MICROBIAL METABOLIC ACTIVITY AND NUTRIENT TURNOVER AT GROUNDWATER-SURFACE WATER INTERFACES

By

PAUL ROMEIJN

A thesis submitted to the University of Birmingham
for the degree of

DOCTOR OF PHILOSOPHY

School of Geography, Earth and Environmental Sciences

College of Life and Environmental Sciences

University of Birmingham

May 2018

Abstract

Rivers and streams have crucial ecohydrological functions and are much more than just transport systems for excess water. Active exchange across groundwater-surface water interfaces facilitates many biogeochemical processes. However, natural functions of microbial metabolic activity (MMA) are disturbed by excess nutrient inputs from anthropogenic disturbances such as agriculture or wastewater treatment plants. Key results of this thesis are: (1) streambed MMA and greenhouse gas production are driven by quantity and quality of the organic matter, and streambed CO_2 production rates can account for up to 35% of estimated total stream evasion. (2) Streambed heterogeneity drives MMA and nutrient turnover. While dissolved organic carbon was not limiting, high organic matter structures can control nutrient concentrations. (3) Macrophyte cover was negatively related to hyporheic exchange. Mowing of macrophytes as a management practice does therefore not negatively influence MMA and can improve transient storage in urban streams. (4) MMA in dual-porosity Chalk groundwater aquifers is sensitive to fertilisation by carbon that can be introduced during groundwater flood events and can be responsible for problems drinking water production quality. These results improve understanding of MMA, nutrient turnover and greenhouse gas production at groundwater-surface water interface and anticipate on the impacts of anthropogenic disturbances.

Acknowledgements

I would like to thank Amaia for her patience and all her support over the past years. We saw many places together and shared many experiences, and you have always been there for me when I needed it. Now we finally have more relaxed times ahead!

I'm very grateful for the support from my supervisors, Professor Stefan Krause and Professor David Hannah. I couldn't have done this without your inspiration and guidance. The meetings with you always gave me a boost in motivation and inspiration that brought me back on track. Thank you as well to the Hypotrain people for the work in Chapter 3, as well as Dr. Jesús Gomez-Velez for the inspiration and his help with the data in Socorro. I'm grateful for the support I received in Berlin from Dr. Jörg Lewandowski, but the cherry on the Berlin pie was of course Jason.

A very special thanks to Sophie Comer-Warner (and Anika!) for your help with the project, but especially the fun times. Rebwar, thank you for your good company and endless patience in the field, and definitely for the sweets from Erbil! Many thanks as well to Dr. Sami Ullah for your support with the analysis, Richard Johnson for your lab and field support, Dr. Mike Rivett for your help in the early stages of my project, and Professor Daren Gooddy and Dr. Nick Kettridge for your inspiration. And a big thank you to all the people from 325 who made the Birmingham times so much fun. The whole experience wouldn't be complete without all the people from the INTERFACES network. It was a great experience to work with you and hopefully we meet again. I would like to acknowledge funding from the EU grants FP7-INTERFACES no 607150 and H2020-MSCA-RISE-2016 no 734317.

Special thanks as well to my friends from the Netherlands, whose visits to everywhere I stayed were always something to look out for.

And last but certainly not least, I owe much gratitude to my parents and sister. You kept supporting me over the years, even when I wasn't sure what to do. I don't know if you imagined me finishing a PhD thesis 15 years ago, but your support definitely brought me this far.

Table of contents

List of figures

List of tables

Introduction

Scientific context

Rivers and streams are vital for the world's fresh water supply. Although this knowledge is commonly accepted, their ecohydrological role has not always been acknowledged. Up to several decades ago streams were viewed as pipelines that merely transport water. It was not until the 1980s that the ecohydrological significance became more accepted (Bencala, 1993; Boulton *et al.*, 1998; Cardenas, 2015). While water flows through a river, there is constant exchange of water between the active channel, the subsurface and the riparian zone (Figure 1). The zone where water is exchanged is referred to as the hyporheic zone (HZ), coming from the Greek 'hypo' for below and 'rheos' for flow. It's believed that water in most streams is completely exchanged with the porewater of the hyporheic zone while flowing downstream (Jones & Mulholland, 2000; Kiel & Bayani Cardenas, 2014). This exchange facilitates a wide variety of biogeochemical interactions between water in the stream, pore water and up- or downwelling groundwater, with the mineral surfaces of the streambed material and biofilms that thrive there (Boulton *et al.*, 1998; McClain *et al.*, 2003; Claret & Boulton, 2009; Singer *et al.*, 2010; Besemer, 2015; Battin *et al.*, 2016).

Hyporheic exchange flow is driven by hydraulic properties of the stream and other features such as meanders or pool-riffle sequences (Gomez-Velez *et al.*, 2014; Fox *et al.*, 2016). This promotes contact with sediment surfaces and provides good habitats for microorganisms that drive nutrient turnover (Pinay *et al.*, 2002, 2015; Hupfer *et al.*, 2018), pollutant attenuation (Schaper *et al.*, 2018) and other ecosystem services (Peralta-Maraver *et al.*, 2018). Depending on the position in the landscape, conditions can be more suitable for aerobic microbial metabolic activity (MMA) and the water fluxes vary (Figure 1).

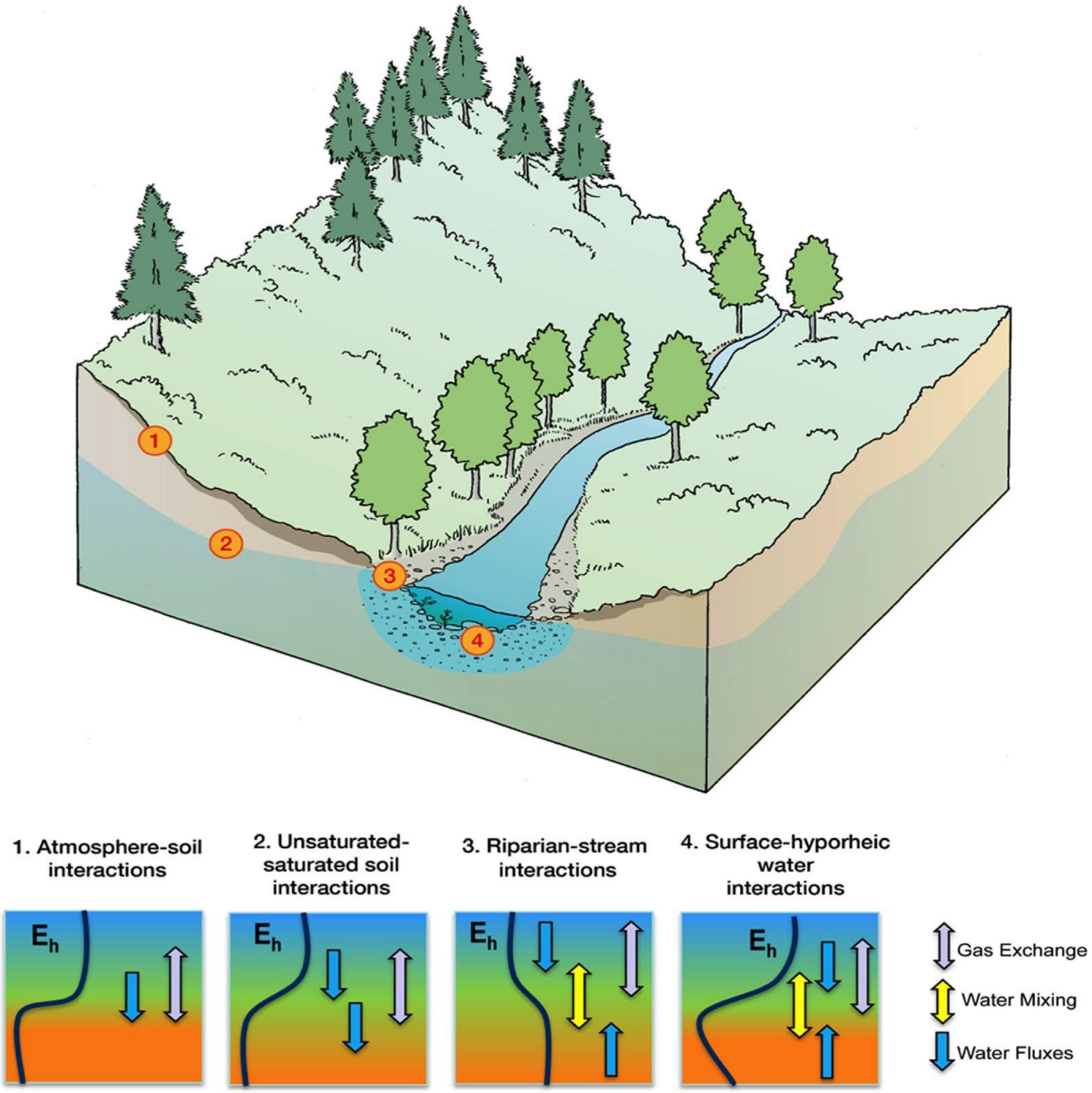

Figure 1. The most common compartments that water passes in the hyporheic zone and their main properties (Krause *et al.*, 2017).

A substantial part of all fresh water in streams worldwide flows through areas with strong anthropogenic influence, such as agriculture, urban runoff or effluents from wastewater treatment plants (Wahl *et al.*, 1997; Kronvang *et al.*, 2005; Dodds & Smith, 2016; Loiselle *et al.*, 2016; Rice & Westerho, 2017). Despite advances in the field of GW-SW exchange, there are still many open questions about the effect of anthropogenic disturbances to hyporheic flow (Cardenas, 2015). Streams and rivers worldwide have been observed to produce

substantial amounts of greenhouse gases (Aufdenkampe *et al.*, 2011; Butman & Raymond, 2011; Raymond *et al.*, 2013). While the total outgassing of rivers and streams to the atmosphere has been studied, the contribution of the top layer of streambed sediments in smaller streams in agricultural areas remained unclear (Cole *et al.*, 2007). In anthropogenically disturbed areas GHG outgassing has been observed to increase (Crawford *et al.*, 2016; Schade *et al.*, 2016). Spatial variation of OM quality and quantity in sediments may be expected to influence microbial metabolic activity (MMA) and associated GHG production. However, it is not only the top layer of streambed sediments that plays a role at the GW-SW interfaces.

In zones with groundwater upwelling, water flow patterns can be affected by spatial variations in streambed heterogeneity (Krause *et al.*, 2012; Gomez-Velez *et al.*, 2014). These variations in water flow patterns drive differences in residence time and nutrient turnover (Krause *et al.*, 2013, 2017; Pinay *et al.*, 2015). However, the influence of variations in residence time in streambeds on MMA remains largely unknown. Residence time becomes an important factor in surface water, represented as transient storage zones in the stream compartment, that can be increased by macrophyte growth (Vereecken *et al.*, 2006; Hensley & Cohen, 2012). Under low flow conditions the increased vegetation can lead to increased nutrient turnover (Kurz *et al.*, 2017). Eutrophication can lead to excess biomass in the channel and reduce flow (Kantrud, 1990), triggering water authorities to clear waterways in urban areas of macrophytes on a frequent basis as a management practice (Ochs *et al.*, 2018). Yet the influence of this mowing on total stream MMA and the degree of disturbance to the habitat caused are not fully understood.

While GW-SW interactions are often discussed closer to the surface, it is crucial to consider processes deeper towards the aquifer level as well. Rivers and their hyporheic zones can be

up- or downwelling and the interactions between downwelling surface water and aquifers can be complex (Allen *et al.*, 2010). However, there is evidence that loading of contaminants from stream to aquifer can be significant (Manamsa *et al.*, 2016). During prolonged rainfall events, the groundwater table can rise to a point that a groundwater flood event occurs (Robins & Finch, 2012), especially in so-called dual porosity aquifers that are connected by fractures that facilitate relatively fast flow (Macdonald & Allen, 2001). Still, any effects of these flood events in terms of possible fertilisation effects on MMA are unknown. The work outlined in this thesis used a combination of novel tracer applications and high frequency measurements across different scales to understand how aquifer-surface water interfaces act as hotspots for interconnected carbon and nitrogen cycling and greenhouse gas production.

Aims and objectives of the research

The aim of this thesis was to investigate the drivers and controls of MMA in groundwater, surface water and at their interfaces across a range of scales from microcosm to reach scale, with a particular focus on spatial and temporal dynamics, and under the influence of anthropogenic disturbances. The objectives of this work were:

- To investigate the drivers of microbial metabolic activity at various types of groundwater-surface water interfaces
- To investigate the role of microbial metabolic activity as driver of nutrient turnover and biogeochemical processes at several extremes of groundwater-surface water interfaces.

Thesis layout

This thesis will explain the role of microbial metabolic activity (MMA) and nutrient turnover at groundwater-surface water (GW-SW) interfaces by first discussing the role of organic

matter quantity and quality on MMA in a microcosm experiment in Chapter 1. Using the knowledge gained under controlled laboratory conditions, it will then provide evidence how MMA and nutrient turnover behave on a small scale inside a heterogeneous streambed of a stream in an agricultural setting (Chapter 2). The next step will show (in Chapter 3) how MMA is controlled in an urban stream that is even more anthropogenically disturbed urban stream. Finally, it is demonstrated in Chapter 4 that GW-SW interfaces are relevant for MMA even at the groundwater level. All the studied GW-SW interfaces were in areas with strong anthropogenic influence in terms of nutrient loading. Novel applications of the reactive tracer resazurin (Haggerty *et al.*, 2009) were used as a proxy to measure MMA throughout the thesis.

Chapter 1. "Streambed organic matter controls on greenhouse gas emissions from streams."

In this chapter greenhouse gas (GHG) production in streams is addressed. GHG production is an understudied topic in streambed environments. An incubation experiment is conducted using a combination of the fluorescent tracer resazurin and GHG analysis under controlled conditions. This study aims to close the knowledge gap of the influence of OM quality and quantity on MMA and GHG production across contrasting streambed sediments.

Chapter 2. "Streambed heterogeneity drives microbial metabolic activity through residence time."

Chapter 2 addresses an *in situ* experiment performed at the River Tern in the UK using a novel push-pull tracer injection method with resazurin. The experiment remains at the smaller plot scale. Injection locations were chosen in a reach with upwelling groundwater and sharp gradients in hydraulic conductivity. These sharp gradients have implications for organic carbon, dissolved oxygen and nitrate turnover in the shallow hyporheic zone. The aim is to

find significant drivers and controls of MMA and nutrient turnover around low hydraulic conductivity structures and possible consequences for hotspot activity.

Chapter 3. "Macrophyte controls on total stream microbial metabolic activity in an urban stream."

In Chapter 3 the study is taken to the reach scale. Here the interplay between MMA and transient storage is studied in an urban stream receiving large inputs of wastewater treatment effluents. Macrophyte growth in channels is sensitive to eutrophication and can lead to decreased drainage. Mowing of macrophyte as a management practice is commonly applied and alters the transient storage inside a stream. The aim of this chapter is to study the influence of macrophyte removal on total stream MMA in relation to transient storage. Concurrent resazurin and conservative tracer slug injections were performed before and after a macrophyte removal.

Chapter 4. "Groundwater flooding induced fertilization and enhanced microbial metabolic activity of a dual-porosity aquifer system."

In the last chapter, the focus shifts to the other part of the GW-SW interface at the groundwater side. During prolonged periods of rainfall, it is possible that the soils become saturated. Groundwater recharge in areas with Chalk aquifers in the UK often happens along fractures in the rock, in so called dual-porosity systems. Although the water is deeper than most hyporheic zones, the water is still strongly influenced by processes at the surface. During periods of high recharge after rain, the amount of water can transport substantial amounts of carbon and nutrients, e.g. due to saturated soils. The aim of the last chapter is to study the impact of groundwater flood events on fertilisation of the microbial communities and potentially increased MMA in aquifers.

References

Allen DJ, Darling WG, Gooddy DC et al. (2010) Interaction between groundwater, the hyporheic zone and a Chalk stream: A case study from the River Lambourn, UK. *Hydrogeology Journal*, **18**, 1125–1141.

Aufdenkampe AK, Mayorga E, Raymond PA et al. (2011) Riverine coupling of biogeochemical cycles between land, oceans, and atmosphere. *Frontiers in Ecology and the Environment*, **9**, 53–60.

Battin TJ, Besemer K, Bengtsson MM, Romani AM, Packmann AI (2016) The ecology and biogeochemistry of stream biofilms. *Nature Reviews Microbiology*, **14**, 251–263.

Bencala KE (1993) A Perspective on Stream-Catchment Connections. *Journal of the North American Benthological Society*, **12**, 44–47.

Besemer K (2015) Biodiversity, community structure and function of biofilms in stream ecosystems. *Research in Microbiology*, **166**, 774–781.

Boulton AJ, Findlay S, Marmonier P, Stanley EH, Valett HM (1998) The functional significance of the hyporheic zone in streams and rivers. *Annual Review of Ecology and Systematics*, **29**, 59–81.

Butman D, Raymond PA (2011) Significant efflux of carbon dioxide from streams and rivers in the United States. *Nature Geoscience*, **4**, 839–842.

Cardenas MB (2015) Hyporheic zone hydrologic science: A historical account of its emergence and a prospectus. *Water Resources Research*, **51**, 3601–3616.

Claret C, Boulton AJ (2009) Integrating hydraulic conductivity with biogeochemical gradients and microbial activity along river - Groundwater exchange zones in a subtropical stream. *Hydrogeology Journal*, **17**, 151–160.

Cole JJ, Prairie YT, Caraco NF et al. (2007) Plumbing the global carbon cycle: Integrating inland waters into the terrestrial carbon budget. *Ecosystems*, **10**, 171–184.

Crawford JT, Loken LC, Stanley EH, Stets EG, Dornblaser MM, Striegl RG (2016) Basin scale controls on CO2 and CH4 emissions from the Upper Mississippi River. *Geophysical Research Letters*, **43**, 2015GL067599.

Dodds WK, Smith VH (2016) Nitrogen, phosphorus, and eutrophication in streams. *Inland Waters*, **6**, 155–164.

Fox A, Laube G, Schmidt C, Fleckenstein JH, Arnon S (2016) The effect of losing and gaining flow conditions on hyporheic exchange in heterogeneous streambeds. *Water Resources Research*, **52**, 7460–7477.

Gomez-Velez JD, Krause S, Wilson JL (2014) Effect of low-permeability layers on spatial patterns of hyporheic exchange and groundwater upwelling. *Water Resources Research*, **50**, 5196–5215.

Haggerty R, Martí E, Argerich A, Von Schiller D, Grimm NB (2009) Resazurin as a "smart" tracer for quantifying metabolically active transient storage in stream ecosystems. *Journal of Geophysical Research: Biogeosciences*, **114**.

Hensley RT, Cohen MJ (2012) Controls on solute transport in large spring-fed karst rivers. *Limnology and Oceanography*, **57**, 912–924.

Hupfer M, Engesgaard P, Jensen H, Krause S, Nützmann G (2018) Aquatic interfaces and linkages: An emerging topic of interdisciplinary research. *Limnologica*, **68**, 1–4.

Jones JB, Mulholland PJ (2000) *Streams and ground waters*. Academic Press, San Diego, 425 pp.

Kantrud H (1990) *Sago pondweed (Potamogeton pectinatus L.): a literature review*.

Kiel BA, Bayani Cardenas M (2014) Lateral hyporheic exchange throughout the Mississippi River network. *Nature Geoscience*, **7**, 413–417.

Krause S, Blume T, Cassidy NJ (2012) Investigating patterns and controls of groundwater up-welling in a lowland river by combining Fibre-optic Distributed Temperature

Sensing with observations of vertical hydraulic gradients. *Hydrology and Earth System Sciences*, **16**, 1775–1792.

Krause S, Tecklenburg C, Munz M, Naden E (2013) Streambed nitrogen cycling beyond the hyporheic zone: Flow controls on horizontal patterns and depth distribution of nitrate and dissolved oxygen in the upwelling groundwater of a lowland river. *Journal of Geophysical Research: Biogeosciences*, **118**, 54–67.

Krause S, Lewandowski J, Grimm NB et al. (2017) Ecohydrological interfaces as hot spots of ecosystem processes. *Water Resources Research*, **53**, 6359–6376.

Kronvang B, Jeppesen E, Conley DJ, Søndergaard M, Larsen SE, Ovesen NB, Carstensen J (2005) Nutrient pressures and ecological responses to nutrient loading reductions in Danish streams, lakes and coastal waters. *Journal of Hydrology*, **304**, 274–288.

Kurz MJ, Drummond JD, Martí E et al. (2017) Impacts of water level on metabolism and transient storage in vegetated lowland rivers: Insights from a mesocosm study. *Journal of Geophysical Research: Biogeosciences*, **122**, 628–644.

Loiselle SA, Gasparini Fernandes Cunha D, Shupe S et al. (2016) Micro and Macroscale Drivers of Nutrient Concentrations in Urban Streams in South, Central and North America (ed Douglas ME). *PLOS ONE*, **11**, e0162684.

Macdonald AM, Allen DJ (2001) Aquifer properties of the Chalk of England. *Quarterly Journal of Engineering Geology and Hydrogeology*, **34**, 371–384.

Manamsa K, Lapworth DJ, Stuart ME (2016) Temporal variability of micro-organic contaminants in lowland chalk catchments: New insights into contaminant sources and hydrological processes. *Science of the Total Environment*, **568**, 566–577.

McClain ME, Boyer EW, Dent CL et al. (2003) Biogeochemical Hot Spots and Hot Moments at the Interface of Terrestrial and Aquatic Ecosystems. *Ecosystems*, **6**, 301–312.

Ochs K, Rivaes RP, Ferreira T, Egger G (2018) Flow Management to Control Excessive Growth of Macrophytes – An Assessment Based on Habitat Suitability Modeling .

Frontiers in Plant Science , **9**, 356.

Peralta-Maraver I, Reiss J, Robertson AL (2018) Interplay of hydrology, community ecology and pollutant attenuation in the hyporheic zone. *Science of the Total Environment*, **610**–**611**, 267–275.

Pinay G, Clément JC, Naiman RJ (2002) Basic principles and ecological consequences of changing water regimes on nitrogen cycling in fluvial systems. *Environmental Management*, **30**, 481–491.

Pinay G, Peiffer S, De Dreuzy JR et al. (2015) Upscaling Nitrogen Removal Capacity from Local Hotspots to Low Stream Orders' Drainage Basins. *Ecosystems*, **18**, 1101–1120.

Raymond PA, Hartmann J, Lauerwald R et al. (2013) Global carbon dioxide emissions from inland waters. *Nature*, **503**, 355–359.

Rice J, Westerho P (2017) High levels of endocrine pollutants in US streams during low flow due to insufficient wastewater dilution. *Nature Geoscience*, **10**, 587–591.

Robins NS, Finch JW (2012) Groundwater flood or groundwater-induced flood? *Quarterly Journal of Engineering Geology and Hydrogeology*, **45**, 119–122.

Schade JD, Bailio J, McDowell WH (2016) Greenhouse gas flux from headwater streams in New Hampshire, USA: Patterns and drivers. *Limnology and Oceanography*, **61**, S165–S174.

Schaper JL, Seher W, Nützmann G, Putschew A, Jekel M, Lewandowski J (2018) The fate of polar trace organic compounds in the hyporheic zone. *Water Research*.

Singer G, Besemer K, Schmitt-Kopplin P, Hödl I, Battin TJ (2010) Physical heterogeneity increases biofilm resource use and its molecular diversity in stream mesocosms (ed Bell T). *PLoS ONE*, **5**, e9988.

Vereecken H, Baetens J, Viaene P, Mostaert F, Meire P (2006) Ecological management of aquatic plants: Effects in lowland streams. *Hydrobiologia*, **570**, 205–210.

Wahl MH, McKellar HN, Williams TM (1997) Patterns of nutrient loading in forested and urbanized coastal streams. *Journal of Experimental Marine Biology and Ecology*, **213**, 111–131.

Chapter 1. Streambed organic matter controls on carbon dioxide and methane emissions from streams

Paul Romeijn[†], Sophie A. Comer-Warner[†], Sami Ullah, David M. Hannah, Stefan Krause

[†] *Joint first authorship*

Abstract

Greenhouse gas (GHG) production in streams is a much understudied topic. Lateral inputs of CO_2 from terrestrial organic, inorganic, or lotic metabolism sources alone cannot account fully for estimates of total evasion reported in the literature. There is a paucity of research exploring organic matter controls on GHG production by microbial metabolic activity in streambeds, which is a major gap given the increased inputs of allochthonous carbon to streams, especially in agricultural catchments. This study aims to close the knowledge gap by quantifying how contrasting organic matter contents in different sediments affect streambed greenhouse gas production and associated microbial metabolic activity. We demonstrate, by means of an incubation experiment, that streambed sediments have the potential to produce substantial amounts of GHG, controlled by sediment organic matter quantity and quality. We observed streambed CO_2 production rates that can account for up to 35% of total stream evasion estimated in previous studies. Moreover, our results indicate that streambed sediments may produce much more CO_2 than quantified to date, depending on the quantity and quality of the organic matter, which has direct implications for global estimates of C fluxes in stream ecosystems.

1.1. Introduction

River corridors, and in particular the interface between groundwater and surface water in hyporheic and riparian zones, provide crucial ecosystem functions such as nutrient spiralling, pollutant attenuation, organism distribution and fish spawning (Boulton *et al.*, 1998; Battin *et al.*, 2009; Krause *et al.*, 2011; Trimmer *et al.*, 2012; Cardenas *et al.*, 2016; Catalán *et al.*, 2016; Freixa *et al.*, 2017; Mendoza-Lera & Datry, 2017). In terms of biogeochemical functions, freshwater-sediment at groundwater-surface water interfaces at streambeds have been identified as significant contributors to both the global carbon (C) cycle and greenhouse gas (GHG) production (Hedin, 1990; Fischer & Pusch, 2001; Battin *et al.*, 2008; Tank *et al.*, 2010; Aufdenkampe *et al.*, 2011; Ciais *et al.*, 2013; Marín-Spiotta *et al.*, 2014; Freixa *et al.*, 2016). Streambed and river C cycling is strongly affected by the composition and turnover of organic matter (OM) in rivers and streambeds (Hedin, 1990; Battin *et al.*, 2009; Aufdenkampe *et al.*, 2011; Ciais *et al.*, 2013; Catalán *et al.*, 2016). Rivers have been shown to be important reactors that promote processing of OM and contribute significantly to the global GHG budget (Trimmer *et al.*, 2012; Raymond *et al.*, 2013). Despite early findings in forest streams that streambed sediment OM can be an important driver in sediment respiration (Hedin, 1990), GHG production as a result of aerobic or anaerobic respiration in streambed sediments has remained understudied in nutrient-rich, agricultural, lowland streams. Enhanced nutrient and C loads (and often larger streambed residence time) in lowland agricultural streams offer the potential to alter significantly aquatic ecosystems worldwide (Allan, 2004; Blann *et al.*, 2009; Fuß *et al.*, 2017), by most critically increasing GHG production (Helton *et al.*, 2014; Crawford *et al.*, 2016; Schade *et al.*, 2016).

The drivers and controls of GHG contributions from agricultural streams less than 100 m wide, and in particular those less than 10 m wide, draining nutrient enriched catchments

remain unknown (Cole *et al.*, 2007; Raymond *et al.*, 2013; Lauerwald *et al.*, 2015), despite these systems showing some of the highest CO_2 (Aufdenkampe *et al.*, 2011; Hotchkiss *et al.*, 2015) and N_2O (Turner *et al.*, 2015) outgassing per surface area. One reason for this is the limited knowledge of the impacts of heterogeneous spatial patterns in geologies, streambed substrates and, in turn, sediment chemical conditions (Bardini *et al.*, 2012; Gomez-Velez *et al.*, 2014; Krause *et al.*, 2014; Trauth *et al.*, 2014). Microbial communities in the streambed vary strongly between different substrates (Cardinale *et al.*, 2002; Fierer *et al.*, 2007; Mosher *et al.*, 2010; Mosher & Findlay, 2011), along the river length (Savio *et al.*, 2015; Freixa *et al.*, 2016) and with surrounding land use (Zhang *et al.*, 2016), suggesting spatially heterogeneous patterns in GHG production. Understanding the relevance and spatial patterns of GHG production from lowland river streambeds requires consideration of variability in OM quantity (as prime control of lowland river respiration processes) as well as the quality of the OM (as control for OM turnover efficiency).

Sources of OM in streambed sediments range from agricultural erosion to local primary production within the stream channel (Wang *et al.*, 2014; Cooper *et al.*, 2015; Rathburn *et al.*, 2017; Rowland *et al.*, 2017), all of which vary in OM quality. As a consequence, C contents of streambed sediments are likely to reflect that of the surrounding erosional surfaces (Cooper *et al.*, 2015; McCorkle *et al.*, 2016). Signatures of the underlying geology are found in stream particulate organic matter (POM) and dissolved organic matter (DOM) from the headwater to the river mouth (Longworth *et al.*, 2007; Mosher *et al.*, 2010). There is evidence that catchment geology plays an important role in river nutrient turnover (Lansdown *et al.*, 2016; Stuart & Lapworth, 2016), local groundwater exchange, ecohydrological and hydrogeological properties (Harvey *et al.*, 2008; Kolbe *et al.*, 2016) which suggests a potential role for OM quality as a driver of MMA and GHG production in streambed sediments. However, there is poor understanding of OM controls on streambed microbial

metabolic activity, GHG production and the role of OM quality and quantity. Given 0.47% of the Earth's surface area is covered by streams (Raymond *et al.*, 2013), it is important to quantify contribution of GHG production from the whole stream ecosystems, including under-researched streambed sediments.

In this context, this paper aims to quantify CO_2 and CH_4 (GHG) production from lowland streambed sediments across a gradient of streambed OM contents and different catchment geological backgrounds, focussing on sandstone and chalk. Production of CO_2, CH_4 and N_2O was measured alongside aerobic microbial metabolic activity in microcosms containing six different sediment types of varying OM content from UK lowland streams underlain by chalk or sandstone.

Table 1-1. Sampling location characteristics from the River Tern and the River Lambourn.

River	**Location**	**Dominating geology**	**Average discharge[#]**	**Stream order**	**Catchment size[#]**
Lambourn	Berkshire, UK, 52°51'20.5" N 2°32'44.7" W	Chalk[*]	1.03 $m^3 s^{-1}$	2	234 km^2
Tern	Shropshire, UK, 51°26'41.7" N 1°22'59.1" W	Permotriassic Sandstone[*]	0.856 $m^3 s^{-1}$	2	192 km^2

[#] Averages over 1962 – 2015, measured at Eaton upon Tern and Newbury, obtained from the National River Flow Archive (NRFA, 2015).
[*] Wheater & Peach (2004)

1.2. Methods

Streambed sediments were incubated under controlled conditions. Rather than measuring directly C cycling and GHG production, previous studies considered total stream evasion (Butman & Raymond, 2011; Hotchkiss *et al.*, 2015; Worrall *et al.*, 2016), or indirectly calculated CO_2 approaches (Raymond *et al.*, 2013), which may be sensitive to overestimation or underestimation (Abril *et al.*, 2015). Furthermore, field measurements are challenged by the difficulty of isolating the governing processes and drivers.

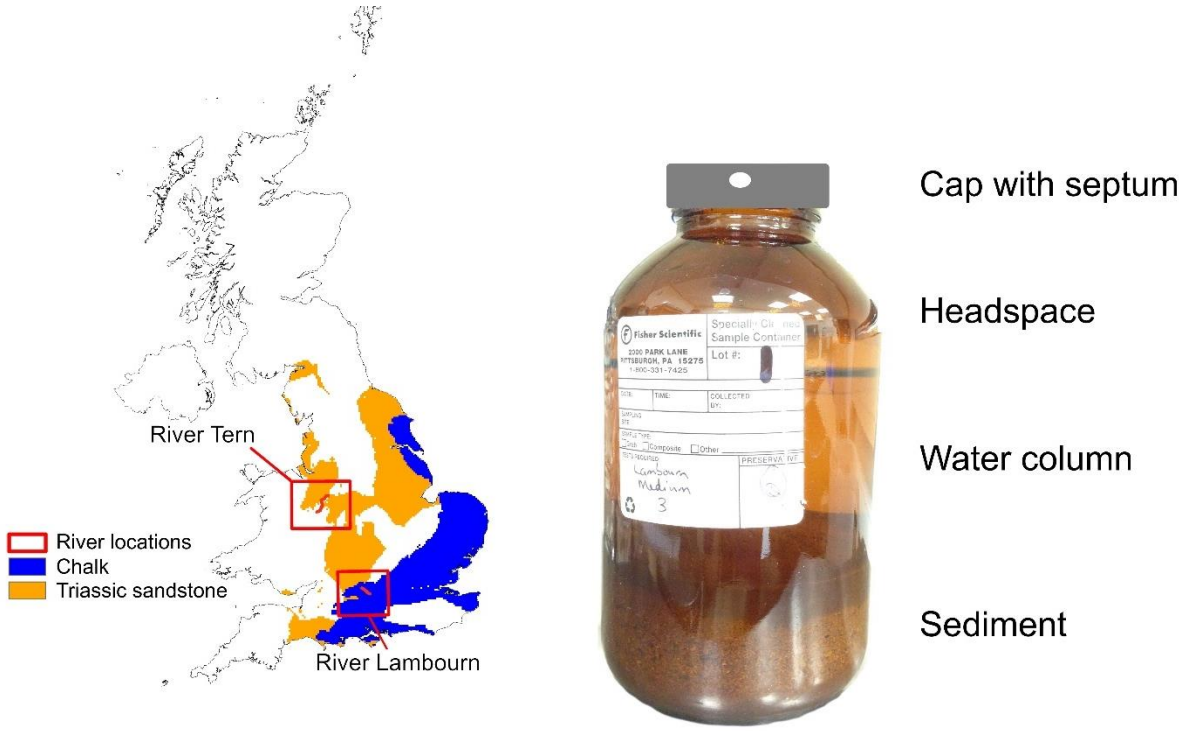

Figure 1-1. Sampling location of sediments used in the microcosm incubations (left). The River Tern is in a sandstone catchment and the River Lambourn in a chalk catchment. An example of a microcosm is shown (right), indicating the how these were filled.

1.2.1. Sediment

Sediments used in microcosm incubations were collected from two rivers with contrasting geological substrates, though similar land use (Wheater & Peach, 2004): River Lambourn and River Tern (Figure 1-1; Table 1-1). Both rivers are in agricultural catchment areas with

similar discharge (NRFA, 2015). Three locations were chosen within each river based on estimated organic matter content to achieve a gradient (fine sediment under vegetation, non-vegetated armoured streambed and non-vegetated sand-dominated straight channel section). Vegetated patches consisted of submerged macrophytes that were not further determined. Macrophyte stands were denser and more clustered in the Lambourn than in the Tern. The total of 6 field-wet sediment types (Table 1-2) was collected in September 2015 by scooping off the top 10 cm of the streambed. Bulk sediments were sieved: fine sediments from under vegetation (CH and SH) at 0.8 cm to clear large organic debris and the others at 1.6 cm, homogenised, stored airtight in the dark and refrigerated at 4.4±0.8°C until start of the experiments. The sieving sizes were chosen to preserve as much of the size characteristics present in the field, while removing larger stones and debris that would otherwise occupy disproportionally large volume inside the microcosms. The storage temperature was monitored using a Tinytag Aquatic 2 temperature logger (Gemini Data Loggers Ltd, Chichester, United Kingdom).

Organic matter content was determined by loss on ignition. Samples were prepared in threefold for each geology OM type (chalk, sandstone, and: low, medium, high). Sediment was milled by hand, sieved at 2mm, homogenised and dried at 105°C for a minimum of 12 hours. OM quantity was measured by loss on ignition (LOI) using an oven at 550°C for 6 hours (Hoogsteen *et al.*, 2015). Carbonate content was then determined using the same oven at a temperature of 950°C for 6 hours (Hoogsteen *et al.*, 2015). Weight loss relative to original dry sample weight was measured immediately to prevent ambient moisture uptake and then used as the fraction of OM or carbonate, respectively.

Table 1-2. OM quantity, carbonate contents and specific ultraviolet absorbance (SUVA) as a measure for OM quality, as measured from the bulk sediment. The new sediment name has been chosen to reflect actual OM content, and varies between chalk and sandstone sediments. Mean values listed with SD and $n = 3$.

Geological background	**Sediment origin**	**Sediment name**	**%OM**	**%carbonate**	**SUVA (L mg^{-1} m^{-1})**
Chalk	Under vegetation	ChalkHigh (CH)	3.625±0.069	11.620±0.499	2.098±0.180
	Straight section, no vegetation	ChalkMedium (CM)	1.847±0.063	18.668±1.423	1.277±0.109
	Gravel section	ChalkLow (CL)	1.409±0.047	17.170±2.259	1.498±0.092
Sandstone	Under vegetation	SandstoneHigh (SH)	3.616±0.116	0.357±0.017	2.642±0.511
	Gravel section	SandstoneMedium (SM)	0.838±0.031	0.234±0.016	1.813±0.252
	Straight section, no vegetation	SandstoneLow (SL)	0.667±0.014	0.253±0.028	3.209±0.263

We compared quality of OM between all sediments by measuring aromaticity of the available organic carbon as specific ultraviolet absorbance (SUVA) at 254 nm wavelength (Weishaar *et al.*, 2003; Ullah *et al.*, 2014). OM quality was measured by taking sediments sieved at 2 mm in triplicate and extracting DOC from the sediments using 2M KCl (Jones & Willett, 2006). DOC content of the sediment extracts was determined using a Shimadzu TOC-L analyser (Shimadzu Corporation, Japan), after which the sediment extracts were measured for SUVA (Weishaar *et al.*, 2003; Ullah *et al.*, 2014). Absorption was measured using a Varian Cary

Eclipse UV-Vis spectrophotometer (Agilent Technologies, Santa Clara, USA). We used a 10 mm path length quartz cuvette, recording the absorbance between 250 and 280 nm at full wavelength scanning and ultrapure water for blank correction.

1.2.2. Microcosm preparation

Microcosms were 1 litre amber jars with 53/400 size septa-capped lids (Fisher Scientific Ltd., UK). The glassware was acid rinsed with 10% HCl before use and triple washed with 18.2MΩ deionised (DIW) water. Incubation of each sediment type was done in triplicate. Each of the 6 sediment types was measured by wet volume using a 300 ml glass beaker and transferred into the microcosms. To control for background concentrations, we added 500 ml DIW to the wet sediment. Headspace volume for each jar was calculated after the experiment, based on total water and sediment volume. The sediments were then laterally shaken for 30 seconds to promote mixing of wet sample and DIW in the water column, while keeping all sediment in suspension. Three control treatments were prepared as 3 jars with 500 ml DIW only. The microcosms were then left 48 hours in the dark at the incubation temperature of 15.35±0.15°C to settle the sediment and minimise turbidity. The caps were loosely placed on top allowing air to flow out, but to minimise evaporation by the air circulation. The refrigerated incubator used was a generic type with forced air circulation, internal light switched off and the internal temperature was monitored using 2 Tinytag Aquatic 2 temperature loggers (Gemini Data Loggers Ltd, Chichester, United Kingdom). One logger was placed on the top shelf and one at the bottom to monitor effects of air circulation.

1.2.3. Experimental procedure

During the experiment, the following steps were undertaken at T = 0, 5, 10, 24 and 29 hours after the microcosms were prepared as described above.

- Take microcosm out of the incubator
- Take two 15 ml headspace gas samples through septum and store in Exetainer, and then open lid (this step is skipped before the addition of raz). This sample will represent the final GHG concentration of this incubation time step
- Open jar and take a 15 ml water sample, filter and measure on fluorometer
- The first timestep only, follow these steps:
    - Take 15 ml water sample from water column and store for calibrations
    - Add 10 ml of raz stock solution and gently stir the water column, trying to minimise turbidity to bring raz to the target concentration
- Place sample from fluorometer back into microcosm using syringe
- Periodically check pH of water column
- Replace headspace air with ambient air by pushing in ambient air using a 100 ml syringe and repeat 5 times
- Close jar and take two 15 ml headspace samples again. This sample will represent starting headspace GHG concentration for this incubation time step
- Return microcosm back to the incubator

1.2.4. Microbial metabolic activity

Aerobic microbial respiration can be successfully measured using the "smart" tracer resazurin. It was first used in ecohydrological applications by Haggerty *et al.* (2008). It proved to be useful in many different setups, such as reach-scale field experiments (Argerich *et al.*, 2011; González-Pinzón *et al.*, 2012, 2015; Lemke *et al.*, 2013a; Knapp *et al.*, 2017), flume-scale (Haggerty *et al.*, 2014) to microcosm setups (Baranov *et al.*, 2016a, 2016b). The resazurin/resorufin tracer system (Haggerty *et al.*, 2008) was used to measure microbial metabolic activity in the microcosms to be able to objectively compare activity across the

different sediment types. This allows to measure aerobic microbial metabolic respiration by acting as a terminal electron acceptor. In this process resazurin (raz) is irreversibly reduced to the strongly fluorescent resorufin (rru), which can be measured using a fluorometer with excitation and emission wavelengths of 570 nm and 585 nm, respectively. Two Albillia GGUN-FL30 fluorometers (Albillia SARL, Switzerland) were used to measure rru production (Lemke *et al.*, 2013b). The fluorometers were calibrated to either water extracts of the sandstone or chalk at the start of the experiment to ensure best accuracy and to control for variations in background fluorescence. These water extracts were sampled from the incubation jars just before start of the experiment. For calibration, we used stock solutions of raz and rru made up in tap water, which were made into final solutions of 108.67 and 95.33 ng/L for raz and rru, using water extracts of sandstone or chalk sediments. The appropriate calibration curve was applied in data analysis. The conversion of raz to rru is reported as μg rru produced per μg of added raz, to normalise for slightly varying initial raz concentrations. pH of the microcosms was monitored using a handheld Hanna HI-98129 pH meter (Hanna Instruments, Woonsocket, USA). The instrument was calibrated before the experiment to ensure pH was near 8 for good fluorometric detection of rru (Lemke *et al.*, 2013b). The detection limit, calculated precision and accuracy of this type of fluorometers are listed in Table 1-3. The target concentration of raz for the starting conditions inside the microcosms was 150 ng/L.

At each sampling moment, a 20 ml sample was extracted from the microcosms using a syringe, which was filtered to control for turbidity using a 0.45 μm nylon syringe filter (ThamesRestek, High Wycombe, UK), which was pre-soaked in DIW to prevent leaching of DOC. The filtered sample was injected directly into the measurement chamber of the fluorometer and measured for at least 3 minutes at a 10-second measurement interval, which was then averaged to calculate the concentration. Approximately half of a randomly chosen

set of samples was measured again on the second fluorometer to control and correct for drift and instrument errors. The samples were transferred back into the microcosm after measurement on the fluorometer to keep the volume constant and the instruments were cleaned with DIW.

Table 1-3. Accuracy, precision and limit of detection for fluorometers used. All concentrations are in ng l^{-1}.

(ng L^{-1})	Accuracy	Precision	Limit of detection[#]	Standard concentration
raz	0.06	0.19	1	108.67
rru	0.08	0.43	1	95.33

[#] Lemke *et al.* (2013b)

1.2.5. Greenhouse gas measurements

Headspace gas concentrations were measured before and after each incubation time step, to calculate the increase in concentrations. A 15 ml gas sample was taken in duplicate using a 20 ml syringe with a hypodermic needle and stopcock to pierce the septum. The duplicate served as a backup and for a randomly picked amount served as a quality control. The syringe was purged three times with ultrapure helium 5.0 (BOC Industrial gases, Manchester, UK) before each sampling. The 15 ml gas sample was then transferred to a 12 ml pre-evacuated Exetainer (Labco Limited, Lampeter, UK), causing it to be slightly over-pressurised. The Exetainers were stored at room temperature until analysis.

Samples were analysed on an Agilent 7890A gas chromatograph (GC), equipped with a 1 ml sample loop, a microECD detector for N_2O detection, a platinum catalyst for CO_2-to-CH_4 conversion and an FID for CH_4 detection (Agilent Technologies, Santa Clara, USA). Samples

eluted from the column at: CH_4 = 3.5 minutes, CO_2 = 5.7 minutes and N_2O = 6.4 minutes. The GC was setup in splitless mode with an oven temperature of 60°C. The microECD was set at 350°C, FID at 250°C, H_2 flow at 48 ml min^{-1}, air flow at 500 ml min^{-1} and N_2 make-up flow at 2 ml min^{-1}. Total run time was 9 minutes per sample. Samples were manually injected into the sample loop using a gas-tight syringe with valve (SGE Analytical Science, Australia). The detection limits for CO_2, CH_4 and N_2O were calculated by dilution of a gas mixture of known concentration and are listed in Table 1-4. We measured samples of known concentrations as quality controls throughout the experiment to calculate accuracy and precision (Table 1-4).

Table 1-4. Limits of detection, precision and accuracy for GHG measurements on Agilent 7890A gas chromatograph, based on standards with listed concentration. All units in parts-per-million (ppm).

(ppm)	Accuracy	Precision	Limit of detection	Standard concentration
CO_2	13.4	14.8	8.2	1051
CH_4	0.07	0.11	0.15	9.8
N_2O	0.13	0.08	0.011	6.2

1.2.6. Statistical analysis

We used descriptive statistics to compare results between sediment types. All mean values listed are noted as mean±standard deviation. Error bars in figures represent standard deviation, unless stated otherwise. For bivariate analysis comparing two sediment types, data were first tested for normal distribution using Shapiro-Wilkes test. Welch's T-test was used to compare two groups of normally distributed samples and results reported as *t*(degrees of freedom), *p* and sample size *n*. Mann-Whitney-Wilcoxon test was used where the distribution

followed a nonparametric distribution with results reported as *U*, *p* and sample size *n*. Kruskall-Wallis test was used to compare whole geology groups, including all different sediment subgroups (results only in supplementary information). Simple linear regression was applied in some cases with results reported as F(degrees of freedom, degrees of freedom), *p*, R^2 and sample size *n*.

1.3. Results

Sediment types are referred to per their OM content (Table 1-2). All means are given with standard deviation. Mean incubation temperature was 15.35±0.15°C (mean ± SD). MMA was clearly detected (Figure 1-2a), indicated by the conversion of raz to rru (interpreted as µg rru produced per hour, normalised for initial raz concentration). CO_2 and CH_4 production was observed in all but the control microcosms. None of the sediments were net N_2O producers under the available instrumental limits of detection. In general, sediments with higher OM content produced more rru, CO_2, and CH_4, and were substantially influenced by the aromaticity of the OM.

Organic matter quality, measured as aromaticity of sediment extractions, varied between 1.207 and 3.469 L mg^{-1} m^{-1} as SUVA (Table 1-2). Mean aromaticity was significantly higher ($t(16) = 3.5546$, $p = 0.00264$, $n = 18$) in the sandstone sediments (2.554±0.684 L mg^{-1} m^{-1}), compared to chalk sediments (1.624±0.385 L mg^{-1} m^{-1}). Aromaticity and OM content were not correlated by simple linear regression ($F(1, 16) = 0.01309$, $p = 0.91$, $R^2 = 0.0008$, $n = 18$).

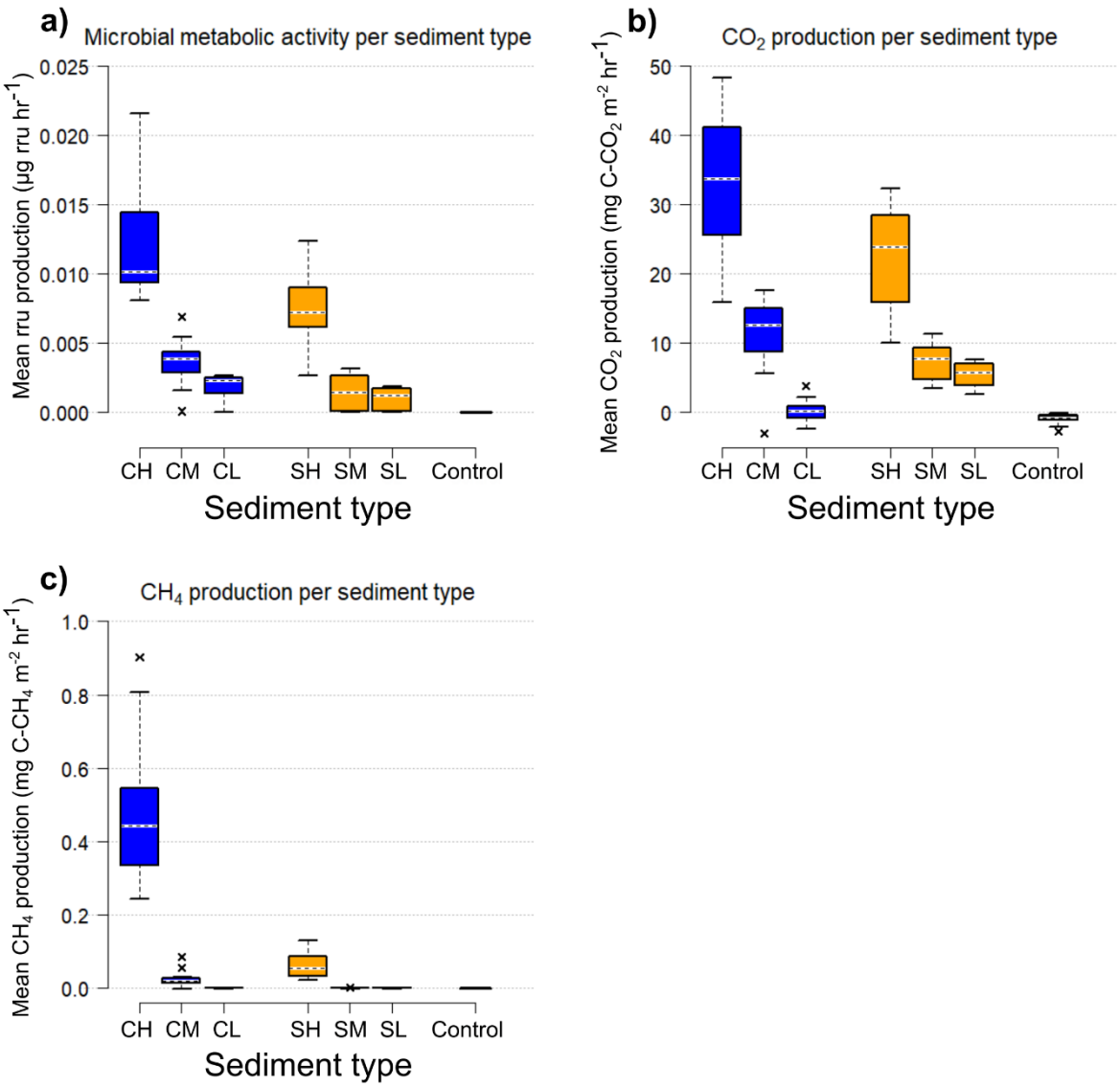

Figure 1-2. Mean hourly production per sediment type for **a**) microbial metabolic activity expressed as normalised rru production, **b**) carbon dioxide production and **c**) methane production. All values are mean hourly production for each incubation time step. Error bars indicate standard deviation within each group (n = 12) of three replicates. Sediment type names correspond to abbreviations given in Table 1-2.

MMA varied for different sediment types (Figure 1-2a). Sediments with the highest OM content of 3.6% were responsible for 65% of the total MMA in streambed sediments of both geological backgrounds (CH and SH). Overall, chalk sediments produced on average 67% more rru per hour than the sandstone sediments. A generally increased trend in MMA with increasing OM content was observed (Figure 1-3a). Mean hourly MMA in chalk sediments

was 0.00584±0.00612 µg rru hr^{-1} and for sandstone 0.00349±0.00492 µg rru hr^{-1}. See also Table A-1 for full results of statistical tests between groups. The strongest MMA was found in CH sediments, with a mean production rate of 0.011±0.0078 µg rru hr^{-1}. CH saw 53% higher MMA than the second highest sediment SH, which experienced production rates of 0.00721±0.0066 µg rru hr^{-1}. CH produced 163% and 370% more rru than lower OM content sediments CM and CL, respectively. SH produced 262% and 463% more than SM and SL, respectively.

CO_2 production followed similar patterns as observed for MMA (Figure 1-2a, b, Figure 1-3b). Mean hourly CO_2 production in chalk sediments was 14.97±15.54 mg C-CO_2 m^{-2} hr^{-1} and for sandstone 11.83±9.03 mg C-CO_2 m^{-2} hr^{-1}, which was 27% higher in chalk compared to sandstone. Like MMA, also the highest CO_2 production was found in CH sediments, with a mean of 33.40±10.55 mg C-CO_2 m^{-2} hr^{-1}. CH produced 48% more CO_2 than the second highest sediment SH, which produced 22.53±7.72 mg C-CO_2 m^{-2} hr^{-1}. CH produced 197% more CO_2 than the lower OM content sediment CM and CL produced virtually nothing. SH produced 203% and 308% more CO_2 than SM and SL, respectively. See also Table A-2 for full results of comparison between sediment groups. Sediments with the highest OM content (CH and SH) were responsible for 62% of total CO_2 production in both chalk and sandstone.

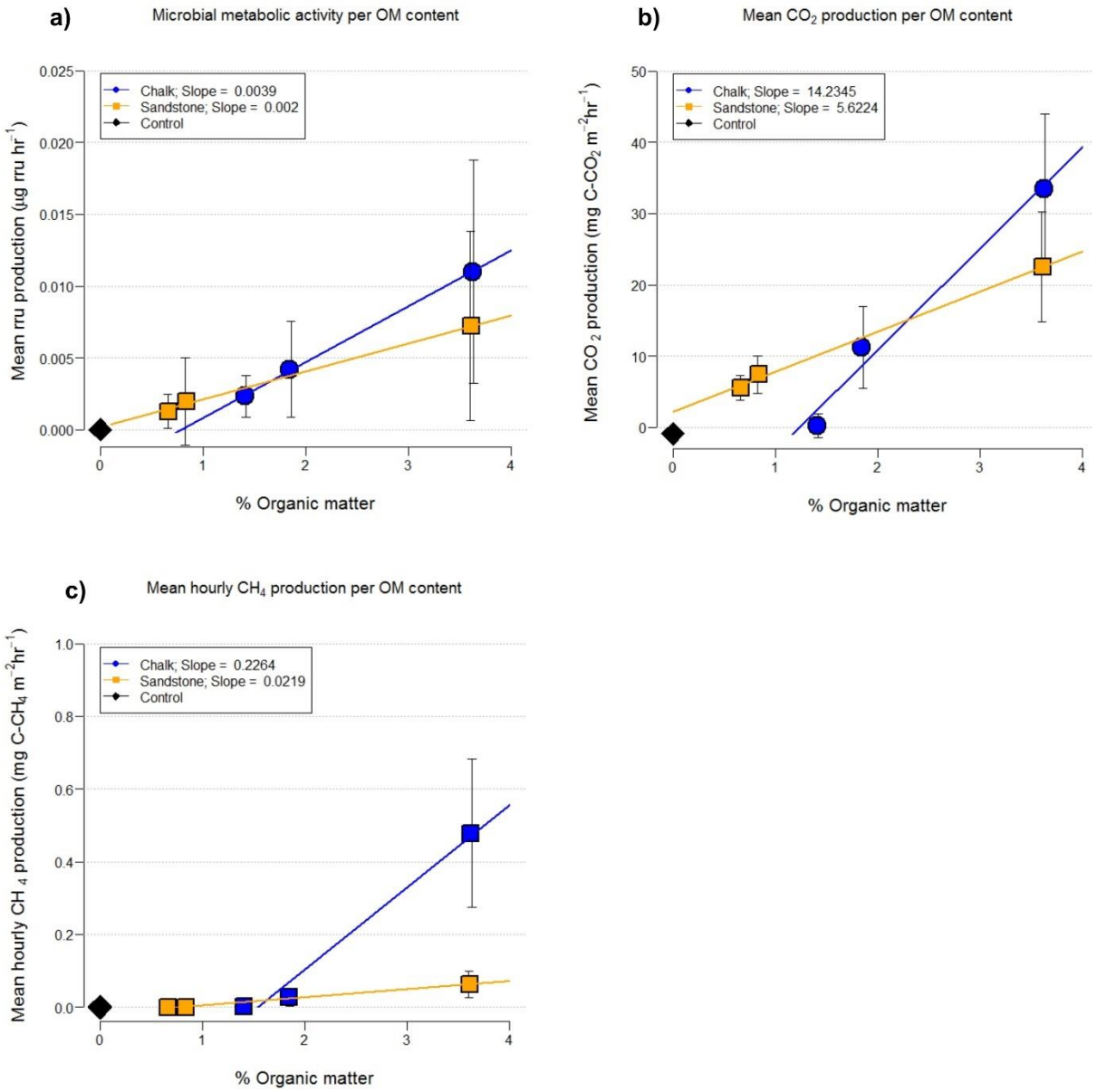

Figure 1-3. Mean hourly production per organic matter content for **a**) microbial metabolic activity expressed as normalised rru production, **b**) carbon dioxide production and **c**) methane production. Error bars indicate standard deviation within each group (n = 12) of three replicates. A trend line has been fitted for comparison between groups.

Patterns of methane production from different sediment types did differ from those observed for MMA and CO_2 (Figure 1-2c, Figure 1-3c). Overall, chalk sediments produced on average 0.1685±0.2503 mg C-CH_4 m^{-2} hr^{-1}, compared to only 0.0213±0.0365 mg C-CH_4 m^{-2} hr^{-1} in sandstone. This was 692% more methane in chalk compared to sandstone. Again, CH sediment experienced the highest methane production with a mean of 0.4778±0.2042 mg C-

CH_4 m^{-2} hr^{-1}. CH produced 656% more than the second highest producer SH, which produced only 0.0632±0.0369 mg C-CH_4 m^{-2} hr^{-1}. Compared to lower OM content sediments, CH produced 1689% more than CM, whereas nothing was detected in CL. See also Table A-3 for full results of comparisons between groups. In SM and SL no methane production was observed at all. Sediments with the highest OM content produced 95% and 100% of all methane in chalk and sandstone, respectively. Methane production accounted for 1.1% of total C losses in chalk sediments, compared to only 0.2% in sandstone.

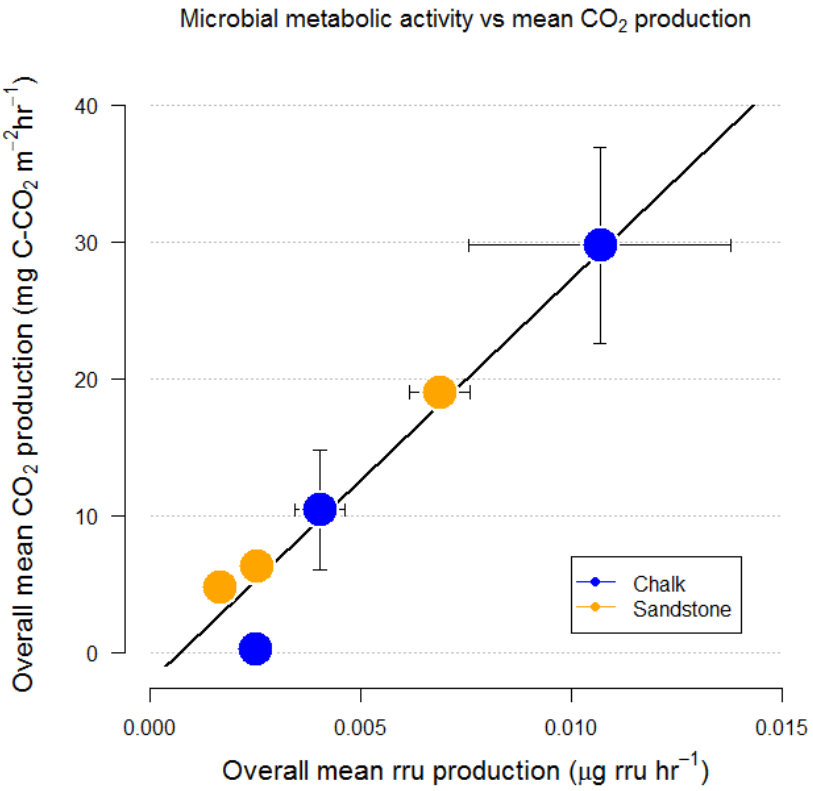

Figure 1-4. Mean CO_2 production increased with mean microbial metabolic activity. All values are based on overall means of all time steps. Error bars indicate standard deviation (n=12). A trend line has been fitted through the combined chalk and sandstone data points to illustrate the general rru-to-CO_2 relation, independent of sediment type. This trend line represents the simple linear regression model that has been fitted.

1.4. Discussion

Our results highlight the substantial potential for streambed sediments from agricultural lowland rivers to produce significant amounts of greenhouse gas. We sampled only the top of the streambed (see methods), although respiration can well take place at greater depths of the streambed, depending on availability of OM and oxic/anoxic zonation (Schindler & Krabbenhoft, 1998; Hlaváčová *et al.*, 2005; Krause *et al.*, 2011, 2014). Despite this, we still measured substantial MMA, CO_2 and CH_4 production that were in a similar range of forest stream sediments *in situ* (Hedin, 1990) and ponds (Yvon-Durocher *et al.*, 2017), lower CO_2 and CH_4 production than from Mediterranean natural stream sediment incubations (Tortosa *et al.*, 2011).

MMA increased with higher OM content. Rru production was found to be linearly correlated by simple linear regression with CO_2 production and proved a good measure for respiration (Figure 1-4; $F(1, 70) = 32.91$, $p << 0.001$, $R^2 = 0.320$, $n = 72$). Higher MMA was observed in chalk sediments compared to sandstone, and the finer sediments in both geologies represented 62% of MMA. OM quantity alone cannot explain the discrepancy in MMA. We find the likely explanation in the OM quality, expressed as aromaticity. Sandstone sediments had significantly higher aromaticity than chalk sediments. Higher aromaticity is typically associated with lower carbon quality and higher recalcitrance (Weishaar *et al.*, 2003; Ullah *et al.*, 2014) and can therefore explain our observations of generally lower MMA, and lower CO_2 and CH_4 production in sandstone. This suggests that OM in sandstone sediments is more recalcitrant due to higher aromaticity and thus more difficult to metabolise by microbial communities (Marschner & Kalbitz, 2003), while it is not simply a consequence of total OM content.

Our results suggest that the observed headspace CO_2 concentrations did not originate from inorganic carbonate weathering (McDonald *et al.*, 2013; Marcé *et al.*, 2015). First, although average hourly CO_2 production in CL sediment with 17.2% carbonate content was slightly, but significantly different from the control treatment (U = 113, p = 0.017, n = 12), the means were both negative and very close to zero (0.266±1.674 and -0.878±0.796 mg C-CO_2 m^{-2} hr^{-1} for CL and control, respectively). We interpret a negative production in this context as a net CO_2 uptake from the headspace into the water column. Second, the sediments with highest and lowest carbonate contents (CM: 18.67%, SM: 0.23%), did not show a significantly different hourly CO_2 production from each other (t(16) = 2.0912, p = 0.053, n = 12). This suggests that it is unlikely that inorganic carbonate weathering alone was an important source of CO_2 measured in the headspace of the microcosms.

Our findings extend previous knowledge from forest streams. We expected higher GHG production in agricultural streams than in forest streams. Hedin (1990) found mean hourly CO_2 production of 5.8 mg C m^{-2} hr^{-1}, between 1.1-14.2 mg C m^{-2} hr^{-1} (mean temperature 14.6°C). The streambed from our agricultural sites produced substantially more with an average CO_2 production rate for all sediments accounted for in this study of 13.40±12.72 mg C m^{-2} hr^{-1}. This highlights the influence of land use: streambeds in agricultural streams can easily produce twice as much CO_2 compared to those in forest streams.

The streambed produces a substantial part of total CO_2 in streams. Higher MMA in chalk sediments and a possible difference in carbon quality are reflected in CO_2 production, where sediments with similar OM content (3.6%) produce more CO_2 in different geologic environments. The average CO_2 production rate for all sediments of 13.40±12.72 mg C-CO_2 m^{-2} hr^{-1} equals to 117.36 g C m^{-2} yr^{-1}. When applying this average value to the UK, and considering a UK land surface cover by streams and rivers of 0.86% (Raymond *et al.*, 2013),

we estimate the potential CO_2 production from streambed sediments to be 1.01 t C km^{-2} yr^{-1}. When comparing this number with estimates of 2.9 t C km^{-2} yr^{-1} total excess CO_2 evasion from the UK (Worrall & Lancaster, 2005), we can conclude that the top of the streambed and riverbed sediments alone can be responsible for up to 35% of total CO_2 fluxes from streams in the UK, which is crucial for estimates of global C budgets, but also has significant consequences for the design of excess nutrient attenuation strategies. Many strategies in strongly nutrient and carbon enriched agricultural lowland streams target enhancing groundwater–surface water exchange (Krause *et al.*, 2011, 2014).

Methane production varied strongly between chalk and sandstone sediments. Our method has not considered any potential methane oxidation. CH was the single highest methane producer. We believe this can be explained by difference in OM quality or microbial communities, such as more productive microbial communities in the chalk sediments. Similar median emission rates (by ebullitive transport) of 0.375 mg C-CH_4 m^{-2} hr^{-1} were found in an extensive global study (Stanley *et al.*, 2016) and Sanders *et al.* (2007) found similar mean emission rates from the water column in chalk streams of 0.168 mg C-CH_4 m^{-2} hr^{-1}. Although both our CH and SH sediments were collected from underneath macrophytes, only CH produced at rates like those observed in the field (Sanders *et al.*, 2007). The fine sediments trapped by the vegetated patches are associated with a higher diversity of methanogenic archaea in the hyporheic zone and streambed (Brablcová *et al.*, 2015). Average OM contents were higher in chalk sediments and sediments with higher OM content produced more CH_4 than sediments with lower OM contents. Streambed OM content has previously been shown to control CH_4 production, although this was only significant at OM contents in excess of 8% (Crawford & Stanley, 2016). This supports our observations that, although there is evidence that OM controls GHG production, the magnitude of production shows substantial differences across different substrates.

No N_2O production was observed in the duration of our experiment. This does not reflect on the occurrence of net-denitrification. Sediments can have a significant denitrification potential, but in case of complete denitrification, total N_2 production will be equal N_2O production (Hlaváčová *et al.*, 2005; Lansdown *et al.*, 2014). If any was produced, N_2O was most likely not the final product of denitrification in our experiments.

We found evidence that OM quality (measured by aromaticity) was a main driver of streambed sediment respiration that varied significantly between sediment types of the two different background geologies. When available substrates vary along a river, and thus with streambed sediment, local microbial communities are expected to adapt and specialise to that reach (Savio *et al.*, 2015; Freixa *et al.*, 2016). This can partially be explained by the fact that reactivity of OM usually decreases with molecule size as it gets further broken down (Amon & Benner, 1996). Fresher OM inputs drove higher respiration rates in our high OM sediments CH and SH. Additionally, the OM quality likely varied between the CH and SH collection site due to differences in macrophyte communities that are expected between sandstone and chalk rivers (Jusik *et al.*, 2015) and differences in macrophytes and vegetation have been demonstrated to result in differences in OM characteristics (Cooper *et al.*, 2015). We may therefore expect differences in streambed microbial communities between chalk and sandstone sediments, despite other physical river characteristics being similar.

There are many variables involved in sediment respiration. We controlled for temperature in this experiment at 15°C as an ideal temperature for these types of streams and hence isolate the impacts of OM and geological background. Further temperature effects are out of the scope of this study. The microcosms used in our experiment resembled lentic water due to the microcosm design and may have limited oxygen availability as opposed to lotic water that better describes *in situ* streambed situations. We could measure aerobic respiration

throughout the experiment; hence we do not expect this to have had any major negative impact on the experiment. Higher streambed CO_2 production may locally be countered by increased photosynthesis of macrophytes (Demars *et al.*, 2016), which we were not able to include in our study.

Rather than measuring directly C cycling and GHG production, previous studies considered total stream evasion (Butman & Raymond, 2011; Hotchkiss *et al.*, 2015; Worrall *et al.*, 2016), or indirectly calculated CO_2 approaches (Raymond *et al.*, 2013), which may be sensitive to overestimation or underestimation (Abril *et al.*, 2015). Furthermore, field measurements are challenged by the difficulty of isolating the governing processes and drivers.

1.5. Conclusions

This study provides new conceptual system level mechanistic understanding of the potential of streambed sediments in agricultural streams to produce substantial amounts of CO_2 and CH_4 across a gradient of OM contents. MMA and associated GHG production are associated with locations of higher OM content as an important driver which is conditioned by different geological backgrounds. These differences in OM between substrate are reflected in significant differences in OM quality (aromaticity) that can support different microbial communities that turnover OM and C at different rates. We provide evidence that mineralisation of OM can produce substantial CO_2 emissions from the streambed. When compared with excess CO_2 fluxes from streams, we find that streambed CO_2 production can represent 35% of total stream CO_2 evasion in the UK. Similar numbers for CO_2 evasion have been estimated before (Hotchkiss *et al.*, 2015), and we now provide new evidence that a large portion of the internal CO_2 production of agricultural streams can be attributed to the top of the streambed. Methane production varies even stronger between sediment from different

geologic backgrounds, suggesting a microbial community-driven variation between streambed sediments. Our findings lead us to the conclusion that both organic matter quantity and quality are important controls on streambed organic matter mineralisation, and improve our understanding of the potential impacts of human-induced land use change in lowland streams.

Acknowledgements

This project has received funding from the European Union's Seventh Framework Programme for research, technological development and demonstration under grant agreement no 607150, the Natural Environment Research Council (NERC) and the Central England NERC Training Alliance.

Author contributions

PR and SCW contributed equally to designing and conceptualising the study, performing the experiments, data collection and analysis. PR wrote the manuscript with support of SCW. SU provided guidance on application of the GHG analysis method, support with data analysis and manuscript revisions. DMH provided support with manuscript revisions. SK instigated the study and advised on the experimental design and the conceptualisation of the results, and supported the data analysis, interpretation, and manuscript revisions.

References

Abril G, Bouillon S, Darchambeau F et al. (2015) Technical Note: Large overestimation of pCO2 calculated from pH and alkalinity in acidic, organic-rich freshwaters. *Biogeosciences*, **12**, 67–78.

Allan JD (2004) Landscapes and riverscapes: the influence of land use on stream ecosystems.

Annual review of ecology, evolution, and systematics, **35**, 257–284.

Amon RMW, Benner R (1996) Bacterial utilization of different size classes of dissolved organic matter. *Limnology and Oceanography*, **41**, 41–51.

Argerich A, Haggerty R, Martí E, Sabater F, Zarnetske J (2011) Quantification of metabolically active transient storage (MATS) in two reaches with contrasting transient storage and ecosystem respiration. *Journal of Geophysical Research: Biogeosciences*, **116**.

Aufdenkampe AK, Mayorga E, Raymond PA et al. (2011) Riverine coupling of biogeochemical cycles between land, oceans, and atmosphere. *Frontiers in Ecology and the Environment*, **9**, 53–60.

Baranov V, Lewandowski J, Krause S (2016a) Bioturbation enhances the aerobic respiration of lake sediments in warming lakes. *Biology letters*, **12**, 269–281.

Baranov V, Lewandowski J, Romeijn P, Singer G, Krause S (2016b) Effects of bioirrigation of non-biting midges (Diptera: Chironomidae) on lake sediment respiration. *Scientific Reports*, **6**, 27329.

Bardini L, Boano F, Cardenas MB, Revelli R, Ridolfi L (2012) Nutrient cycling in bedform induced hyporheic zones. *Geochimica et Cosmochimica Acta*, **84**, 47–61.

Battin TJ, Kaplan LA, Findlay S et al. (2008) Biophysical controls on organic carbon fluxes in fluvial networks. *Nature Geoscience*, **1**, 95–100.

Battin TJ, Luyssaert S, Kaplan LA, Aufdenkampe AK, Richter A, Tranvik LJ (2009) The boundless carbon cycle. *Nature Geoscience*, **2**, 598–600.

Blann KL, Anderson JL, Sands GR, Vondracek B (2009) Effects of Agricultural Drainage on Aquatic Ecosystems: A Review. *Critical Reviews in Environmental Science and*

Technology, **39**, 909–1001.

Boulton A, Findlay S, Marmonier P (1998) The functional significance of the hyporheic zone in streams and rivers. *Annual Review of Ecology and Systematics*, **29**, 59–81.

Brablcová L, Buriánková I, Badurová P, Chaudhary PP, Rulík M (2015) Methanogenic archaea diversity in hyporheic sediments of a small lowland stream. *Anaerobe*, **32**, 24–31.

Butman D, Raymond PA (2011) Significant efflux of carbon dioxide from streams and rivers in the United States. *Nature Geoscience*, **4**, 839–842.

Cardenas MB, Ford AE, Kaufman MH, Kessler AJ, Cook PLM (2016) Hyporheic flow and dissolved oxygen distribution in fish nests: The effects of open channel velocity, permeability patterns, and groundwater upwelling. *Journal of Geophysical Research: Biogeosciences*, **121**, 3113–3130.

Cardinale BJ, Palmer MA, Swan CM, Brooks S, Poff NL (2002) The influence of substrate heterogeneity on biofilm metabolism in a stream ecosystem. *Ecology*, **83**, 412–422.

Catalán N, Marcé R, Kothawala DN, Tranvik LJ (2016) Organic carbon decomposition rates controlled by water retention time across inland waters. *Nature Geoscience*, **9**, 501–504.

Ciais P, Sabine C, Bala G et al. (2013) Carbon and other biogeochemical cycles. In: *Climate Change 2013: The Physical Science Basis. Contribution of Working Group I to the Fifth Assessment Report of the Intergovernmental Panel on Climate Change* (eds Stocker TF, Qin D, Plattner G-K, Tignor M, Allen SK, Boschung J, Nauels A, Xia Y, V. B, Midgley PM), pp. 465–570. Cambridge University Press, Cambridge, United Kingdom and New York, NY, USA.

Cole JJ, Prairie YT, Caraco NF et al. (2007) Plumbing the global carbon cycle: Integrating inland waters into the terrestrial carbon budget. *Ecosystems*, **10**, 171–184.

Cooper RJ, Pedentchouk N, Hiscock KM, Disdle P, Krueger T, Rawlins BG (2015) Apportioning sources of organic matter in streambed sediments: An integrated molecular and compound-specific stable isotope approach. *Science of The Total Environment*, **520**, 187–197.

Crawford JT, Stanley EH (2016) Controls on methane concentrations and fluxes in streams draining human-dominated landscapes. *Ecological Applications*, **26**, 1581–1591.

Crawford JT, Loken LC, Stanley EH, Stets EG, Dornblaser MM, Striegl RG (2016) Basin scale controls on CO2 and CH4 emissions from the Upper Mississippi River. *Geophysical Research Letters*, **43**, 2015GL067599.

Demars BOL, Gíslason GM, Ólafsson JS et al. (2016) Impact of warming on CO2 emissions from streams countered by aquatic photosynthesis. *Nature Geoscience*, **9**, 758–761.

Fierer N, Morse JL, Berthrong ST, Bernhardt ES, Jackson RB (2007) Environmental controls on the landscape-scale biogeography of stream bacterial communities. *Ecology*, **88**, 2162–2173.

Fischer H, Pusch M (2001) Comparison of bacterial production in sediments, epiphyton and the pelagic zone of a lowland river. *Freshwater Biology*, **46**, 1335–1348.

Freixa A, Ejarque E, Crognale S, Amalfitano S, Fazi S, Butturini A, Romaní AM (2016) Sediment microbial communities rely on different dissolved organic matter sources along a Mediterranean river continuum. *Limnology and Oceanography*, **61**, 1389–1405.

Freixa A, Acuña V, Casellas M, Pecheva S, Romaní AM (2017) Warmer night-time temperature promotes microbial heterotrophic activity and modifies stream sediment community. *Global Change Biology*, **23**, 3825–3837.

Fuß T, Behounek B, Ulseth AJ, Singer GA (2017) Land use controls stream ecosystem metabolism by shifting dissolved organic matter and nutrient regimes. *Freshwater*

Biology, **62**, 582–599.

Gomez-Velez JD, Krause S, Wilson JL (2014) Effect of low-permeability layers on spatial patterns of hyporheic exchange and groundwater upwelling. *Water Resources Research*, **50**, 5196–5215.

González-Pinzón R, Haggerty R, Myrold DD (2012) Measuring aerobic respiration in stream ecosystems using the resazurin-resorufin system. *Journal of Geophysical Research: Biogeosciences*, **117**, n/a-n/a.

González-Pinzón R, Ward AS, Hatch CE et al. (2015) A field comparison of multiple techniques to quantify groundwater – surface-water interactions. *Freshwater Science*, **34**, 139–160.

Haggerty R, Argerich A, Martí E (2008) Development of a "smart" tracer for the assessment of microbiological activity and sediment-water interaction in natural waters: The resazurin-resorufin system. *Water Resources Research*, **44**, W00D01.

Haggerty R, Ribot M, Singer GA, Martí E, Argerich A, Agell G, Battin TJ (2014) Ecosystem respiration increases with biofilm growth and bed forms: Flume measurements with resazurin. *Journal of Geophysical Research: Biogeosciences*, **119**, 2013JG002498.

Harvey GL, Gurnell AM, Clifford NJ (2008) Characterisation of river reaches: The influence of rock type. *Catena*, **76**, 78–88.

Hedin LO (1990) Factors Controlling Sediment Community Respiration in Woodland Stream Ecosystems. *Oikos*, **57**, 94.

Helton AM, Bernhardt ES, Fedders A (2014) Biogeochemical regime shifts in coastal landscapes: the contrasting effects of saltwater incursion and agricultural pollution on greenhouse gas emissions from a freshwater wetland. *Biogeochemistry*, **120**, 133–147.

Hlaváčová E, Rulík M, Čáp L (2005) Anaerobic microbial metabolism in hyporheic sediment of a gravel bar in a small lowland stream. *River Research and Applications*, **21**, 1003–1011.

Hoogsteen MJJ, Lantinga EA, Bakker EJ, Groot JCJ, Tittonell PA (2015) Estimating soil organic carbon through loss on ignition: effects of ignition conditions and structural water loss. *European Journal of Soil Science*, **66**, 320–328.

Hotchkiss ER, Hall Jr RO, Sponseller RA et al. (2015) Sources of and processes controlling CO2 emissions change with the size of streams and rivers. *Nature Geoscience*, **8**, 696–699.

Jones DL, Willett VB (2006) Experimental evaluation of methods to quantify dissolved organic nitrogen (DON) and dissolved organic carbon (DOC) in soil. *Soil Biology and Biochemistry*, **38**, 991–999.

Jusik S, Szoszkiewicz K, Kupiec JM, Lewin I, Samecka-Cymerman A (2015) Development of comprehensive river typology based on macrophytes in the mountain-lowland gradient of different Central European ecoregions. *Hydrobiologia*, **745**, 241–262.

Knapp JLA, González-Pinzón R, Drummond JD, Larsen LG, Cirpka OA, Harvey JW (2017) Tracer-based characterization of hyporheic exchange and benthic biolayers in streams. *Water Resources Research*, **53**, 1575–1594.

Kolbe T, Marçais J, Thomas Z et al. (2016) Coupling 3D groundwater modeling with CFC-based age dating to classify local groundwater circulation in an unconfined crystalline aquifer. *Journal of Hydrology*, **543**, 31–46.

Krause S, Hannah DM, Fleckenstein JH et al. (2011) Inter-disciplinary perspectives on processes in the hyporheic zone. *Ecohydrology*, **4**, 481–499.

Krause S, Boano F, Cuthbert MO, Fleckenstein JH, Lewandowski J (2014) Understanding

process dynamics at aquifer-surface water interfaces: An introduction to the special section on new modeling approaches and novel experimental technologies. *Water Resources Research*, **50**, 1847–1855.

Lansdown K, Heppell CM, Dossena M et al. (2014) Fine-scale in situ measurement of riverbed nitrate production and consumption in an armored permeable riverbed. *Environmental Science and Technology*, **48**, 4425–4434.

Lansdown K, McKew BA, Whitby C et al. (2016) Importance and controls of anaerobic ammonium oxidation influenced by riverbed geology. *Nature Geoscience*, **9**, 357–360.

Lauerwald R, Laruelle GG, Hartmann J, Ciais P, Regnier PAG (2015) Spatial patterns in CO2 evasion from the global river network. *Global Biogeochemical Cycles*, **29**, 534–554.

Lemke D, Liao Z, Wöhling T, Osenbrück K, Cirpka O a. (2013a) Concurrent conservative and reactive tracer tests in a stream undergoing hyporheic exchange. *Water Resources Research*, **49**, 3024–3037.

Lemke D, Schnegg P-A, Schwientek M, Osenbrück K, Cirpka O a. (2013b) On-line fluorometry of multiple reactive and conservative tracers in streams. *Environmental Earth Sciences*, **69**, 349–358.

Longworth BE, Petsch ST, Raymond PA, Bauer JE (2007) Linking lithology and land use to sources of dissolved and particulate organic matter in headwaters of a temperate, passive-margin river system. *Geochimica et Cosmochimica Acta*, **71**, 4233–4250.

Marcé R, Obrador B, Josep-Anton Morguí, López JLRP, Joan A (2015) Carbonate weathering as a driver of CO2 supersaturation in lakes. *Nature Geoscience*, **8**, 1–5.

Marín-Spiotta E, Gruley KE, Crawford J et al. (2014) Paradigm shifts in soil organic matter research affect interpretations of aquatic carbon cycling: transcending disciplinary and

ecosystem boundaries. *Biogeochemistry*, **117**, 279–297.

Marschner B, Kalbitz K (2003) Controls of bioavailability and biodegradability of dissolved organic matter in soils. *Geoderma*, **113**, 211–235.

McCorkle EP, Berhe AA, Hunsaker CT, Johnson DW, McFarlane KJ, Fogel ML, Hart SC (2016) Tracing the source of soil organic matter eroded from temperate forest catchments using carbon and nitrogen isotopes. *Chemical Geology*.

McDonald CP, Stets EG, Striegl RG, Butman D (2013) Inorganic carbon loading as a primary driver of dissolved carbon dioxide concentrations in the lakes and reservoirs of the contiguous United States. *Global Biogeochemical Cycles*, **27**, 285–295.

Mendoza-Lera C, Datry T (2017) Relating hydraulic conductivity and hyporheic zone biogeochemical processing to conserve and restore river ecosystem services. *Science of The Total Environment*, **579**, 1815–1821.

Mosher JJ, Findlay RH (2011) Direct and Indirect Influence of Parental Bedrock on Streambed Microbial Community Structure in Forested Streams. *Applied and Environmental Microbiology*, **77**, 7681–7688.

Mosher JJ, Klein GC, Marshall AG, Findlay RH (2010) Influence of bedrock geology on dissolved organic matter quality in stream water. *Organic Geochemistry*, **41**, 1177–1188.

NRFA (2015) NRFA Daily Flow Data. *Natural Environment Research Council - Centre for Ecology & Hydrology*.

Rathburn SL, Bennett GL, Wohl EE, Briles C, McElroy B, Sutfin N (2017) The fate of sediment, wood, and organic carbon eroded during an extreme flood, Colorado Front Range, USA. *Geology*, G38935.1.

Raymond PA, Hartmann J, Lauerwald R et al. (2013) Global carbon dioxide emissions from inland waters. *Nature*, **503**, 355–359.

Rowland R, Inamdar S, Parr T (2017) Evolution of particulate organic matter (POM) along a headwater drainage: role of sources, particle size class, and storm magnitude. *Biogeochemistry*, **133**, 181–200.

Sanders I a., Heppell CM, Cotton J a., Wharton G, Hildrew a. G, Flowers EJ, Trimmer M (2007) Emission of methane from chalk streams has potential implications for agricultural practices. *Freshwater Biology*, **52**, 1176–1186.

Savio D, Sinclair L, Ijaz UZ et al. (2015) Bacterial diversity along a 2600 km river continuum. *Environmental Microbiology*, **17**, 4994–5007.

Schade JD, Bailio J, McDowell WH (2016) Greenhouse gas flux from headwater streams in New Hampshire, USA: Patterns and drivers. *Limnology and Oceanography*, **61**, S165–S174.

Schindler JE, Krabbenhoft DP (1998) The hyporheic zone as a source of dissolved organic carbon and carbon gases to a temperate forested stream. *Biogeochemistry*, **43**, 157–174.

Stanley EH, Casson NJ, Christel ST, Crawford JT, Loken LC, Oliver SK (2016) The ecology of methane in streams and rivers: patterns, controls, and global significance. *Ecological Monographs*, **86**, 146–171.

Stuart ME, Lapworth DJ (2016) Macronutrient status of UK groundwater: Nitrogen, phosphorus and organic carbon. *Science of the Total Environment*, **572**, 1543–1560.

Tank JJL, Rosi-Marshall EJE, Griffiths NA, Entrekin SA, Stephen ML (2010) A review of allochthonous organic matter dynamics and metabolism in streams. *Journal of the North American Benthological Society*, **29**, 118–146.

Tortosa G, Correa D, Sánchez-Raya AJ, Delgado A, Sánchez-Monedero MA, Bedmar EJ (2011) Effects of nitrate contamination and seasonal variation on the denitrification and greenhouse gas production in La Rocina Stream (Do??ana National Park, SW Spain). *Ecological Engineering*, **37**, 539–548.

Trauth N, Schmidt C, Vieweg M, Maier U, Fleckenstein JH (2014) Hyporheic transport and biogeochemical reactions in pool-riffle systems under varying ambient groundwater flow conditions. *Journal of Geophysical Research: Biogeosciences*, **119**, 910–928.

Trimmer M, Grey J, Heppell CM, Hildrew AG, Lansdown K, Stahl H, Yvon-Durocher G (2012) River bed carbon and nitrogen cycling: State of play and some new directions. *Science of The Total Environment*, **434**, 143–158.

Turner PA, Griffis TJ, Lee X, Baker JM, Venterea RT, Wood JD (2015) Indirect nitrous oxide emissions from streams within the US Corn Belt scale with stream order. *Proceedings of the National Academy of Sciences*, **112**, 201503598.

Ullah S, Zhang H, Heathwaite AL, Heppell C, Lansdown K, Binley A, Trimmer M (2014) Influence of emergent vegetation on nitrate cycling in sediments of a groundwater-fed river. *Biogeochemistry*, **118**, 121–134.

Wang X, Cammeraat ELH, Romeijn P, Kalbitz K (2014) Soil Organic Carbon Redistribution by Water Erosion – The Role of CO2 Emissions for the Carbon Budget (ed Bond-Lamberty B). *PLoS ONE*, **9**, e96299.

Weishaar JL, Aiken GR, Bergamaschi BA, Fram MS, Fujii R, Mopper K (2003) Evaluation of specific ultraviolet absorbance as an indicator of the chemical composition and reactivity of dissolved organic carbon. *Environmental Science and Technology*, **37**, 4702–4708.

Wheater HS, Peach D (2004) Developing interdisciplinary science for integrated catchment

management: the UK lowland catchment research (LOCAR) programme. *International Journal of Water Resources Development*, **20**, 369–385.

Worrall F, Lancaster A (2005) The Release of CO2 from Riverwaters – the Contribution of Excess CO2 from Groundwater. *Biogeochemistry*, **76**, 299–317.

Worrall F, Burt TP, Howden NJK (2016) The fluvial flux of particulate organic matter from the UK: The emission factor of soil erosion. *Earth Surface Processes and Landforms*, **41**, 61–71.

Yvon-Durocher G, Hulatt CJ, Woodward G, Trimmer M (2017) Long-term warming amplifies shifts in the carbon cycle of experimental ponds. *Nature Climate Change*, **7**, 209–213.

Zhang X, Gu Q, Long X-E et al. (2016) Anthropogenic activities drive the microbial community and its function in urban river sediment. *Journal of Soils and Sediments*, **16**, 716–725.

Chapter 2. Streambed heterogeneity drives microbial metabolic activity through residence time

Paul Romeijn, Rebwar Dara, David M. Hannah, Stefan Krause

Abstract

The streambed and the hyporheic zone are often characterised by sharp gradients in hydraulic conductivity. These sharp gradients have implications for organic carbon, dissolved oxygen and nitrate turnover in the shallow hyporheic zone. Low-conductivity sediment structures in the streambed can inhibit groundwater upwelling and cause local surface water downwelling, including horizontal pore water flow. These often very local differences cause variability in residence time and provide a place for small-scale differences in microbial activity and associated biogeochemical turnover. We used a novel small scale "push-pull" tracer application, using the resazurin-resorufin tracer system to measure microbial metabolic turnover. The tracer was injected at discrete depths in a UK lowland river strongly impacted by surrounding agriculture that was previously surveyed using ground penetrating radar. This approach provided us with a combined measurement of dilution and a relative comparison for microbial metabolic activity between studied locations. We found hydraulic conductivity and residence time related differences in dissolved oxygen and microbial metabolic activity. Our results suggest microbial metabolic activity is driven by a combination of dissolved oxygen and residence time. In heterogeneous streambed environments, biogeochemical hotspots may be related to deeper lying sediment structures that are not always accounted for. Using this new knowledge, predictions of spatial patterns of nutrient turnover, microbial metabolic activity and potential associated greenhouse gas production in the hyporheic zone can be improved.

2.1. Introduction

Rivers and streams take up approximately 0.47% of the Earth's surface (Raymond *et al.*, 2013). These flowing waters are much more than passive pipes, but instead form a complex interaction of upwelling and downwelling water (Boulton *et al.*, 1998). Downwelling water provides dissolved oxygen to the hyporheic zone (HZ) and where water wells up, the stream is provided with nutrients. Many lowland streams and rivers are located in areas of concentrated agriculture, as lowland river plains are ideal locations for crops and pastures. Nitrate loading into stream water is a problem worldwide (Meybeck & Helmer, 1989; Scanlon *et al.*, 2007; He *et al.*, 2011) and denitrification of excess nitrate is not straightforward across spatial scales (Saunders & Kalff, 2001; Piña-Ochoa & Álvarez-Cobelas, 2006; Stelzer *et al.*, 2011; Zarnetske *et al.*, 2011a; Briggs *et al.*, 2015).

2.1.1. Spatial heterogeneity of streambed nutrient cycling

Spatial groundwater upwelling patterns have been visualised with increasing detail at the streambed level using temperature as a tracer (Conant, 2004; Keery *et al.*, 2007; Krause *et al.*, 2013; Briggs *et al.*, 2014; Abbott *et al.*, 2016). However, upwelling patterns at the streambed surface do not necessarily reflect flow patterns deeper into the hyporheic zone. It is a complex interaction of mixing and no streambed is perfectly heterogeneous, resulting in complex flow patterns. During river evolution streambed is formed of layer after layer. These successive strata may lead to less permeable layers. Hyporheic exchange flow (HEF) depends on a combination of bedforms, hydrodynamic forcing of the stream water and vertical hydraulic gradients (Kasahara & Wondzell, 2003; Keery *et al.*, 2007; Hester & Doyle, 2008; Boano *et al.*, 2014).

Heterogeneities inside the streambed can be abrupt or smooth discontinuities in hydraulic conductivity *K*. In streambeds with high and abrupt heterogeneity, rates of hyporheic water

exchange are expected to increase compared to homogeneous streambeds, which is mostly attributed to preferred flow through connected flow paths, and hence decreased average residence times (Pryshlak *et al.*, 2015). Hydraulic regimes in streams can be upwelling, downwelling, neutral, or more likely a complex combination of those. Upwelling is related to the distribution of hydraulic conductivity and higher vertical hydraulic gradients can be found in zones with higher K (Chen, 2011; Song *et al.*, 2016) and in the middle of the channel (Genereux *et al.*, 2008; Song *et al.*, 2016). However, not only does conductivity change over reach-scale lengths, it can change orders of magnitude over distances as small as 10 cm, suggesting that hyporheic exchange patterns are hyperlocal (Salehin *et al.*, 2004; Wu *et al.*, 2016).

Sediment hydraulic conductivity often shows strong vertical patterns (Ryan & Boufadel, 2007; Chen, 2011; Angermann *et al.*, 2012; Tang *et al.*, 2015), suggesting that including vertical profiles of processes would reveal more information than just the streambed surface alone. Upwelling groundwater also shows strong spatial variability (Hyun *et al.*, 2011; Krause *et al.*, 2012; Binley *et al.*, 2013; Wang *et al.*, 2017). Previous studies have found streambed temperature patterns using distributed temperature sensing that were related to streambed heterogeneity. These patterns identified differences in groundwater upwelling in the streambed (Krause *et al.*, 2012). Residence time generally decreases in heterogeneous streambeds due to faster flow through preferred flow paths (Fox *et al.*, 2016), while heterogeneity may have different effects between different streambeds (Sawyer & Cardenas, 2009). Small-scale flow paths in the streambed may also be related to the presence of low conductivity structures in the streambed and may affect hyporheic exchange patterns (Angermann *et al.*, 2012). Taking this into account, it raises the question to what extent microbial metabolic activity (MMA) and associated nutrient turnover are controlled by streambed heterogeneity.

2.1.2. Carbon and nutrient cycling in hyporheic zones

Groundwater is a major source of N in lowland rivers (Rivett *et al.*, 2008a; Mulholland & Webster, 2010). Recent work has focused largely on spatial variations in the streambed morphology and how they influence groundwater upwelling (and downwelling) patterns (Salehin *et al.*, 2004; Krause *et al.*, 2013; Gomez-Velez *et al.*, 2014, 2015; Pryshlak *et al.*, 2015; Tonina *et al.*, 2016; Wang *et al.*, 2017). In such a heterogeneous streambed environment, water is forced through flow paths other than the governing Darcy flux or the vertical gradient. Heterogeneity may cause a change in residence time and hence control nitrate production or removal (Zarnetske *et al.*, 2011a). Governing DO concentrations and residence time control biogeochemical transformations through exposure time (Gomez *et al.*, 2012; Zarnetske *et al.*, 2012) and define nutrient spiralling (Ensign & Doyle, 2006).

Peat and clay lenses in the streambed are examples of relatively small confined units that have high OM content when compared to the surrounding material, and thus high and abrupt differences. High OM units can therefore act as local sources of mobilised OM or DOM and act as biogeochemical hotspots (Krause *et al.*, 2013). At smaller scales, we can even find complex micro-zones in heterogeneous sediments that favour opposite conditions compared to the environment, such as nitrification and denitrification (Briggs *et al.*, 2015). Nitrate concentrations (both in the case of nitrification and denitrification) can be affected by residence times (Zarnetske *et al.*, 2011a). If there is a vertical flux, we can assume a nonlinear relation between the nitrate concentrations and the time it resides there, although this mainly applies to shorter residence times (Zarnetske *et al.*, 2011a; Briggs *et al.*, 2014, 2015). However, in many streams and rivers, we may find residence times that are much greater than a few hours, as much as several weeks (Sawyer & Cardenas, 2009). Hence, although residence time alone appears to dominate reactivity, other drivers are likely to be key players

in systems with great nitrate loading and where residence times exceed 24 hours (Zarnetske *et al.*, 2011a).

While there is evidence that low conductivity structures in the streambed play an important role in biogeochemical turnover (Krause *et al.*, 2013; Battin *et al.*, 2016), information about differences in microbial metabolic activity (MMA) across the hyporheic zone at different residence times is lacking. More information is needed on the drivers of MMA and nutrient turnover in the hyporheic zone to understand and predict these processes in lowland river environments. Where previous studies focused on the top part of the hyporheic zone (Nogaro *et al.*, 2010; Singer *et al.*, 2010; Mendoza-Lera & Mutz, 2013) or just at a fixed depth (Claret & Boulton, 2009), it is often overlooked that deeper zones of the HZ can contribute substantially to nutrient turnover (Stelzer *et al.*, 2011).

This study aims to provide insight into the drivers and controls of nutrient concentrations and MMA in a heterogeneous streambed environment with focus on spatial variations rather than temporal variation. We address this by analysing significant controls of microbial metabolic activity and nutrient turnover around low conductivity structures and how this can lead to hotspot activity. For the first time ever, we use push-pull injections into the streambed to quantify these processes.

2.2. Methods

2.2.1. Experimental field site

A section was selected of approximately 100 m of the River Tern in Shropshire, UK (Figure 2-1; 52°51'20.4"N 2°32'45.1"W). The reach has a sandy to gravelly streambed surface with a riffle and pool section halfway (Krause *et al.*, 2013). The land use around the study area is heavily impacted by agriculture and farming. The river is incised deeply in the study reach

with banks up to 2 meters above water level. Mean and median daily discharge measured at Tern Hill station from 2013 to 2015 were 0.885 and 0.762 m^3/s, respectively, which is approximately 3.3 km upstream of the studied reach (NRFA, 2016). Experiments were performed on three different moments in May and September 2015 and May 2016, which are referred to as experiments 1, 2, and 3, respectively. Mean daily flow on the experiment days were 0.651, 0.489 and 0.744 m^3/s for experiments 1, 2 and 3, respectively, measured at Tern Hill station.

2.2.2. Streambed physical properties

Locations for installing the mini-piezometers (MP) for the experiments outlined in the following sections were selected based on the structure of the subsurface of the streambed. This structure was recorded in a parallel study using ground penetrating radar (GPR) which was calibrated by sediment core samples to verify subsurface sediment type (personal communication, Rebwar Dara, March 2015). The GPR system used was a PulseEKKO PRO radar system ground penetrating radar device equipped with lightweight bistatic shielded square transducers antennas with a 250 MHz centre frequency. that was mounted on a raft (Sensors and Software Inc., Canada). The raft was used to image the streambed over the length of the studied reach of the River Tern (Figure 2-1). The GPR study provided a non-invasive method to identify sediment structures, such as peat and clay lenses and other sediment heterogeneities, and select the MP locations accordingly, without creating unnecessary holes in the streambed near study sites. Based on the available subsurface information, three types of general sediment structures were differentiated. The mini-piezometers (Figure 2-2) were clustered into these three types, to which we will refer to as cluster one, two and three, as indicated in Figure 2-3. Cluster one is characterised by sandy

clay, cluster two has generally sandy sediments and cluster three is dominated by large peat structures.

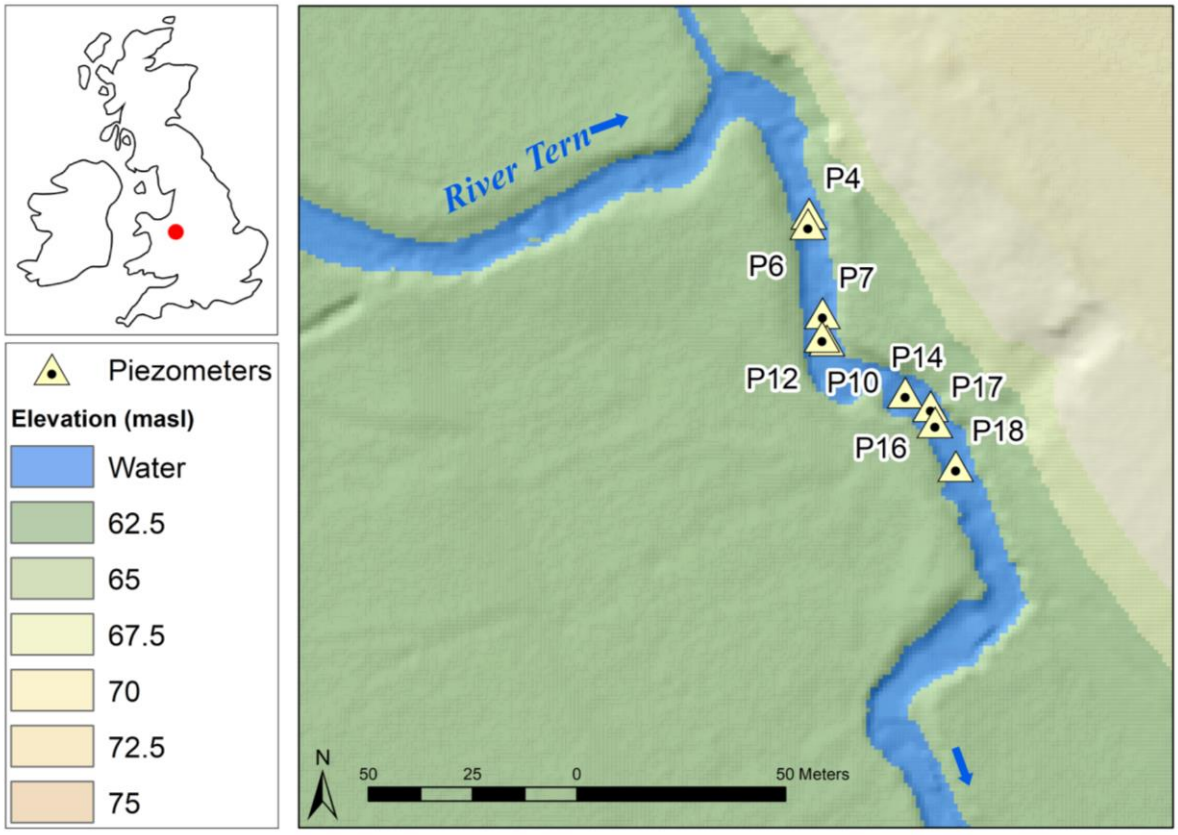

Figure 2-1. River Tern field site location, with locations of piezometers used marked along the profile.

Horizontal hydraulic conductivity K_h was calculated by falling head tests and calculated according to the method of Hvorslev (1951) and Bouwer and Rice (1976), and corrected following the findings of Chapuis (1989). Tests were performed by installing a standard type 40 mm inner diameter (ID) PVC waste pipe with slotted sections to the depths of the piezometers near each of the MP's sampling depth. Usually one test was performed per depth inside each of the clusters (see section 2.2.3 and Figure 2-3). The piezometers used to measure K_h were installed between 10 and 30 cm from the MPs to reflect as accurately as possible the sediment structure of the injection points without causing disturbance to the flow

field of the MPs. Vertical hydraulic gradients (VHG) were measured during each experiment using a Solinst 102 water level indicator with a 4 mm tip (Solinst, Georgetown, ON, Canada) through the centre tube of the MPs (Figure 2-2). VHG were calculated as $\Delta h/\Delta l$, where Δh is the inside and outside difference in piezometer water level and Δl is the distance from the centre of the screened section to streambed surface level (Krause *et al.*, 2013).

2.2.3. Pore-water extraction and tracer injections

Water sampling and push-pull injections were performed using MPs (Figure 2-2) similar to those used by Krause *et al.* (2013) and Rivett *et al.* (2008b). The MPs were built specifically per site (Table B-1), according to results from the GPR surveys of the streambed, with the mini-points attached to depths with structures of interest. The MPs were grouped in clusters 1, 2 and 3 (see also Figure 2-3), in order to cover three specific types of streambed subsurface structures with apparent similar features and hence increase potential sampling size. Although the streambed and hyporheic zone in the study area are heterogeneous, the zones of injection were assumed to be homogeneous and isotropic and to represent a small sub-area of the hyporheic zone.

The MPs consisted of a central 10/13 mm (ID/OD) high-density polyethylene tube (Deutsch & Neumann, Berlin, Germany), to which several 1.6/3.2 mm (ID/OD) PTFE tubes (Tygon® E-3603, Saint-Gobain Performance Plastics, Charny, France) were attached to act as mini-points (Figure 2-2). The central tube had a screened section at the bottom, which was 110 cm below streambed surface, drilled with 24 holes with a 3 mm diameter, covered with a mesh. The tips of the mini-points were covered with a 100 μm nylon mesh to keep most sediments out, while maintaining a good flow. The MPs were then installed into the streambed using a steel guide tube that was retracted after hammering, leaving behind the piezometer in place.

Missing MP numbers (Figure 2-1) were built and installed (Table B-1), but were not functioning when installed in the field.

Residence time (RT) calculation was based on the dilution time of chloride from the MP injections and is defined as the time in hours for the electrical conductivity (EC) to fall back to 0.1% of EC raised by injection, as this was the level at which the EC meter did not display any decimals. RT was then calculated by fitting a linear model through all measured points over time and taking the time *t* where the linear regression intersects y=0.001.

2.2.4. Tracer injection

The tracer injection method was based on the point dilution method (Drost *et al.*, 1968; Lamontagne *et al.*, 2002; Kobr *et al.*, 2005; Piccinini *et al.*, 2016) and adapted to our MP specifications (Figure 2-2). The advantage of this method is a minimal distortion to the flow field under investigation (Drost *et al.*, 1968; Freeze & Cherry, 1979), due to the limited internal diameter size of 1.6 mm of the MP sampling points.

The reactive tracer resazurin (Apollo Scientific, Stockport, UK) was injected at several MPs at various depths as described in Table B-1, where each location was a unique injection and sampling location. Sodium chloride was co-injected with raz to correct for advective losses during the incubation period and calculate RT. A 1500 ng/l raz stock solution was prepared with tap water less than 24 hours before start of the experiment. Chloride was added to approximately double the background conductivity of the pore water.

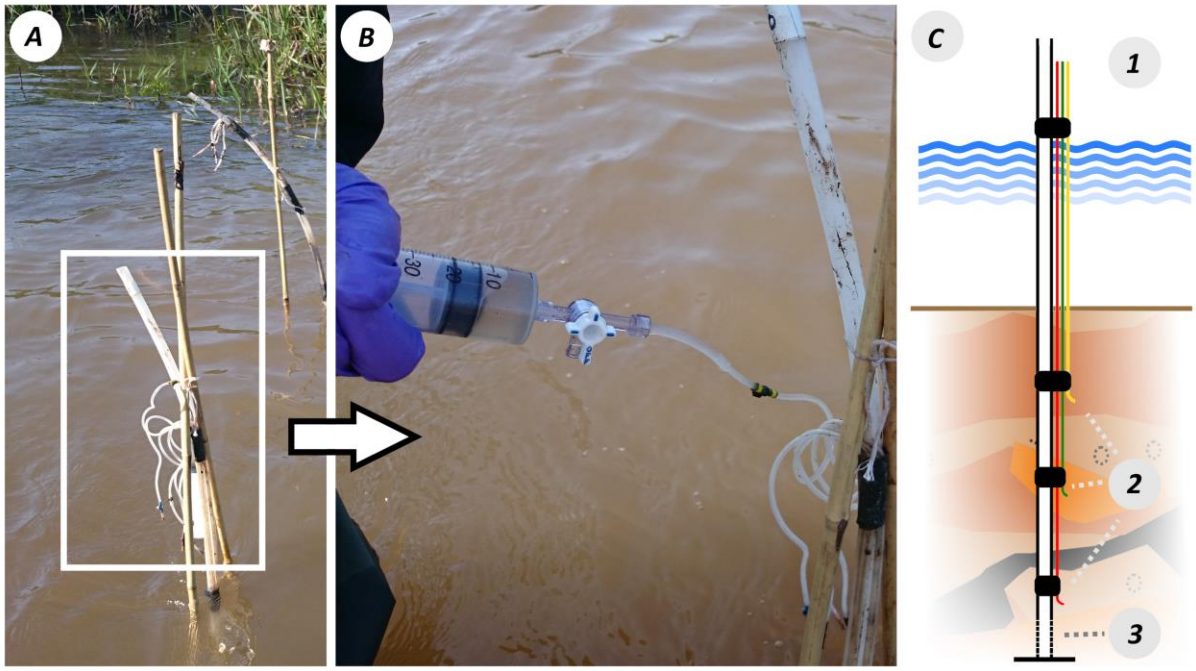

Figure 2-2. Description of piezometers used in experiments. Mini-piezometers were installed in the channel section and held up by bamboo canes during experiment days (**A**). Samples were taken from each depth using a 60-ml syringe that was connected to the tubing via a three-way stopcock (**B**). The tubing on the side of the centre tube leads from above the water surface (**C1**) to different depths along the vertical profile (**C2**). The centre tube has a screened section between 105 and 115 cm depth (**C3**) which is used to measure vertical hydraulic gradient.

The push-pull injection for each MP depth was performed by connecting a three-way stopcock to the MP tubing, extracting twice a 45-ml pore water sample using a 60-ml syringe and keep sample in syringe. A 10-ml syringe loaded with 10 ml of tracer stock solution was connected to the third stopcock inlet and slowly injected simultaneously with each of the syringe, 5 ml of stock solution at a time, sparing 3 ml of pore water from the last syringe to wash all tracer down the tubing. The injectate then had a raz concentration of 150 ng/l. For each time step, starting at t=0 directly following injection, 3 ml was extracted from the MP and discarded to rinse MP tubing. A new 15 ml sample was then taken from the MP point, which is the minimal amount required for the fluorometer. The sample was measured for DO and temperature using a light-shielded, modified 60 ml syringe on a YSI Pro-ODO handheld DO meter (YSI-Xylem, Rye Brook, USA). It was then injected and filtered over a 0.45 µm

syringe filter into the fluorometer chamber (Albillia GGUN-FL30 field fluorometer) and measured for at least 3 minutes. The first sample extraction measurement after injecting was taken as t=0. After measuring the sample was discarded and the fluorometer rinsed. The next sample extraction was performed one hour after tracer injection, and the aforementioned steps of analysis were repeated. Based on the apparent speed of dilution at t=1, for each MP it was decided to extract the next sample at either t=2 or t=3. The last sample extraction was decided when background conductivity was back to normal, which ranged between t=8 and t=24, depending on the MP location.

The average internal volume of the MP tubing is 2.01 ml per meter of mini-point tubing. Because injection volume (100 ml) greatly exceeds the internal volume by approximately 25 times, we neglect any vertical water flow within the observation well (i.e. mini-point tubing). This means that the apparent dilution velocity, v_a, is equal to ratio of v_a to α, the filtration velocity in the layer (Drost *et al.*, 1968; Kobr *et al.*, 2005; Piccinini *et al.*, 2016). The tracer was not allowed to drift. Due to the design of the mini-piezometer, the influence of the well was expected to be negligible on the velocity field around the outlet (Leap & Kaplan, 1988; Hall *et al.*, 1991). Standard estimated effective porosity values were based on McWhorter and Sunada (1977).

2.2.5. Microbial metabolic activity

Resazurin (raz) was used as a tracer for microbial metabolic activity (MMA). Raz reduces irreversibly to resorufin (rru) in the presence of aerobic microbial metabolism rather than anaerobic metabolism (Gumprecht *et al.*, 1995; Haggerty *et al.*, 2008). Both raz and rru can be detected fluorometrically and simultaneously (Lemke *et al.*, 2013a). It has recently been introduced as a “smart” tracer for MMA in aquatic environments (Haggerty *et al.*, 2008). Since, it has been successfully been applied across different scales, from microcosms to

reaches of more than one kilometre (Haggerty *et al.*, 2009, 2014; Argerich *et al.*, 2011; González-Pinzón *et al.*, 2012, 2015; Lemke *et al.*, 2013b; Baranov *et al.*, 2016; Knapp *et al.*, 2017).

After raz was injected and extracted, the concentration of both raz and rru were measured on the fluorometer and the ratio of the two were calculated as:

$$ratio = \ln(\frac{rru}{raz} + 1) \qquad \text{Equation 2-1}$$

The ratio of Equation 2-1 was measured at several timesteps and a linear regression was fitted through each of the timestep points to express the growth of the daughter compound rru relative to the parent compound raz. The slope of the line yields microbial metabolic activity expressed as hourly raz turnover and serves as a measure to compare between different sites.

Due to sporadic measurement errors on the fluorometers, it was not possible to calculate MMA for all the injection locations. The most likely sources of the errors were air bubbles inside the measurement chamber, resulting in scattering of light and incorrect excitation measurements. Fluorescence results from nine piezometer injections were discarded out of a total of 30. However, chloride dilutions and porewater chemistry were retained as these were unaffected by these errors. Sorption differences between raz and rru were assumed to be of negligible influence. MMA varied up to one order of magnitude between long and short RT; it seems unlikely that this large difference is caused by a difference in sorption alone (Lemke *et al.*, 2014).

2.2.6. Analysis of porewater chemistry

Before commencing each experiment, porewater was sampled from the MPs for analysis of nitrate, dissolved organic carbon (DOC) and for experiment 2 and 3 also NH_3+NH_4^+, referred to as NH_x, as new equipment became available. Filters were extracted by attaching a stopcock to the MO tubing, discarding the first 5 ml. A 50 ml sample was divided between 7 ml for nutrients and 25 ml for DOC analysis, with a few ml to spare for pre-rinsing the containers. The samples were filtered immediately using a 0.45 µm nylon syringe filter (Thames Restek, UK), which was pre-soaked in deionised water to prevent DOC leaching. Nitrate and NH_x samples were stored in 15 ml centrifuge tubes (Greiner Bio One, Frickenhausen, Germany). DOC samples were stored in acid washed 50 ml centrifuge tubes (Greiner Bio One, Frickenhausen, Germany). All samples were frozen and stored until analysis due to equipment limitations. Although freezing was expected to alter nutrient concentrations, nutrient concentration alterations are expected to be less than natural variations at time of sampling (Avanzino & Kennedy, 1993). Frozen storage time was similar for all samples (between 4 and 8 weeks). DOC concentrations were assumed unaffected by freezing, which can change due to freezing through precipitation of less labile fractions of DOC (Fellman *et al.*, 2008). On visual inspection no precipitation was observed prior to analysis.

During sampling, DO measured in a flow-through cell using Pro-ODO handheld DO meter (YSI-Xylem, Rye Brook, USA). Background EC was measured by a Hanna HI-98129 EC/pH meter (Hanna Instruments, Woonsocket, USA). Instruments were calibrated before the start of the experiments. DOC was measured as non-purgeable organic carbon using a Shimadzu TOC-V analyser. Nitrate samples from the first experiment were measured on a Dionex IC-2100 analyser (Dionex, Sunnyville, USA). Samples from the other experiments, including

NH_x samples, were measured on a Skalar San^{++} flow analyser (Skalar Analytical BV, Breda, NL).

2.2.7. Data analysis

Results of physical characteristics, chemistry, and MMA between clusters were compared by means of T-test or Mann-Whitney U test, depending on the outcome of a Shapiro-Wilkes test for normality. Trends were compared by simple linear regression or nonlinear least squares regression to fit either linear, exponential (log) or power-law regression (log-log) models. Model fits are reported using residual standard error.

2.3. Results

2.3.1. Streambed fluxes and residence times

Horizontal hydraulic conductivity K_h varied with depth (Figure 2-3a), as expected from residence time. When comparing K_h across the reach, there was a potential for longer residence times due to lower permeability in cluster 3 (near piezometers 14 to 18). The area that was designated as containing a high fraction of peat (black colour in Figure 2-3), had several magnitudes smaller values for K_h compared to the rest of the reach. At greater depths, underneath the peaty area, the hydraulic conductivity appeared to be higher, such as MP 14-100 (piezometer 14 at 100 cm depth). Cluster 2, around MP 10 to 12, was dominated by a more sandy sediment, which was reflected by higher K_h values. Mean hydraulic conductivities were 5.2±2.8, 5.8±3.1 and 2.0±2.8 m d^{-1} for clusters 1, 2 and 3, respectively.

Bulk residence time was calculated from chloride dilutions (Figure 2-3b) and will be referred to as just residence time (RT) for both singular and plural. There was a pronounced difference between RT in cluster 3 where there a dominant area of lower hydraulic conductivity was present. In the middle section of cluster 2, near piezometers 7 to 12, more sandy sediments

were found and RT were shorter. RT in cluster 3 were significantly longer than in cluster 2, with mean RT of 7.72±4.52 and 20.78±17.53 hours for clusters 2 and 3, respectively. Mean RT in cluster 1 was similar to cluster 2 with 8.59±2.67 hours. Shortest RT were in the area with most sandy sediments (cluster 2). Longest RT were found in the area with most peaty and clay areas (cluster 3).

Vertical hydraulic gradients (VHG) were positive during all experiments at all piezometers, indicating a net upwelling regime throughout the entire reach (see also Figure B-1). Mean VHG were 0.33±0.09, 0.29±0.10 and 0.28±0.17 m m^{-1} for clusters 1, 2 and 3 respectively, and 0.29±0.13 m m^{-1} for the entire reach.

2.3.2. Streambed biogeochemical and metabolic conditions

Dissolved oxygen (DO) per piezometer was measured throughout the injection phase. Mean DO concentrations are displayed in Figure 2-3c, which are based on the average of measurements at several time steps. The highest DO concentrations of 4.44±2.17 mg/l were generally found in cluster 2 at the midsection of the reach. Mean DO was lowest in the peaty area of cluster 3, with concentrations of 2.35±0.74 mg/l. Mean DO concentrations in cluster 1 were 3.13±1.42 mg/l. DO concentrations in cluster 3 were significantly lower compared to cluster 2 ($t(10,17) = 3.7069$, $p = 0.00176$, $n = 16$). For comparison, mean DO in the stream water was 9.49±0.35 mg/l.

Microbial metabolic activity (MMA) varied along the reach and with depth as well (Figure 2-3d). Mean MMA was almost twice as high in cluster 1 and 2 (0.155±0.100 hr^{-1} and 0.150±0.064 hr^{-1}) when compared to the most downstream cluster 3 (0.078±0.060 $hr^{-1)}$.

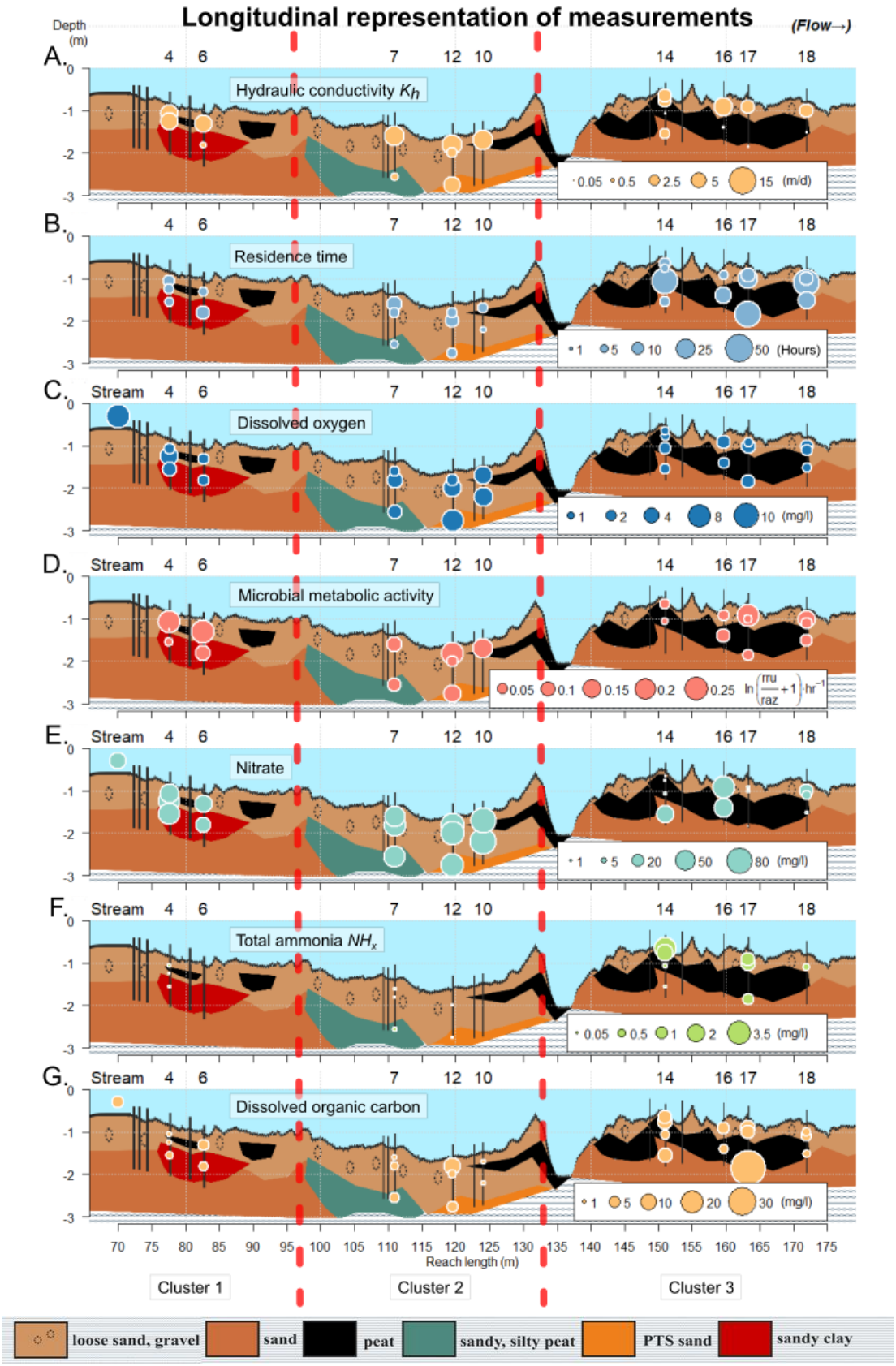

Figure 2-3. Physical and chemical properties of streambed sediments plotted along a longitudinal depth profile for each piezometer. The background is the streambed sediment structure, according to the GPR results.

Mean nitrate concentrations in the three main clusters (Figure 2-3e) were 46.29±11.75, 66.48±11.70, and 14.23±22.10 mg/l in clusters 1, 2, and 3, respectively. The mean concentration in cluster 3 was significantly lower than both cluster 1 and 2 ([Mann–Whitney $U = 48$, $n_1 = 5$, $n_2 = 11$, $P = 0.019$ two-tailed] and [Mann–Whitney $U = 63$, $n_1 = 6$, $n_2 = 11$, $P = 0.001$ two-tailed], respectively). Vertical patterns in nitrate were observed that varied with location. In some cases (e.g. MP 14) concentrations decreased from the lower end towards the streambed, or increased (e.g. MP 18). In other locations, the concentrations remained more or less constant (e.g. MP 4 to 12).

Total ammonia+ammonium (NH_3+NH_4^+) is reported as NH_x (Figure 2-3f). Due to equipment limitations, these concentrations were measured in the last two out of three experiments. Mean NH_x concentrations in the three clusters were 0.097±0.031, 0.084±0.057, and 1.011±0.983 mg/l in clusters 1, 2, and 3, respectively. The mean concentration in the downstream cluster 3 was significantly higher than in clusters 1 and 2 ([Mann–Whitney $U = 24$, $n_1 = 8$, $n_2 = 3$, $P = 0.012$ two-tailed] and [Mann–Whitney $U = 39$, $n_1 = 8$, $n_2 = 5$, $P = 0.003$ two-tailed], respectively), with local concentrations as high as 3.21 mg/l.

Mean DOC concentrations were 2.90±1.54, 4.22±3.64, and 9.81±12.92 mg/l in clusters 1, 2, and 3, respectively (Figure 2-3g). The mean concentration in the downstream cluster 3 was significantly higher than cluster 1, but not cluster 2 ([Mann–Whitney $U = 6$, $n_1 = 5$, $n_2 = 11$, $P = 0.013$ two-tailed] and [Mann–Whitney $U = 16$, $n_1 = 6$, $n_2 = 11$, $P = 0.098$ two-tailed], respectively). Although not significant, higher DOC concentrations were found in the area with high peat presence, cluster 3. One location with noticeably higher DOC was MP 17-115 with 48.24 mg/l, which was more than 5 times the standard deviation of the mean (6.27±7.98 mg/l). Mean streambed DOC concentrations in the entire reach were 6.30±8.37 mg/l, compared to 5.91±0.37 mg/l in the stream.

2.3.3. Residence time and oxygen controls on MMA and nutrient cycling

Lower DO concentrations were generally found at longer RT, which was best described by an exponential relationship (Figure 2-4a). A clear direct relation between DOC and RT was not found (Figure 2-4b). Higher DOC concentrations were mainly found at lower residence times, except for high DOC concentration at MP17-115, which was in an area with higher peat abundance. MMA was more intensive in locations with lowest RT (Figure 2-4c). At longer RT there was less nitrate present (Figure 2-4d). More specifically, the variation in nitrate concentrations dropped sharply at residence times longer than 20 hours. When comparing RT and NH_x concentrations (Figure 2-4e), higher concentrations were found at longer RT, although no significant correlation could be found between the two.

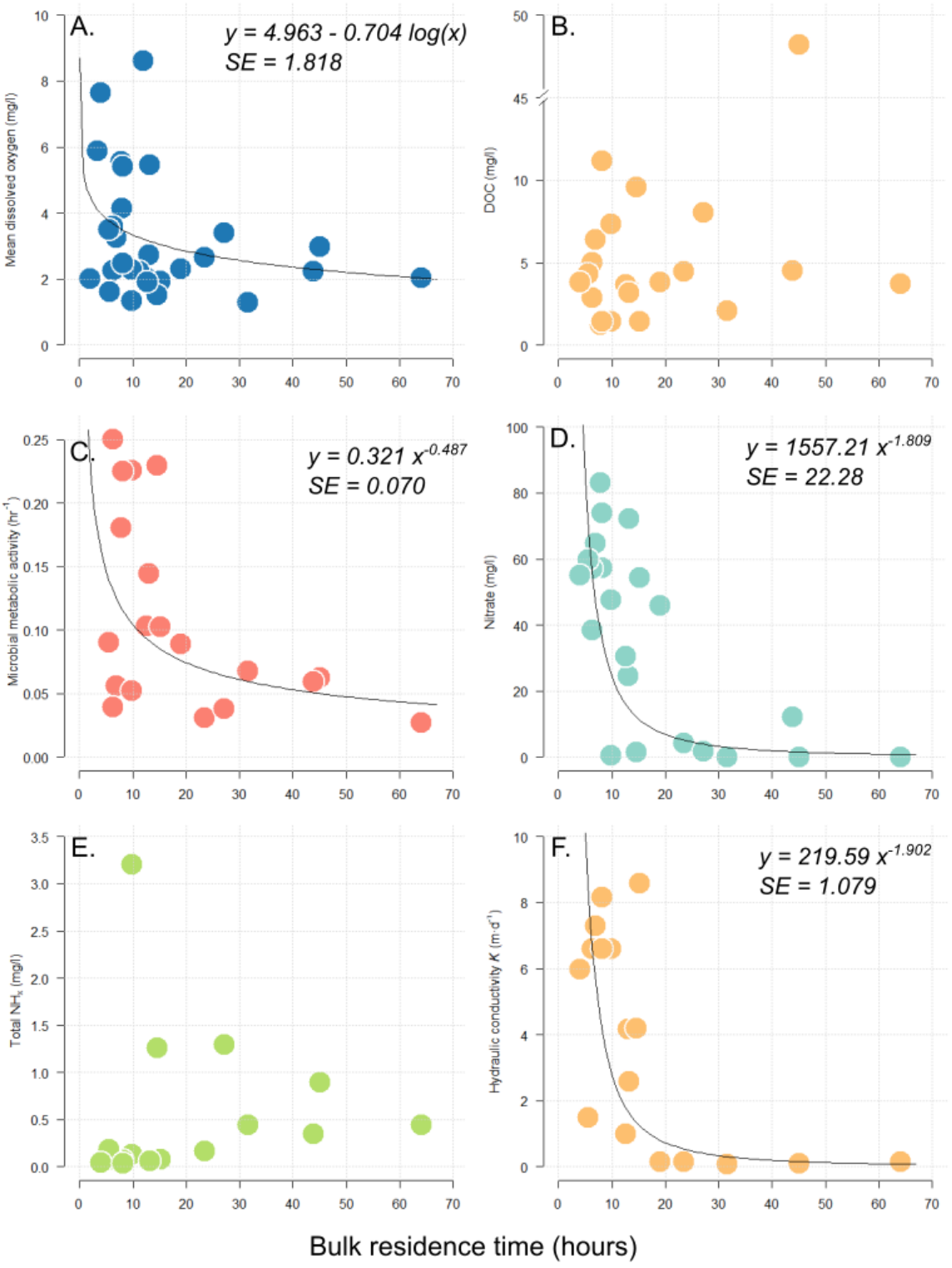

Figure 2-4. Bivariate plots of chemical and physical parameters compared to the bulk residence time. **B)** Note that the y-axis is broken to better display all values. Model fits are plotted where a fit was found, with equation and residual standard error displayed.

Lower DOC concentrations were found at higher DO concentrations, although the relationship was not strong (Figure 2-5a). While both DO and MMA appear to be controlled by RT, there is no strong direct relationship between DO and MMA (Figure 2-5b), even though raz turnover is typically associated with aerobic microbial metabolic activity (see methods). There were four locations with the highest MMA that drew attention which had mean DO concentrations of 1.5-2.5 mg/l, which was not above average. Nitrate concentrations followed a pattern where higher concentrations were generally found at locations with high DO (Figure 2-5c). A threshold value seemed to exist between low and high nitrate concentrations around DO = 2.5 mg/l. NH_x concentrations were lower in areas with lower DO (Figure 2-5d), which were in the peaty area of cluster 3 (Figure 2-3f). Higher DO was generally present at higher hydraulic conductivity (Figure 2-5e). High DO concentrations were not observed at locations with low hydraulic conductivity.

There was no strong relation between MMA and nitrate concentrations (Figure 2-6a), despite both MMA and nitrate decreasing with increasing RT. Based on this study it is unclear whether MMA controlled nitrate concentrations, or vice versa. There were few locations (Figure 2-6a) that had (relatively) low nitrate concentrations (<20 mg/l) and low MMA (<0.1 hr^{-1}). This cluster of points had mean residence times of 34.94±17.61 hours, which was substantially higher than the general mean residence time of 15.32±14.46 hours. Like nitrate, there was no direct relation between NH_x and MMA (Figure 2-6b). In general, NH_x was often present in locations with high OM presence and low breakdown rates, which would yield low MMA, although we cannot find this relation. The four highest values for MMA were found at a large range of DOC contents between 1.44 and 11.18 mg/l (Figure 2-6c). Highest MMA was found where the hydraulic conductivity was higher (Figure 2-6d). Multivariate approaches were attempted for the parameters in Figure 2-6, but no significant model was found that could describe meaningful relations.

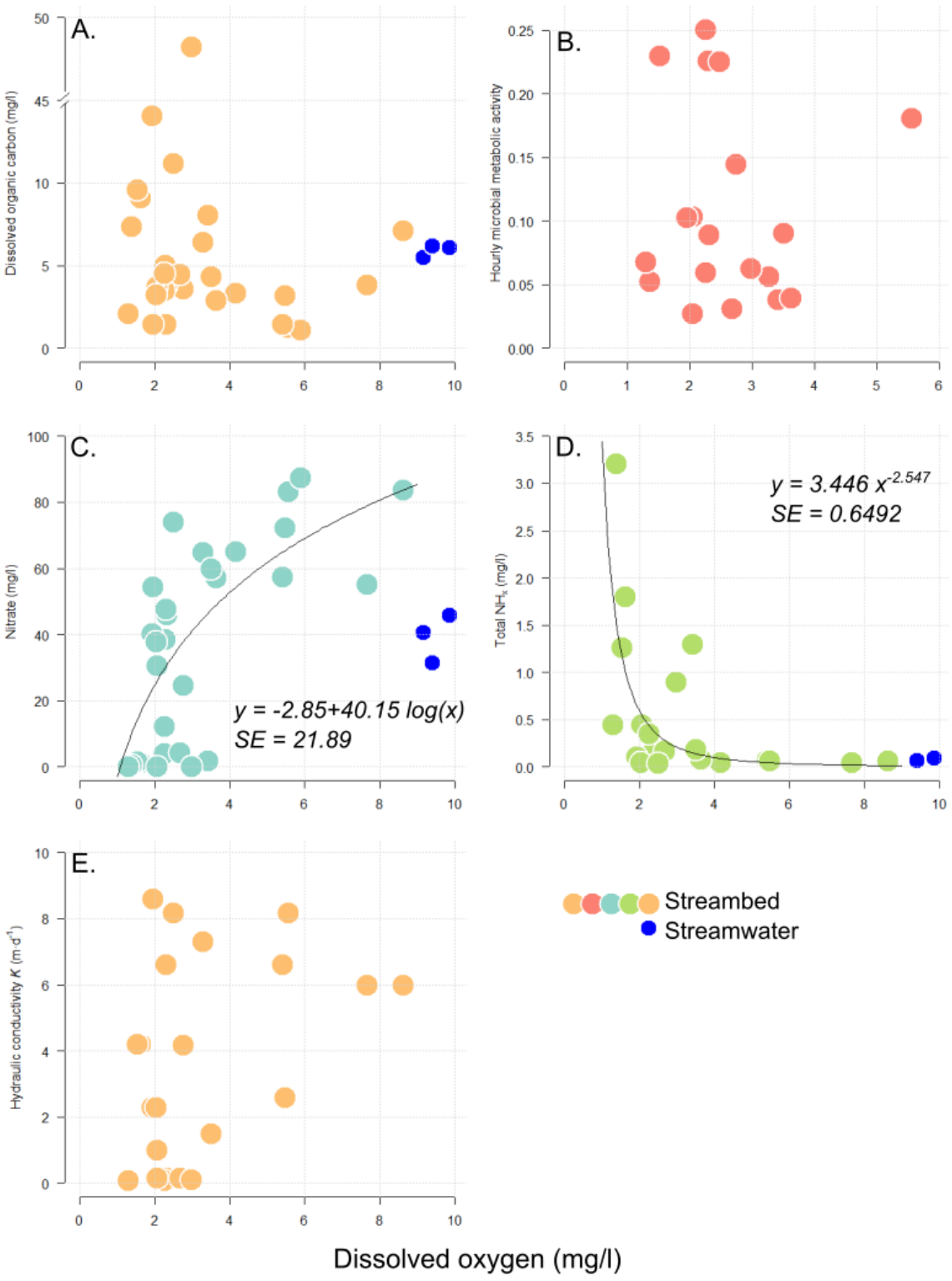

Figure 2-5. Bivariate plots of physical and chemical parameters compared to mean dissolved oxygen concentrations. **A**: note the broken y-axis of DOC concentrations. Trendlines are plotted where linear regression was significant. Model fits are plotted where a fit was found, with equation and residual standard error displayed. Models were fitted to data measured in streambed only. Data measured in stream water is plotted in blue for reference.

When comparing NH_x and DOC concentrations (Figure 2-7a), higher NH_x was generally found in areas with higher DOC. This coincided with the locations of peat abundance in cluster 3. Nitrate and NH_x were inversely related, with the highest NH_x exclusively present in locations with low nitrate (Figure 2-7b). Most nitrate was present at the lower end of our range of DOC concentrations (Figure 2-7c), although there was no clear or significant relation found between DOC and nitrate. No significant multivariate models could be found that could describe meaningful relations in Figure 2-7.

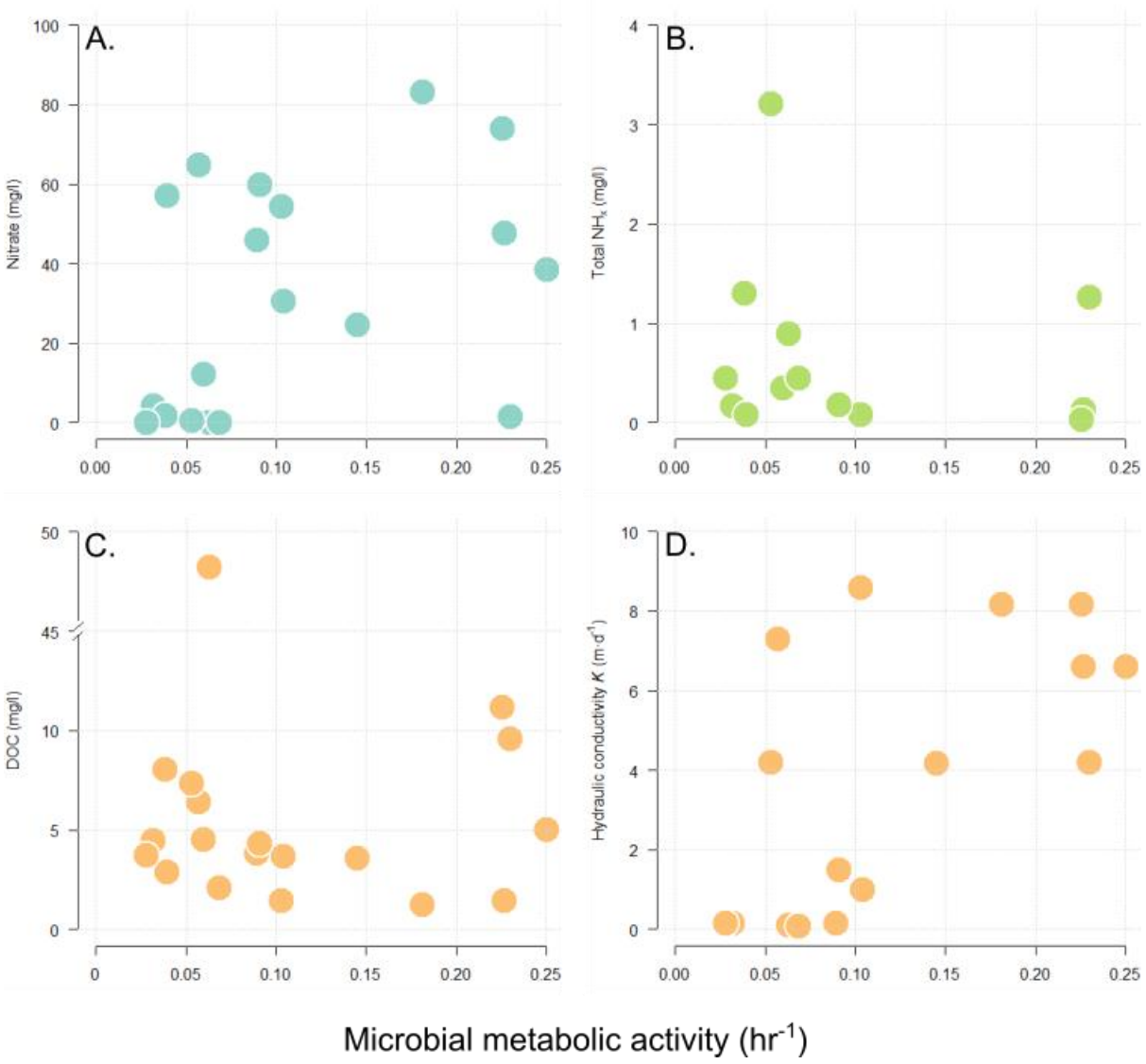

Figure 2-6. Bivariate plots of physical and chemical parameters compared to mean microbial metabolic activity, expressed as hourly resazurin turnover. Only MMA was included that was over the detection limit of the fluorometers.

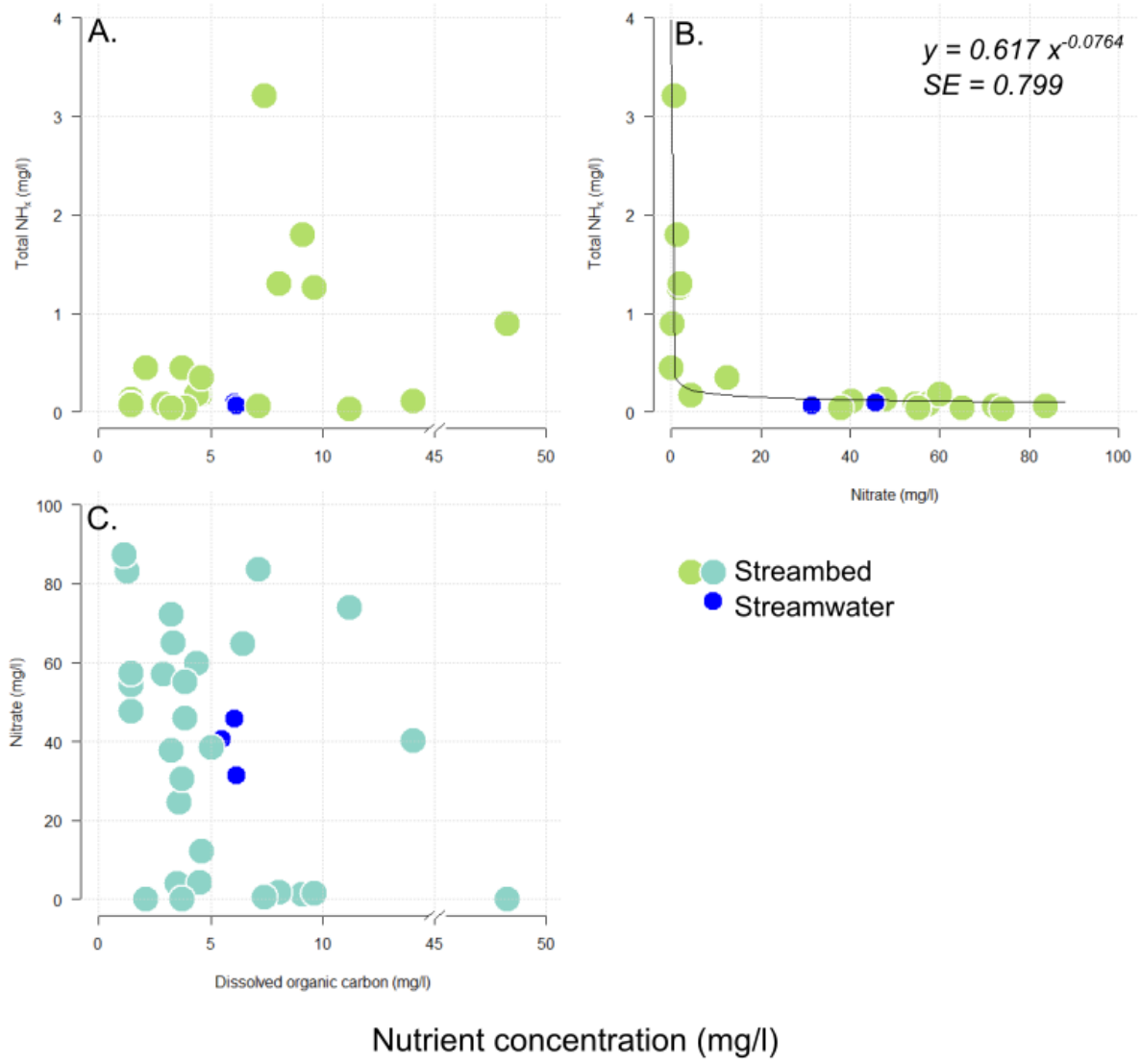

Figure 2-7. Bivariate plots of physical and chemical parameters compared to **A**/**C**: mean dissolved organic carbon and **B**: mean nitrate concentrations. Note the broken x-axis of A and C. Model fit is plotted for B where a fit was found, with equation and residual standard error displayed. Model was fitted to data measured in streambed only. Data measured in stream water is plotted in blue for reference.

2.4. Discussion

Building on the previous work of Krause *et al*. (2012, 2013), this study provides a detailed analysis of the effect of low conductivity strata on streambed on bulk residence times, microbial metabolic activity and nitrogen and carbon cycling.

2.4.1. Streambed sediment controls on residence time distributions

Streambed hydraulic conductivity K_h varied substantially between the clusters and higher RT was associated with lower K_h, driven by differences in sediment characteristics. We found lower values for K_h at structures in the streambed that were expected to be of lower conductivity, such as peat and clay, as represented by the GPR measurements (Figure 2-3a). A high K_h combined with sufficient advective flow reduced residence times (RT) of the water in the subsurface (Figure 2-4f), such as in the areas of cluster 2 with sandy sediments. RT varied between sites, but were longest in cluster 3, where the highest density of low conductivity clusters in the reach were found. Though not significant, the shortest RT were found in cluster 2 where the highest sand content was present. Although RT and K_h were measured using different methods, they reflect similar patterns where high RT and low K_h coincide (Figure 2-4f). In a few cases there were shorter RT present at relatively low K_h, which could have been a consequence of high spatial heterogeneity of the hyporheic sediment (Song *et al.*, 2016). It may also be explained by sediment clogging of the screened section has occurred during measurements of hydraulic conductivity.

2.4.2. Streambed oxygen concentrations as a function of flow pathways and RT

RT were important for DO concentrations at each location. The highest DO concentrations in the reach were found in the stream water and the second highest in the deepest part of our studied reach, which was at MP12-115 cm depth (Figure 2-3c). Based on positive VHG in the reach, the likely source at MP12-115 was upwelling groundwater, rather than hyporheic exchange. DO concentrations decreased from the deeper points at MP12 towards the surface, suggesting there was consumption in cluster 2 along these flow paths. The source of high DO in the deeper surface remains unknown, but may be attributed to relatively short GW upwelling flow paths.

RT was an important control on DO concentrations, driven by streambed heterogeneity (Figure 2-3b and Figure 2-4a). The lowest DO concentrations were found in cluster 3, reflected by longer RT. DO concentrations in cluster 1 were lower than cluster 2 and can be explained by their proximity to layers with lower conductivity, such as the area with sandy clay between MP4 and MP6. The longest RT within cluster 1 was at MP6-70, which coincided with one of the lowest DO concentrations.

2.4.3. The impact of RTD and resulting oxygen conditions on MMA

The novel application of push-pull raz injections in the streambed provided us with new insights into microbial metabolic activity (MMA) at very local scales. DO concentrations at locations with low K_h were predominantly low, more DO is consumed by MMA at longer RT and eventually MMA slows down when it becomes limiting. In areas with low K_h this causes faster oxygen consumption than resupply, suggesting that MMA controls DO concentrations. Despite this observed control, a direct relation between DO and MMA could not be quantified (Figure 2-4c). The relation between MMA and DO is not straightforward: our results do not suggest that MMA is highest in locations with consistently high DO. Highest MMA was in locations with DO between 1.5-2.5 mg/l, suggesting that high MMA is responsible for DO consumption along the flow path (Sobczak & Findlay, 2002). DO concentrations are merely a snapshot of the situation at a specific moment. It is not simply a closed system, and there is continuous advection, dilution and diffusion taking place (Malcolm *et al.*, 2006). This illustrates the dynamic nature of MMA, similar to a continuum as presented in Zarnetske *et al*. (2011a), where DO was limiting to control biogeochemical processes.

In general, areas with low K_h have lower MMA and longer RT, suggesting MMA was also influenced by streambed structure and heterogeneity, possibly due to sediment clogging

(Nogaro *et al.*, 2010). Higher MMA was found in areas with higher K_h, such as closer to the streambed surface and where sandy deposits dominate and RT are shorter, such as cluster 2. In other words, streambed K_h appeared to be an important control for hyporheic microbial metabolic activity. The variation of MMA between different sites decreased substantially when residence times were longer than 20 hours, which were all located in the downstream part of the reach. However, the shortest RT were not exclusively associated with highest MMA, which may be due to the presence of micro-zones with unique redox characteristics that are not accurately reflected by the K_h measurements (Briggs *et al.*, 2015).

2.4.4. Nutrient cycling

Nitrate concentrations varied strongly around low conductivity structures in the streambed (Figure 2-3e) and followed a pattern around a threshold value of DO (Figure 2-5c), which is similar to previous findings at this site (Krause *et al.*, 2013). This threshold is around 2 mg/l of DO, which appears to be similar for the threshold DO concentration where NH_x is observed (Figure 2-5). This value seems on the higher end of a range of observed threshold values between 0.2 and 4 described in a literature review by Rivett *et al.* (2008a, and references therein). Due to the nature of sampling in this experiment, where a certain volume is sampled, it averages out any anoxic microsites that could be present where DO concentrations are lower than the measured 2 mg/l (Zarnetske *et al.*, 2011a). The results suggest such microsites were present in the studied area and DO conditions around 2 mg/l demonstrated presence of nitrate spiralling (Briggs *et al.*, 2014). In areas of longer RT, nitrate concentrations were lower compared to a shorter RT area such as cluster 2. Considering the predominantly upwelling hydraulic regime, we observe strong concentration changes along the vertical profiles in cluster 3, whereas the variation along profiles in cluster 2 and 1 are substantially smaller. We hypothesise that the low conductivity structures in cluster 3 act as a

boundary to provide a relatively isolated environment below, where hyporheic exchange flow is effectively cut off.

During our study DOC was not identified as a limiting factor for MMA. Even at the lowest DOC concentrations measured in our reach there was substantial MMA detected. A direct relation between DO and DOC could not be confirmed. An explanation that the link is not too strong, is possibly that there was no information on the carbon quality in the system. In a recent study by (Zarnetske *et al.*, 2011b) it was shown that mainly labile carbon acts as a main control in biogeochemical cycling. DOC concentrations in this study were higher, which supports the hypothesis that DOC in general was not a limiting factor.

2.4.5. Peat as control for NH_4

NH_x concentrations were strongly location-dependent. The most likely source of NH_x in the streambed is from OM mineralisation (ammonification) inside the streambed. Within cluster 3 we identified high peat and clay presence with large deposits of OM which provided ammonium to the overlying pore water (e.g. Koretsky *et al.*, 2006). We believe that in cluster 3 there is mineralisable, exchangeable and non-exchangeable ammonium present. Under conditions with low pH a low concentration of NH_4^+ in the upwelling water may have been sorbed by the available sorption potential of the peat as well to sustain high concentrations in the pore water above (Triska *et al.*, 1994). Since our results suggest that in this section upwelling is more complex due to the presence of the low conductivity strata, this chemical signature of the hyporheic water is rather restricted to this particular area. Ammonification is common in sections with accumulation of DOC at the soil-water interface near the riparian zone (Hedin *et al.*, 1998) and in pool sections where flow conditions are calmer (Lefebvre *et al.*, 2004). In this study, increasing NH_x concentrations were observed from the stream

downwards to zones with high peat content inside the streambed, suggesting the low-flow, but high-DOC peat layer to be the source.

DNRA, although probably present, was not believed to be a major contributing factor, which is usually observed in highly anoxic and organic-rich environments (Mitsch & Gosselink, 2010). Locations in this study with high NH_x still have DO present, albeit at low concentrations. Hyporheic zones in areas with high peat content are known to be a stronger source of ammonium than those that have no or little peat (Greenwald *et al.*, 2008). Similar patterns can be observed in our reach: clusters 1 and especially 2 have more sandy sediment type (i.e. alluvial) and contribute only marginally to the NH_x content. Cluster 3 on the other hand is by far the largest contributor with pore water concentrations over 12 times higher than cluster 2.

Over the studied reach there were several locations with substantial NH_x concentrations; e.g. MP14-20 has only 1.24 mg/l nitrate, but there is 3.2 mg/l NH_x. This study's spatial sampling resolution for the streambed above the low conductivity (LC) peat layer in cluster 3 was not fine enough to capture the full ammonium dynamics, as these concentrations and such strong gradients were not expected. Future studies could increase the resolution to find whether nitrification is a major pathway between source and sediment-water interface.

2.4.6. Streambed heterogeneity and related hotspot activity

The results suggest that the heterogeneous streambed environment hosts a variety of nutrient turnover rates. Not only was a mechanistic control of LC layers in the streambed observed like in earlier studies (Conant, 2004; Krause *et al.*, 2013), but also strong spatial changes in concentrations of nitrate, NH_x, DO and DOC. These changes appeared to be preferentially located in zones with larger sections of LC layers (e.g. Figure 2-3c and e) and coincided with

enhanced nutrient turnover. The anaerobic zones in the streambed were important controls for the spatial patterns of nitrate and ammonium, similar to water at soil-stream interfaces (McNamara *et al.*, 2008). Although hotspots of nitrate spiralling were identified in this study, future studies could focus on temporal dynamics of nitrate to identify hot moments. Due to relatively high flow and the heterogeneity of the streambed, the hyporheic zone is possibly of shallow depth. In heterogeneous streambeds, a plume of mixing stream water may move back and forth and create local delays in mass transport, hence locally increasing these RT (Hester *et al.*, 2017). However, RT are mainly expected to be lower when higher K strata are connected throughout the streambed, as these will act as preferential flow paths (Pryshlak *et al.*, 2015).

LC structures partially disconnect lower regions of the streambed (Figure 2-8). Such disconnections, combined with a predominantly upwelling hydraulic regime, reduce the size of the hyporheic zone, which leads to shorter residence times in the higher parts above the LC structures and effectively a smaller hyporheic zone (Gomez *et al.*, 2012; Fox *et al.*, 2016). Groundwater upwelling can inhibit deeper hyporheic cycling (Boano *et al.*, 2008), although these shorter residence times create an environment promoting higher turnover and promote the presence of biogeochemical hotspots due to the presence of the LC structures. On the other hand, water that slowly flows through these LC structures will have a relatively high RT. In these high RT areas, biogeochemical processes slow down due to the lack of oxygen (Zarnetske *et al.*, 2011a). We see this clearly reflected by the decline in DO at higher RT (Figure 2-4a). We demonstrate how biogeochemical processes can be very local within the reach scale and choosing a study site for a higher resolution study requires careful consideration.

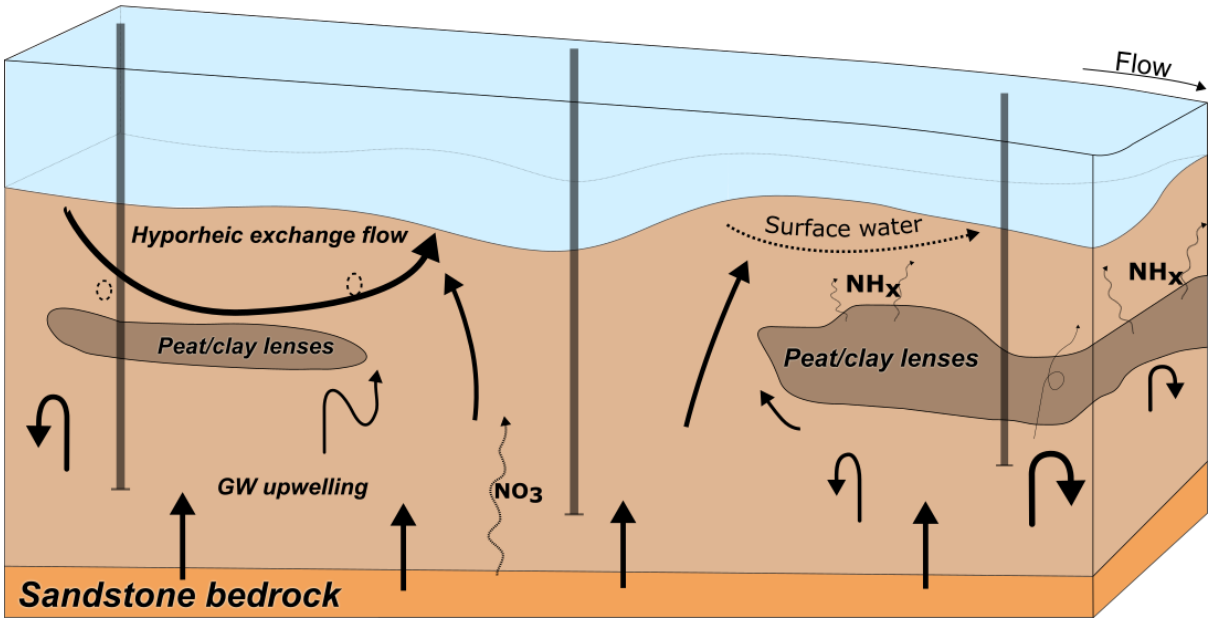

Figure 2-8. Conceptual model of streambed processes adapted from Krause *et al*. (2012). Upwelling groundwater (GW) is forced around low-conductivity (LC) structures, such as peat and clay lenses, increasing its residence time (RT). In some sections (e.g. middle section) the upwelling GW is well connected with the stream and has shorter RT, with higher DO concentrations and high MMA, but lower potential for denitrification. In the upstream and downstream part there is increased hyporheic exchange flow possible due to the LC structures. The peat and clay strata have higher RTs and lower DO concentrations due to depletion. MMA slows down, but there is increased potential and hotspots for denitrification and ammonification.

We were unable to find a model that correctly describes the relation between most or each of the most important physical and chemical parameters, such as bulk RT, nitrate, ammonium, DOC and MMA. Finding such a relation may prove difficult, not only because of the heterogeneous environment where processes can be hyperlocal, but also because of confounded process controls that may have hidden feedbacks. To capture relevant parameters on timescales that are necessary to accurately model complex flow behaviour, an extensive piezometer network would be required to capture even sharper gradients, which is beyond the scope of this study.

2.5. Conclusions

Microbial metabolic activity and nutrient concentrations were measured during a novel push-pull experiment in a heterogeneous streambed environment of a lowland stream in the UK. Unprecedented detailed knowledge of streambed sediment structure revealed direct control of K_h on MMA and nutrient concentrations. Spatial patterns of K_h were found to control hyporheic exchange flow velocity and RT distributions. DO concentrations were controlled by RT, where higher DO concentrations were generally found at shorter RT. MMA was lower at longer RT, where DO became limiting. Nitrate cycling was strongly linked to DO concentrations, which in turn were controlled by RT. DOC was not limiting for MMA in the studied reach and was not controlled by aerobic MMA. NH_x concentrations were controlled by the presence of low conductivity structures with high OM content in the streambed and were found to release substantial amounts into the streambed. Heterogeneous streambeds and hyporheic zones host a wide range of environments with sharp gradients that cannot always be observed from the streambed surface. Hotspot activity may be related to deeper lying sediment structures which are not always accounted for in studies. The presented results shed new light on the role of LC structures and their role in nutrient cycling and possible impacts on MMA related greenhouse gas production.

Acknowledgements

This project has received funding from the European Union's Seventh Framework Programme for research, technological development and demonstration under grant agreement no 607150.

Author contributions

PR wrote the manuscript and was responsible for designing and conceptualising the study, performing the experiments, data collection and analysis. RD was responsible for data collection of the ground-penetrating radar dataset, performing experiments and data collection. DMH provided support with manuscript revisions. SK instigated the study and advised on the experimental design and the conceptualisation of the results, and supported the data analysis, interpretation, and manuscript revisions.

References

Abbott BW, Baranov V, Mendoza-Lera C et al. (2016) Using multi-tracer inference to move beyond single-catchment ecohydrology. *Earth-Science Reviews*, **160**, 19–42.

Angermann L, Krause S, Lewandowski J (2012) Application of heat pulse injections for investigating shallow hyporheic flow in a lowland river. *Water Resources Research*, **48**.

Argerich A, Martí E, Sabater F, Ribot M (2011) Temporal variation of hydrological exchange and hyporheic biogeochemistry in a headwater stream during autumn. *Journal of the North American Benthological Society*, **30**, 635–652.

Avanzino RJ, Kennedy VC (1993) Long-term frozen storage of stream water samples for dissolved orthophosphate, nitrate plus nitrite, and ammonia analysis. *Water Resources Research*, **29**, 3357–3362.

Baranov V, Lewandowski J, Krause S (2016) Bioturbation enhances the aerobic respiration of lake sediments in warming lakes. *Biology letters*, **12**, 269–281.

Battin TJ, Besemer K, Bengtsson MM, Romani AM, Packmann AI (2016) The ecology and biogeochemistry of stream biofilms. *Nature Reviews Microbiology*, **14**, 251–263.

Binley A, Ullah S, Heathwaite AL et al. (2013) Revealing the spatial variability of water fluxes at the groundwater-surface water interface. *Water Resources Research*, **49**, 3978–3992.

Boano F, Revelli R, Ridolfi L (2008) Reduction of the hyporheic zone volume due to the stream-aquifer interaction. *Geophysical Research Letters*, **35**, L09401.

Boano F, Harvey JW, Marion A, Packman AI, Revelli R, Ridolfi L, Wörman A (2014) Hyporheic flow and transport processes: Mechanisms, models, and biogeochemical

implications. *Reviews of Geophysics*, **52**, 603–679.

Boulton A, Findlay S, Marmonier P (1998) The functional significance of the hyporheic zone in streams and rivers. *Annual Review of Ecology and Systematics*, **29**, 59–81.

Bouwer H, Rice RC (1976) A slug test for determining hydraulic conductivity of unconfined aquifers with completely or partially penetrating wells. *Water Resources Research*, **12**, 423–428.

Briggs MA, Lautz LK, Hare DK (2014) Residence time control on hot moments of net nitrate production and uptake in the hyporheic zone. *Hydrological Processes*, **28**, 3741–3751.

Briggs MA, Day-Lewis FD, Zarnetske JP, Harvey JW (2015) A physical explanation for the development of redox microzones in hyporheic flow. *Geophysical Research Letters*, **42**, 4402–4410.

Chapuis RP (1989) Shape Factors for Permeability Tests in Boreholes and Piezometers. *Ground Water*, **27**, 647–654.

Chen X (2011) Depth-dependent hydraulic conductivity distribution patterns of a streambed. *Hydrological Processes*, **25**, 278–287.

Claret C, Boulton AJ (2009) Integrating hydraulic conductivity with biogeochemical gradients and microbial activity along river - Groundwater exchange zones in a subtropical stream. *Hydrogeology Journal*, **17**, 151–160.

Conant B (2004) Delineating and Quantifying Ground Water Discharge Zones Using Streambed Temperatures. *Ground Water*, **42**, 243–257.

Drost W, Klotz D, Koch A, Moser H, Neumaier F, Rauert W (1968) Point dilution methods of investigating ground water flow by means of radioisotopes. *Water Resources Research*, **4**, 125–146.

Ensign SH, Doyle MW (2006) Nutrient spiraling in streams and river networks. *Journal of Geophysical Research: Biogeosciences*, **111**.

Fellman JB, D'Amore D V., Hood E (2008) An evaluation of freezing as a preservation technique for analyzing dissolved organic C, N and P in surface water samples. *Science of The Total Environment*, **392**, 305–312.

Fox A, Laube G, Schmidt C, Fleckenstein JH, Arnon S (2016) The effect of losing and gaining flow conditions on hyporheic exchange in heterogeneous streambeds. *Water Resources Research*, **52**, 7460–7477.

Freeze RA, Cherry JA (1979) Groundwater. 604.

Genereux DP, Leahy S, Mitasova H, Kennedy CD, Corbett DR (2008) Spatial and temporal variability of streambed hydraulic conductivity in West Bear Creek, North Carolina, USA. *Journal of Hydrology*, **358**, 332–353.

Gomez JD, Wilson JL, Cardenas MB (2012) Residence time distributions in sinuosity-driven hyporheic zones and their biogeochemical effects. *Water Resources Research*.

Gomez-Velez JD, Krause S, Wilson JL (2014) Effect of low-permeability layers on spatial patterns of hyporheic exchange and groundwater upwelling. *Water Resources Research*, **50**, 5196–5215.

Gomez-Velez JD, Harvey JW, Cardenas MB, Kiel B (2015) Denitrification in the Mississippi River network controlled by flow through river bedforms. *Nature Geoscience*, **8**, 941–945.

González-Pinzón R, Haggerty R, Myrold DD (2012) Measuring aerobic respiration in stream ecosystems using the resazurin-resorufin system. *Journal of Geophysical Research: Biogeosciences*, **117**, n/a-n/a.

González-Pinzón R, Ward AS, Hatch CE et al. (2015) A field comparison of multiple techniques to quantify groundwater – surface-water interactions. *Freshwater Science*, **34**, 139–160.

Greenwald MJ, Bowden WB, Gooseff MN, Zarnetske JP, McNamara JP, Bradford JH, Brosten TR (2008) Hyporheic exchange and water chemistry of two arctic tundra streams of contrasting geomorphology. *Journal of Geophysical Research: Biogeosciences*, **113**, n/a-n/a.

Gumprecht R, Gerlach H, Nehrkorn A (1995) FDA hydrolysis and resazurin reduction as a measure of microbial activity in sediments from the south-east Atlantic. *Helgoländer Meeresuntersuchungen*, **49**, 189–199.

Haggerty R, Argerich A, Martí E (2008) Development of a "smart" tracer for the assessment of microbiological activity and sediment-water interaction in natural waters: The resazurin-resorufin system. *Water Resources Research*, **44**, W00D01.

Haggerty R, Martí E, Argerich A, Von Schiller D, Grimm NB (2009) Resazurin as a "smart" tracer for quantifying metabolically active transient storage in stream ecosystems. *Journal of Geophysical Research: Biogeosciences*, **114**.

Haggerty R, Ribot M, Singer GA, Martí E, Argerich A, Agell G, Battin TJ (2014) Ecosystem respiration increases with biofilm growth and bed forms: Flume measurements with resazurin. *Journal of Geophysical Research: Biogeosciences*, **119**, 2013JG002498.

Hall SH, Luttrell SP, Cronin WE (1991) A Method for Estimating Effective Porosity and Ground-Water Velocity. *Ground Water*, **29**, 171–174.

He B, Kanae S, Oki T, Hirabayashi Y, Yamashiki Y, Takara K (2011) Assessment of global nitrogen pollution in rivers using an integrated biogeochemical modeling framework. *Water Research*, **45**, 2573–2586.

Hedin LO, von Fischer JC, Ostrom NE, Kennedy BP, Brown MG, Robertson GP (1998) Thermodynamic constraints on nitrogen transformations and other biogeochemical processes at soil–stream interfaces. *Ecology*, **79**, 684–703.

Hester ET, Doyle MW (2008) In-stream geomorphic structures as drivers of hyporheic exchange. *Water Resources Research*.

Hester ET, Cardenas MB, Haggerty R, Apte S V. (2017) The importance and challenge of hyporheic mixing. *Water Resources Research*, **53**, 3565–3575.

Hvorslev MJ (1951) *Time Lag And Soil Permeability In Ground-water Observations*, Vol. 36. Vicksburg, Mississippi, 1-50 pp.

Hyun Y, Kim H, Lee S-S, Lee K-K (2011) Characterizing streambed water fluxes using temperature and head data on multiple spatial scales in Munsan stream, South Korea. *Journal of Hydrology*, **402**, 377–387.

Kasahara T, Wondzell SM (2003) Geomorphic controls on hyporheic exchange flow in mountain streams. *Water Resources Research*, **39**, SBH 3-1-SBH 3-14.

Keery J, Binley A, Crook N, Smith JWN (2007) Temporal and spatial variability of groundwater–surface water fluxes: Development and application of an analytical method using temperature time series. *Journal of Hydrology*, **336**, 1–16.

Knapp JLA, González-Pinzón R, Drummond JD, Larsen LG, Cirpka OA, Harvey JW (2017) Tracer-based characterization of hyporheic exchange and benthic biolayers in streams. *Water Resources Research*, **53**, 1575–1594.

Kobr M, Mareš S, Paillet F (2005) Geophysical Well Logging. In: *Hydrogeophysics*, pp. 291–331. Springer Netherlands, Dordrecht.

Koretsky CM, Haas JR, Ndenga NT, Miller D (2006) Seasonal variations in vertical redox stratification and potential influence on trace metal speciation in minerotrophic peat sediments. *Water, Air, and Soil Pollution*, **173**, 373–403.

Krause S, Blume T, Cassidy NJ (2012) Investigating patterns and controls of groundwater up-welling in a lowland river by combining Fibre-optic Distributed Temperature Sensing with observations of vertical hydraulic gradients. *Hydrology and Earth System Sciences*, **16**, 1775–1792.

Krause S, Tecklenburg C, Munz M, Naden E (2013) Streambed nitrogen cycling beyond the hyporheic zone: Flow controls on horizontal patterns and depth distribution of nitrate

and dissolved oxygen in the upwelling groundwater of a lowland river. *Journal of Geophysical Research: Biogeosciences*, **118**, 54–67.

Lamontagne S, Dighton J, Ullman W (2002) *Estimation of groundwater velocity in riparian zones using point dilution tests*. CSIRO Land and Water.

Leap DI, Kaplan PG (1988) A single-well tracing method for estimating regional advective velocity in a confined aquifer: Theory and preliminary laboratory verification. *Water Resources Research*, **24**, 993–998.

Lefebvre S, Marmonier P, Pinay G (2004) Stream regulation and nitrogen dynamics in sediment interstices: comparison of natural and straightened sectors of a third-order stream. *River Research and Applications*, **20**, 499–512.

Lemke D, Schnegg P-A, Schwientek M, Osenbrück K, Cirpka O a. (2013a) On-line fluorometry of multiple reactive and conservative tracers in streams. *Environmental Earth Sciences*, **69**, 349–358.

Lemke D, Liao Z, Wöhling T, Osenbrück K, Cirpka O a. (2013b) Concurrent conservative and reactive tracer tests in a stream undergoing hyporheic exchange. *Water Resources Research*, **49**, 3024–3037.

Lemke D, González-Pinzón R, Liao Z, Wöhling T, Osenbrück K, Haggerty R, Cirpka OA (2014) Sorption and transformation of the reactive tracers resazurin and resorufin in natural river sediments. *Hydrology and Earth System Sciences*, **18**, 3151–3163.

Malcolm IA, Soulsby C, Youngson AF (2006) High-frequency logging technologies reveal state-dependent hyporheic process dynamics: Implications for hydroecological studies. *Hydrological Processes*, **20**, 615–622.

McNamara JP, Kane DL, Hobbie JE, Kling GW (2008) Hydrologic and biogeochemical controls on the spatial and temporal patterns of nitrogen and phosphorus in the Kuparuk River, arctic Alaska. *Hydrological Processes*, **22**, 3294–3309.

McWhorter DB, Sunada DK (1977) *Ground-water hydrology and hydraulics*. Water Resources Publications, 290 pp.

Mendoza-Lera C, Mutz M (2013) Microbial activity and sediment disturbance modulate the vertical water flux in sandy sediments. *Freshwater Science*, **32**, 26–38.

Meybeck M, Helmer R (1989) The quality of rivers: From pristine stage to global pollution. *Global and Planetary Change*, **1**, 283–309.

Mitsch WJ, Gosselink JG (2010) *Wetlands*, 4th edn. Wiley, New York, 582 pp.

Mulholland PJ, Webster JR (2010) Nutrient dynamics in streams and the role of J-NABS.

Journal of the North American Benthological Society, **29**, 100–117.

Nogaro G, Datry T, Mermillod-Blondin F, Descloux S, Montuelle B (2010) Influence of streambed sediment clogging on microbial processes in the hyporheic zone. *Freshwater Biology*, **55**, 1288–1302.

NRFA (2016) National River Flow Archive; UK Daily Flow Data. *Natural Environment Research Council - Centre for Ecology & Hydrology*.

Piccinini L, Fabbri P, Pola M (2016) Point dilution tests to calculate groundwater velocity: an example in a porous aquifer in northeast Italy. *Hydrological Sciences Journal*, **61**, 1512–1523.

Piña-Ochoa E, Álvarez-Cobelas M (2006) Denitrification in Aquatic Environments: A Cross-system Analysis. *Biogeochemistry*, **81**, 111–130.

Pryshlak TT, Sawyer AH, Stonedahl SH, Soltanian MR (2015) Multiscale hyporheic exchange through strongly heterogeneous sediments. *Water Resources Research*, **51**, 9127–9140.

Raymond PA, Hartmann J, Lauerwald R et al. (2013) Global carbon dioxide emissions from inland waters. *Nature*, **503**, 355–359.

Rivett MO, Buss SR, Morgan P, Smith JWN, Bemment CD (2008a) Nitrate attenuation in groundwater: A review of biogeochemical controlling processes. *Water Research*, **42**, 4215–4232.

Rivett MO, Ellis PA, Greswell RB et al. (2008b) Cost-effective mini drive-point piezometers and multilevel samplers for monitoring the hyporheic zone. *Quarterly Journal of Engineering Geology and Hydrogeology*, **41**, 49–60.

Ryan RJ, Boufadel MC (2007) Evaluation of streambed hydraulic conductivity heterogeneity in an urban watershed. *Stochastic Environmental Research and Risk Assessment*, **21**, 309–316.

Salehin M, Packman AI, Paradis M (2004) Hyporheic exchange with heterogeneous streambeds: Laboratory experiments and modeling. *Water Resources Research*, **40**.

Saunders DL, Kalff J (2001) Nitrogen retention in wetlands, lakes and rivers. *Hydrobiologia*, **443**, 205–212.

Sawyer AH, Cardenas MB (2009) Hyporheic flow and residence time distributions in heterogeneous cross-bedded sediment. *Water Resources Research*, **45**.

Scanlon BR, Jolly I, Sophocleous M, Zhang L (2007) Global impacts of conversions from natural to agricultural ecosystems on water resources: Quantity versus quality. *Water*

Resources Research, **43**.

Singer G, Besemer K, Schmitt-Kopplin P, Hödl I, Battin TJ (2010) Physical heterogeneity increases biofilm resource use and its molecular diversity in stream mesocosms (ed Bell T). *PLoS ONE*, **5**, e9988.

Sobczak W V, Findlay S (2002) Variation in Bioavailability of Dissolved Organic Carbon among Stream Hyporheic Flowpaths. *Ecology*, **83**, 3194.

Song J, Jiang W, Xu S et al. (2016) Heterogeneity of hydraulic conductivity and Darcian flux in the submerged streambed and adjacent exposed stream bank of the Beiluo River, northwest China. *Hydrogeology Journal*, **24**, 2049–2062.

Stelzer RS, Bartsch LA, Richardson WB, Strauss EA (2011) The dark side of the hyporheic zone: Depth profiles of nitrogen and its processing in stream sediments. *Freshwater Biology*, **56**, 2021–2033.

Tang Q, Kurtz W, Brunner P, Vereecken H, Hendricks Franssen H-J (2015) Characterisation of river–aquifer exchange fluxes: The role of spatial patterns of riverbed hydraulic conductivities. *Journal of Hydrology*, **531**, 111–123.

Tonina D, de Barros FPJ, Marzadri A, Bellin A (2016) Does streambed heterogeneity matter for hyporheic residence time distribution in sand-bedded streams? *Advances in Water Resources*, **96**, 120–126.

Triska FJ, Jackman AP, Duff JH, Avanzino RJ (1994) Ammonium sorption to channel and riparian sediments: A transient storage pool for dissolved inorganic nitrogen. *Biogeochemistry*, **26**, 67–83.

Wang L, Jiang W, Song J et al. (2017) Investigating spatial variability of vertical water fluxes through the streambed in distinctive stream morphologies using temperature and head data. *Hydrogeology Journal*, **25**, 1283–1299.

Wu G, Shu L, Lu C, Chen X (2016) The heterogeneity of 3-D vertical hydraulic conductivity in a streambed. *Hydrology Research*, **47**, 15–26.

Zarnetske JP, Haggerty R, Wondzell SM, Baker M a. (2011a) Dynamics of nitrate production and removal as a function of residence time in the hyporheic zone. *Journal of Geophysical Research*, **116**, G01025.

Zarnetske JP, Haggerty R, Wondzell SM, Baker M a. (2011b) Labile dissolved organic carbon supply limits hyporheic denitrification. *Journal of Geophysical Research*, **116**, G04036.

Zarnetske JP, Haggerty R, Wondzell SM, Bokil V a., González-Pinzón R (2012) Coupled transport and reaction kinetics control the nitrate source-sink function of hyporheic

zones. *Water Resources Research*, **48**.

Chapter 3. Macrophyte controls on total stream microbial metabolic activity in an urban stream

Paul Romeijn, David M. Hannah, Stefan Krause

Abstract

Many streams worldwide are under direct influence of wastewater treatment plant effluents. Properly managed drainage is important in these mostly urban areas as flooding is unwanted. Macrophyte growth in the channels is sensitive to eutrophication and is one of the causes of reduced drainage. Therefore, macrophytes are mowed from the channel bed on a frequent basis as a management practice. However, the impact of mowing on the streambed and microbial metabolic activity (MMA) is not fully understood. Tracer slug injections were performed with conservative tracer uranine and the reactive tracer resazurin before and after mowing the macrophytes. Contrary to the hypothesis, mowing of the macrophytes did not lead to a significant decrease in whole-stream MMA. Although MMA was slightly lower in mowed segments than before, the decrease in the unmowed segments was much larger, despite a substantially lower travel time in the mowed segments because of mowing. Transient storage index was calculated for each segment and was found to have slightly increased. The results suggest that removing macrophytes exposed the sediment and combined with increased flow velocity improved hyporheic exchange through the sediment. Even though the storage compartment of the macrophytes had disappeared, the storage compartment of the hyporheic zone was improved. The hyporheic zone provided better metabolically active transient storage so that net MMA in the mowed segments, although a slight net decrease, was relatively improved. Thus, macrophyte mowing did not lead to

significant losses of stream microbial metabolic activity and potential nutrient and pollutant attenuation.

3.1. Introduction

In many streams worldwide, and urban streams in particular, local water management depends on reliable waterway functioning for water transport and nutrient management from wastewater treatment plant (WWTP) effluents (Hellström *et al.*, 2000; Paul *et al.*, 2001; Cotton *et al.*, 2006; Brown *et al.*, 2009; Marlow *et al.*, 2013). In urban and agricultural settings, a surplus of nutrients may be expected with a high potential for eutrophication. Macrophytes growth inside channels is often sensitive to eutrophication and increasingly blocks waterways (Kantrud, 1990). To maintain a good flow through natural and strongly anthropogenically modified streams, macrophyte removal by mowing is used as a common management practice (Vereecken *et al.*, 2006; Ochs *et al.*, 2018) that potentially disturbs instream habitats (Kaenel *et al.*, 1998; Baattrup-Pedersen *et al.*, 2016).

Macrophyte growth may increase stream storage capacity (Vereecken *et al.*, 2006; Hensley & Cohen, 2012), increase the potential for fine sediment trapping (Sand-Jensen, 1998; Madsen *et al.*, 2001) and increase stream temperature (Wilcock *et al.*, 1999). While it may seem trivial to assume that increased fine sediment retention may promote higher microbial metabolic respiration in streambed sediment communities, this is not always confirmed in field observations (O'Brien *et al.*, 2014).

The biogeochemical role of macrophytes growing inside channels is not yet fully understood. Although macrophytes are important for instream biogeochemical cycling, this is often attributed to autotrophic metabolism (Riis *et al.*, 2012; O'Brien *et al.*, 2014), while the combination with heterotrophic demand seems more important (García *et al.*, 2017).

However, macrophytes can be important in high-nutrient lowland rivers for NH_4^+ attenuation by uptake (Levi *et al.*, 2015) and epiphytic biofilm formation (Alnoee *et al.*, 2016).

While transient storage is important for nutrient turnover, urban streams are among those with lowest storage due to low complexity of the channel morphology (Gooseff *et al.*, 2007). Optimal management in urban streams could benefit from knowledge about the impacts of macrophyte removal, since it is a common management practice. Previous studies focused on headwater streams or focused specifically on macrophyte nutrient uptake rates (Kaenel *et al.*, 2000; Hensley & Cohen, 2012). In urban streams there are still knowledge gaps on the effects of removal as management practises on total stream microbial metabolic activity.

We hypothesise that (I) removal of macrophyte vegetation reduces transient storage and increases flow velocity, leaving a less favourable habitat for microbial communities. Also, (II) when transient storage is reduced, a reduced residence time may lead to reduced microbial metabolic activity. As a result, whole reach reactivity and nutrient turnover are expected to be lower in mowed streams, giving urban streams less opportunity to break down pollutants received from WWTP. This study used concurrent conservative and reactive tracer injections to compare situations before and after a macrophyte removal on total stream respiration effects of macrophyte stands.

3.2. Methods

Fluorescent tracer injections were carried out on two occasions: one before a macrophyte removal, and one after removal. The study location was the river Erpe on the border of Berlin and Brandenburg, Germany (Figure 3-1), a strongly modified section of urban stream. Discharge in the Erpe has strong diurnal patterns driven by WWTP output, from which the river receives the largest part of the water. Diurnal discharge can vary from 0.35 m^3/s at night

to around 1 m^3/s during daytime. A part of the discharge is lost to side channels in section 3 that later re-join the main channel (Figure 3-1). Tracer that enters the side channels is considered lost, as the water does not re-enter the main channel during the course of one tracer experiment due to the low flow velocity relative to the main channel. Discharge in side channels was measured and main channel discharge and tracer recovery corrected for the loss.

Macrophytes were removed on 17 June 2016 by a specialised company using mowing buckets attached to tractors, mowing over the sediment surface and slightly disturbing the sediment without dredging it. Local authorities apply this management strategy on a yearly basis to control macrophyte growth. Upstream segments 1 and 2 were not mowed, serving as reference sections between tracer injections, while segments 3 through 7 were mowed (Figure 3-1).

Total microbial metabolic activity was measured using slug injections of the "smart" tracer resazurin (Haggerty *et al.*, 2009). Resazurin (raz) is transformed irreversibly to resorufin (rru) in the presence of aerobic microbial metabolism and has been successfully applied from microcosm scale (Baranov *et al.*, 2016a, 2016b) to reach scale (Argerich *et al.*, 2011; Lemke *et al.*, 2013b; González-Pinzón *et al.*, 2016; Knapp & Cirpka, 2017; Blaen *et al.*, 2018). Both parent and daughter compound raz and rru can be fluorometrically detected in water. Resazurin was injected alongside the conservative tracer uranine (ura), which was used to measure hydrodynamic flow parameters of the river.

High-frequency fluorometric tracer measurements were used (Lemke *et al.*, 2013a, 2013b). All tracers raz, rru and ura were detected online using Albillia GGUN FL30 field fluorometers (Albillia, Neuchatel, CH), measuring at 10-second intervals at 7 different

stations along the river (Figure 3-1). An additional FL30 fluorometer was set up out of the water to measure grab samples taken at each station and used to check for consistency across different fluorometers. All fluorometers were calibrated in stream conditions immediately prior to tracer injections. Temperature was relatively constant, turbidity low and constant, and pH was above 8 at all times throughout the experiment (Blaen *et al.*, 2017). Fluorometers were all placed in the river attached to a frame to be able to optimally measure inside the water velocity profile and raising it above streambed sediments. Dissolved oxygen and temperature were measured at each station using MiniDOT loggers (Precision Measurement Engineering, Inc, Vista, CA, USA) at 5-minute intervals.

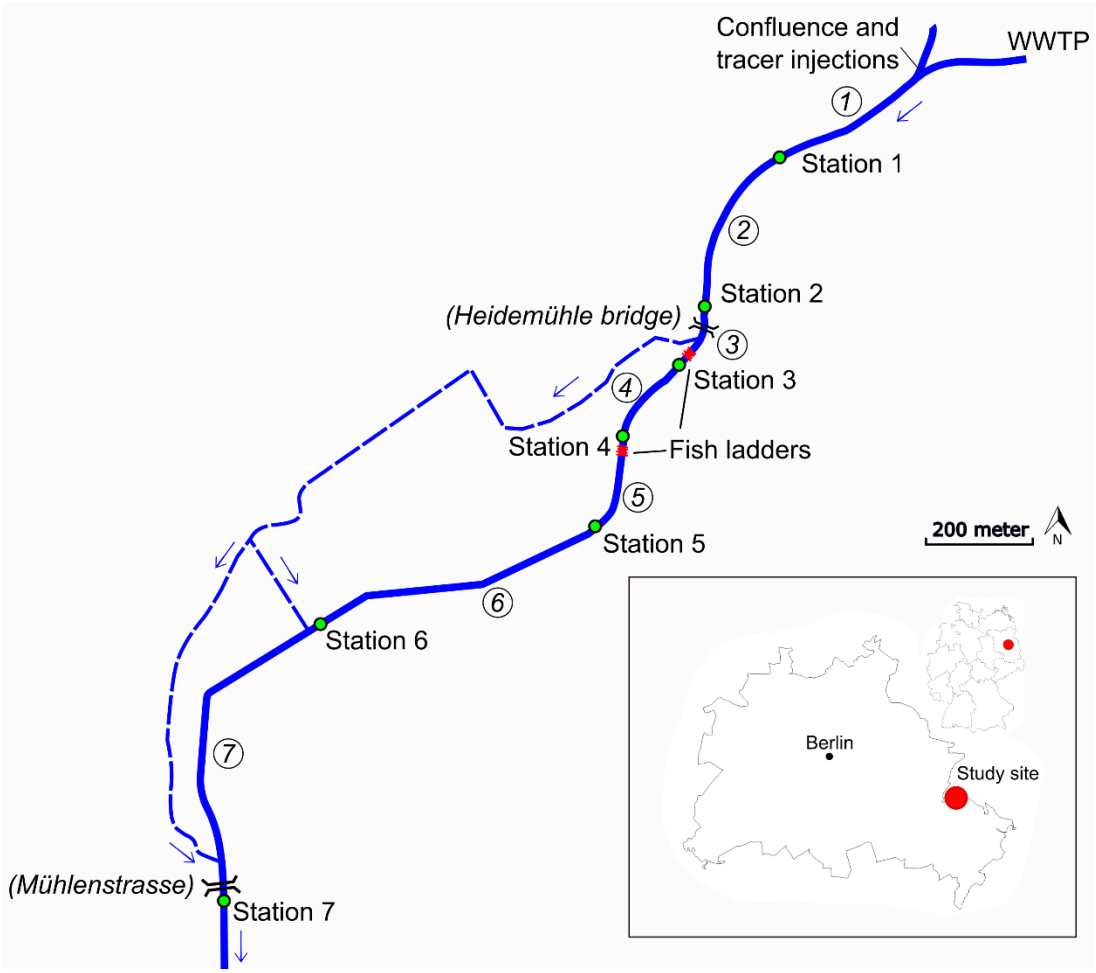

Figure 3-1. Study site of the River Erpe on the border of Berlin and Brandenburg. The river is strongly channelled and transports mainly effluents from the wastewater treatment plant. Several side channels transport a small part through the meadows surrounding the main

channel. Fish ladders are indicated by red zigzag lines. Segment numbers are indicated by circled numbers. For reference, location Heidemühle Bridge is at 52°28'48.1"N, 13°38'12.1"E.

Tracer injections were performed on 16 and 21 June 2016 during daytime when discharge in the Erpe was most stable. Photodegrading effects on raz were assumed negligible due to cloudy weather (Haggerty *et al.*, 2008). Tracer slugs were prepared for each injection by dissolving approximately 25 grams of uranine (Fluka Chemicals, Seelze, DE) and 75 grams of resazurin (Apollo Scientific, Stockport, UK) into 10 liters of stream water, targeting an instream concentration of 33 µg/l and 100 µg/l for ura and raz, respectively. Slugs were instantaneously released across the width of the channel at the injection point, giving a 246-metre mixing length (Figure 3-1) to station 1.

Tracer breakthrough curves (BTC) were truncated below 0.1 µg/l (Lemke *et al.*, 2013a). Flow metrics were calculated from the truncated conservative tracer BTCs for each segment (Ward *et al.*, 2013; Schmadel *et al.*, 2016). Recovered mass was estimated by numerically integrating the area under the conservative tracer BTC. Advective time t_{ad} was calculated as the time from tracer injection to t_{peak}. The window of detection t_w was calculated as time of first tracer arrival t_1 to t_{99}, where 99% of tracer mass has passed and is normalised by dividing by t_{ad}. All temporal and statistical moments were calculated using normalised tracer masses:

$$c(t) = \frac{C(t)}{\int_{t=0}^{t=99} C(t)dt}, \qquad \text{Equation 3-1}$$

where *C(t)* is the total tracer mass that passed through a given segment and *c(t)* is the normalised tracer mass. The first temporal moment (central moment) is an estimate of mean tracer arrival time was calculated as:

$$M_1 = \int_{t=0}^{t=99} tc(t)dt$$ Equation 3-2

The n^{th} moments for $n>1$ were calculated as:

$$\mu_n = \int_{t=0}^{t=99} (t - M_1)^n c(t)dt$$ Equation 3-3

The second and third temporal moments (μ_2 and μ_3) were used to calculate skewness γ, which is a measure for the late time tailing of the BTC relative to symmetrical spreading:

$$\gamma = \frac{\mu_3}{\mu_2^{3/2}}$$ Equation 3-4

To estimate the amount of transient storage in a reach, the time necessary for tracer concentrations to fall back to background concentrations was calculated as the transient storage index, normalised for t_{ad} to standardise advective variations:

$$TSI = \frac{(t_{99} - t_{peak})}{t_{ad}}$$ Equation 3-5

Microbial respiration R_{coeff} (hr^{-1}) was calculated per reach segment, based on raz turnover, as:

$$R_{coeff} = \frac{ln\left(m_0^{up} / m_0^{down}\right)}{\tau}$$ Equation 3-6

where τ is the travel time within a given segment between the upstream and downstream segment calculated as $t_{ad,downstream}$-$t_{ad,upstream}$, based on the conservative tracer BTCs

(González-Pinzón & Haggerty, 2013; González-Pinzón *et al.*, 2014) and zeroth moment m_0 is the mass of raz at the upstream and downstream end of a given reach. Dividing raz turnover by reach length allows for comparison between treatments where a difference in residence time is expected. All above metrics were calculated from the conservative tracer BTCs.

Relationships between before and after treatment of parameters were compared by type III sums of squares two-way ANOVA according to a simple unbalanced before-after-control-impact (BA*CI) design in the form of $y = BA + CI + (BA:CI)$, where *BA* represents the effect for before and after the mowing treatment and *CI* the effect for control and impact sites (Schwarz 2018). Results of the ANOVA are reported as an estimated effect of the BACI treatment as estimated changes of the means of the dependent variables of interest estimated by least-square means, along with a standard error and 95% confidence interval estimated from the least-square means method. Other parameters were analysed by a two-tailed T-test. Results between different parameters were compared by simple linear regression shown with R^2 or nonlinear least squares regression where the model was selected according to the lowest standard residual error. Other results are shown with their standard deviations.

3.3. Results

Mean macrophyte density was 176.18±87.31 g m^{-2} dry biomass, based on 3 random plots inside the study area. Dominant species were *Stuckenia pectinate* (80%), *Callitriche hamuata* (12%) and *Sparganium emersum* (7%). Macrophyte mowing removed an estimated 75% of biomass inside the stream and, based on visual inspection, perturbed the top layer of the streambed sediment. Water turbidity caused by loose sediments went down soon after mowing had finished (the same day) and was similarly low during both tracer injections.

Table 3-1. Overview of important parameter results, before and after mowing, with one standard deviation.

	Mowed		*Unmowed*	
	Before	**After**	**Before**	**After**
Mean discharge (m^3/s) [1]	0.65±0.02	0.63±0.03	0.82±0.02	0.84±0.02
Flow velocity (m/s)	0.15±0.05	0.21±0.06	0.11±0.02	0.11±0.02
Travel time total (hour) [2,3]	3.97	2.69	1.47	1.45
TSI (hour)	0.869±0.244	0.927±0.244	0.494±0.101	0.448±0.162
Skewness (gamma)	0.375±0.128	0.589±0.211	0.456±0.139	0.437±0.007
R_{coeff} (hr^{-1})	0.077±0.055	0.072±0.030	0.060±0.003	0.041±0.009
R_{coeff} (m^{-1}) (* 10^{-3})	0.132±0.062	0.10±0.043	0.156±0.032	0.100±0.009
[1] Mean discharge during passing of solute BTC				
[2] From injection to first moment (M1) at station 2				
[3] From M1 at station 2 to arrival at station 7				

Discharge was similar during both experiments in all segments (Table 3-1/Figure 3-2). Flow velocity increased in the mowed segments by 0.055±0.065 m s^{-1} (38%), although the treatment effect was not significant (F(2,10); p=0.417). Flow velocity remained similar in the unmowed segments. Total travel time was substantially reduced in the mowed section of the river: after macrophyte removal, travel time of the solute tracer was only 66% of the time before removal. The difference was not significantly different by comparison with a t-test. Travel time in the unmowed section was similar before and after and was only slightly lower.

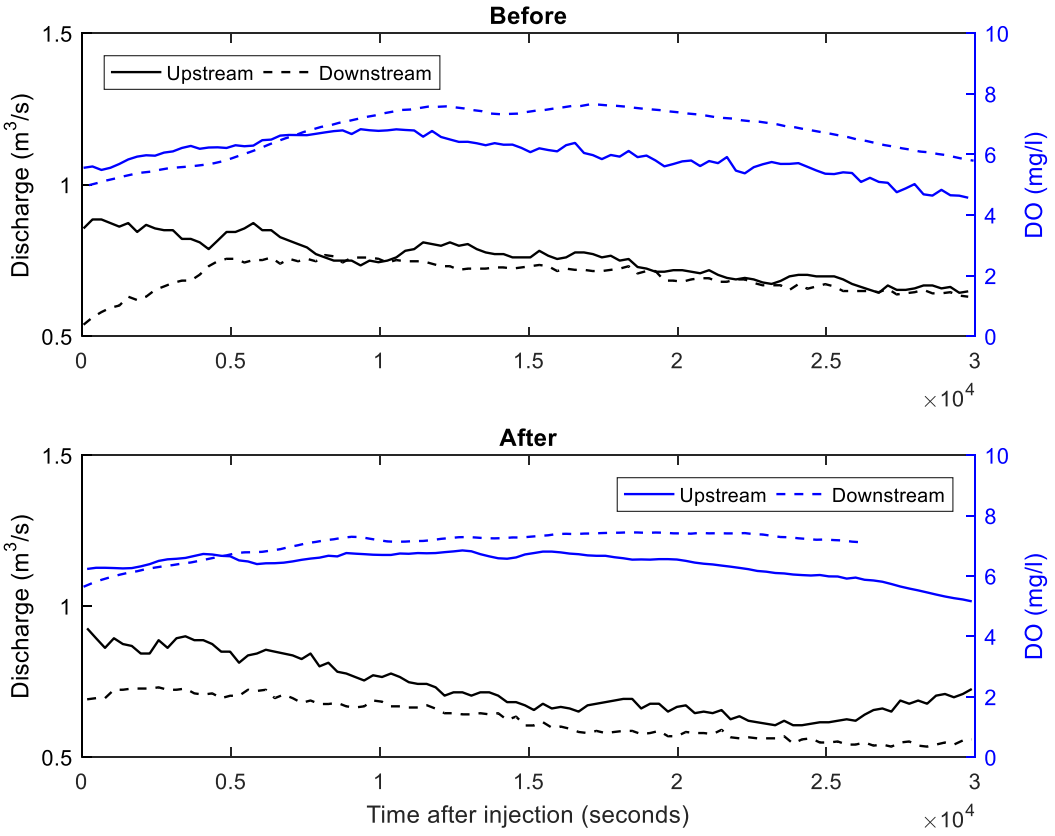

Figure 3-2. Discharge and dissolved oxygen concentrations during the tracer injections. Discharge is displayed for stations 2 and 7 (see Figure 3-1) for upstream and downstream, respectively. DO was measured at stations 2 (upstream), and 6 (downstream). Downstream DO logger data after vegetation removal was incomplete near the end of measurements.

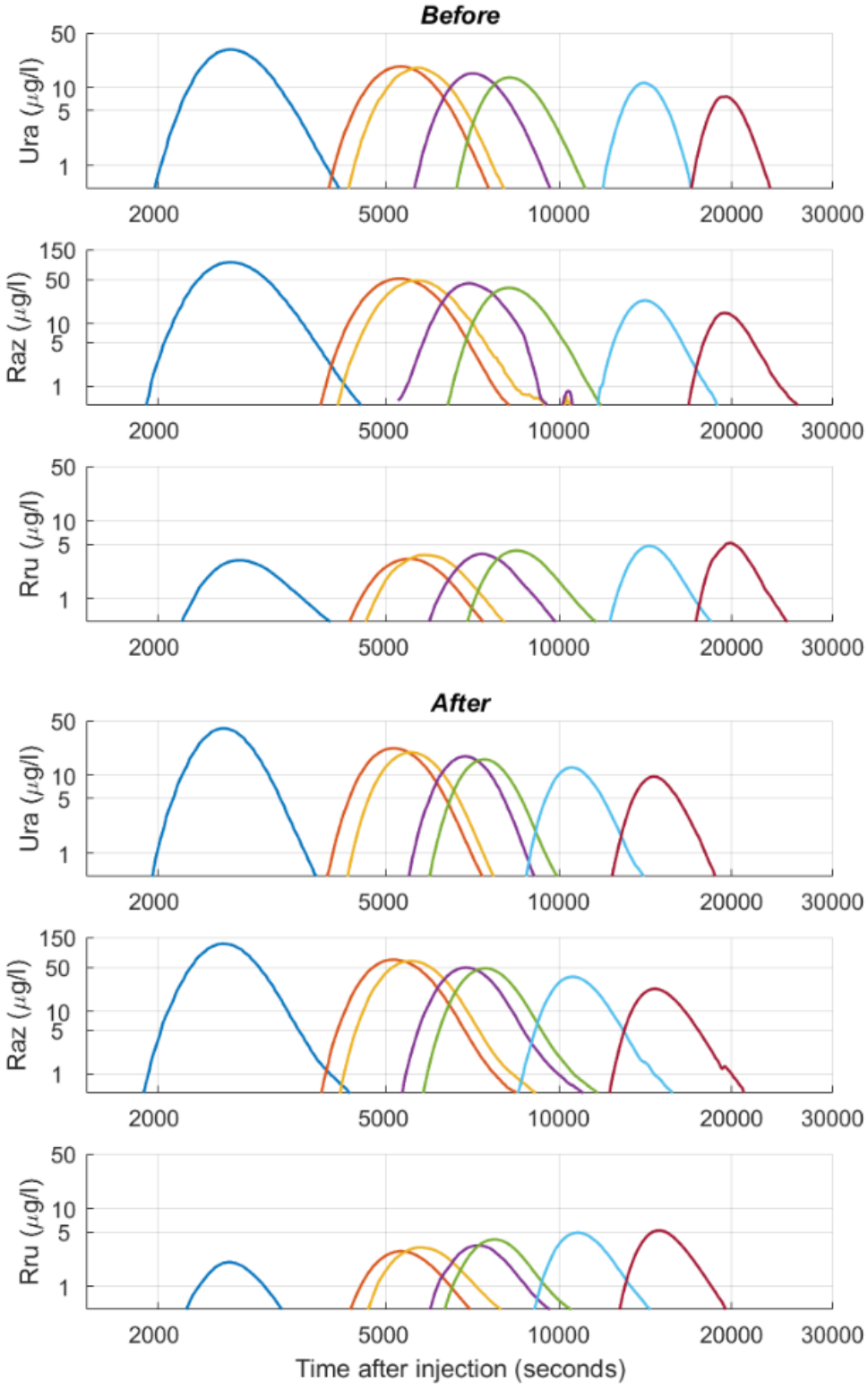

Figure 3-3. Breakthrough curves (BTC) for uranine and resazurin tracer injections, and the formed daughter compound resorufin (logarithmic axes). Above are BTCs before macrophyte removal and below are results after removal. BTC colours correspond incrementally to individual segments, from segment 1 on the left (blue) to segment 7 on the right (burgundy).

The solute BTC passed quicker after removing the vegetation (Figure 3-3). The (normalised) window of detection $t_{w,norm}$ of the conservative tracer BTC decreased after mowing by 0.050±0.076 (corresponding to 0.39 hours or 17%) in the mowed segments (Figure 3-4b), while $t_{w,norm}$ in the unmowed segments remained unchanged. The decrease in the mowed segments due to the treatment was not significant (*F(2,10); p = 0.75*).

Advective time, t_{ad}, was compared before and after removal (Figure 3-4a) and decreased on average by 12% in the mowed section with increasing difference towards the most downstream stations 6 and 7, while t_{ad} decreased only 4.4% in the unmowed segments 1 and 2. The decrease in the mowed section after treatment was not significant ($t(4) = 1.6093$, $p = 0.1828$, $n = 5$).

Skewness γ of the solute BTC increased due to mowing of vegetation by 0.23±0.22 (57%), while the unmowed section was on average slightly lower by 4% (Figure 3-5a). Although the change in γ was substantial, it was not significant (*F(2,10); p = 0.32*). The largest increase in γ occurred in the downstream segments 5 and 6. While a decrease of 8.6% in transient storage (normalised for t_{ad} shown in Figure 3-4a) was observed in the unmowed segments, removal of macrophytes led to an increase in (normalised) transient storage of 0.065±0.057 (15%) in the mowed segments. Segments with the largest increase were the most downstream segments 5 through 7. Although the increased TSI_{norm} in mowed segments was not significant (*F(2,10); p = 0.28*), removal of storage capacity within macrophyte stands leading to increased TSI was unexpected. Transient storage increased linearly and significantly with advective time (Figure 3-5d), described by a simple linear regression model ($F(1, 12) = 84.94$, $p < 0.001$, $R^2 = 0.7883$, $n = 14$).

Mean dissolved oxygen concentrations were similar before and after macrophyte removal in all instrumented segments (Figure 3-6a). Generally increasing DO concentrations were measured from the WWTP in downstream direction, with the highest DO increase measured in the first three segments of the river. Later segments are more clustered, but not strongly affected by mowing. Dissolved oxygen varied throughout the river and highest concentrations were found in locations with lowest discharge (Figure 3-6b). The relationship could be described by a significant simple linear regression model ($F(1, 8) = 84.94$, $p < 0.001$, $R^2 = 0.9139$, $n = 10$), both before and after macrophyte removal.

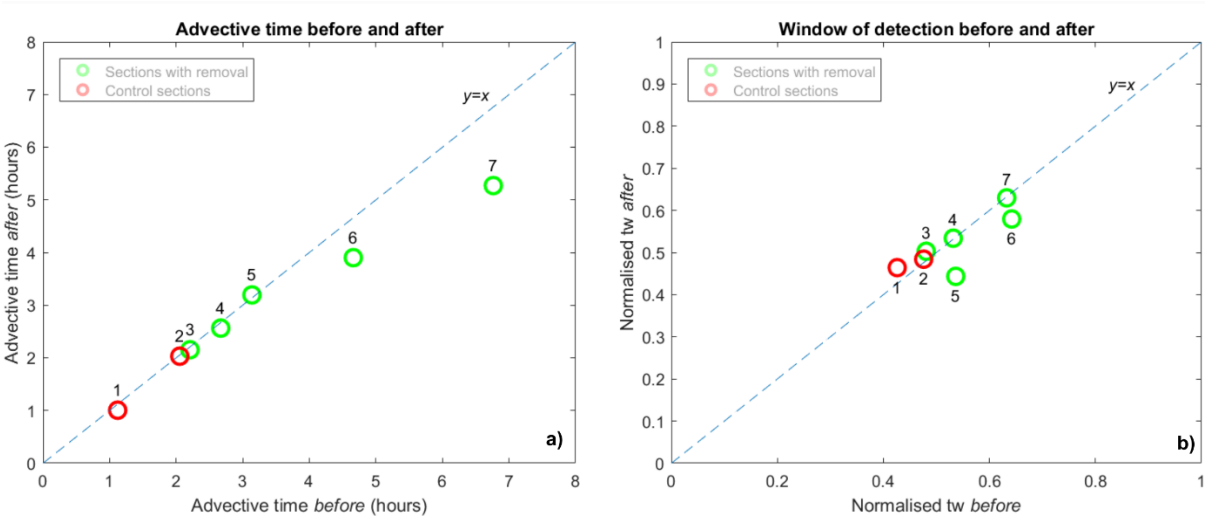

Figure 3-4. **a)** Change in advective time (hours), before and after macrophyte removal. Segment numbers indicated at points. t_{ad} were calculated from conservative tracer uranine. **b)** Comparison of the window of detection (t_w), before and after macrophyte removal normalised by advective time t_{ad}.

Macrophyte removal did not lead to a notable increase in minimum diel dissolved oxygen during the night, which was in the unmowed segments 2.05±0.45 mg l^{-1} and 2.48±0.08 mg l^{-1} before and after removal, respectively, and in the mowed segments 2.03±0.47 mg l^{-1} and 2.32±1.93 mg l^{-1} before and after removal, respectively. When comparing R_{coeff}, macrophyte removal caused a slight and insignificant decrease of 6% in respiration activity normalised

for residence time per reach (Equation 3-6). When R_{coeff} was normalised for reach length, respiration per meter decreased by approximately 25% in the mowed segments.

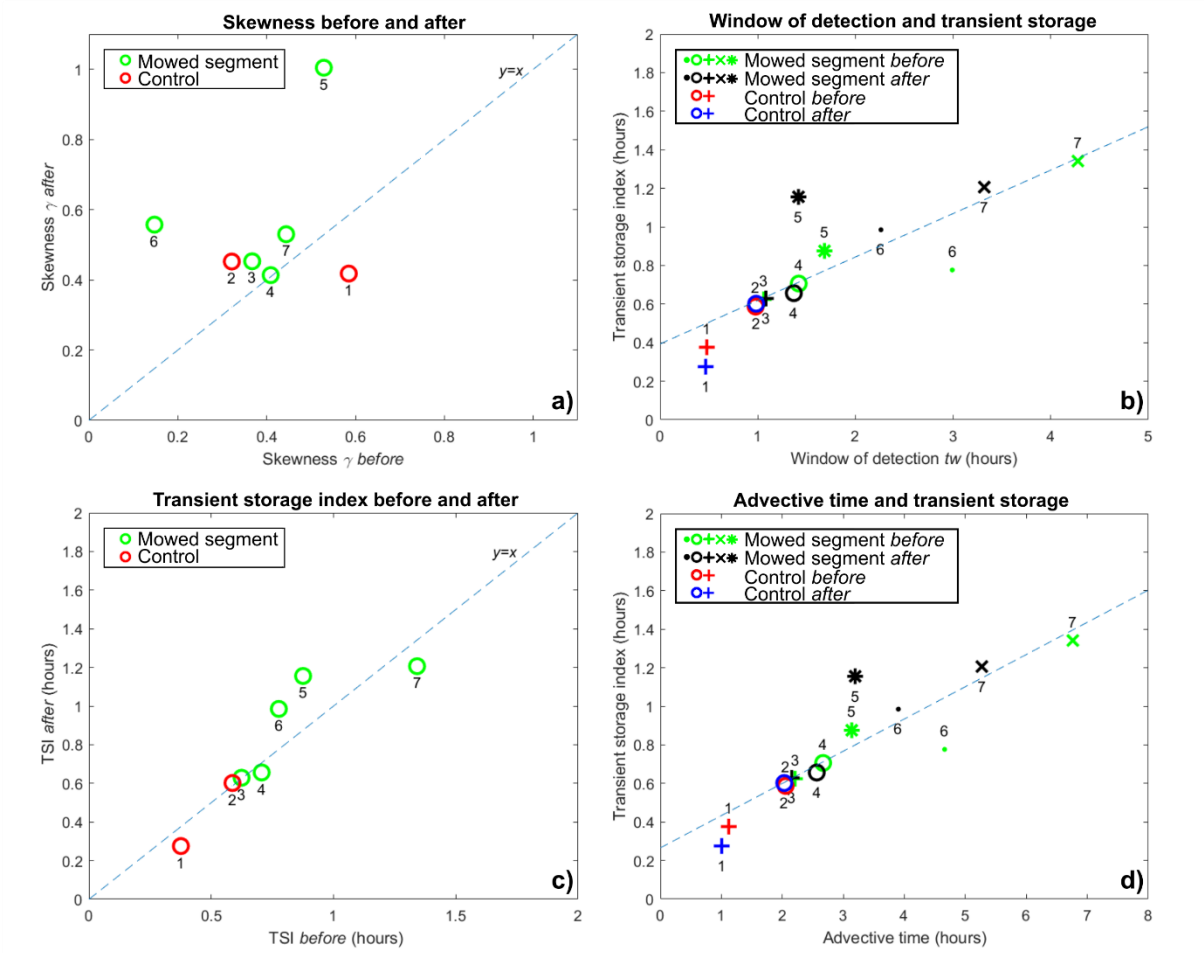

Figure 3-5. **a)** Change in skewness γ of the solute breakthrough curves of the conservative tracer, before and after vegetation removal. **b)** Window of detection time t_w and transient storage index (*TSI*). A simple linear regression model describing the relation is drawn. **c)** Change in *TSI*, before and after vegetation removal. **d)** Advective time t_{ad} and *TSI*. A simple linear regression model describing the relation is drawn.

Respiration in each segment varied, although mowing effects were different for each segment (Figure 3-7a). In the mowed section, R_{coeff} decreased slightly after mowing by 5.7%. However, in the unmowed section a substantially stronger decrease of 32% was observed in R_{coeff}. Therefore, corrected for the treatment effect according to the BA*CI analysis (see section 3.2. Methods), the observed change due to the treatment actually corresponded to a

slight increase of 0.014±0.05 hr^{-1}, although this change was not significant (*F(2,10); p* = 0.80). When comparing R_{coeff} normalised for reach length (Figure 3-7b), we found that there was a negligible difference of 0.002±0.02 m^{-1} as R_{coeff} normalised for length, which was not significant after correcting for treatment effects (*F(2,10); p = 0.91*). A decrease in R_{coeff} was observed that was less strong in mowed segments. The difference in decrease was less pronounced between mowed and unmowed segments, with 25% and 36%, respectively, which was not significant ($t(4) = 1.9918$, $p = 0.1172$, $n = 5$). Both methods suggest more microbially active segments after macrophyte mowing.

Table 3-2. Respiration coefficients per segment normalised for travel time and length.

R_{coeff}		***Before***		***After***		***Change***	
		h^{-1}	$10^{-3}\ m^{-1}$	h^{-1}	$10^{-3}\ m^{-1}$	h^{-1}	$10^{-3}\ m^{-1}$
Unmowed	1	0.063	0.187	0.031	0.091	↓ 51%	↓ 51%
	2	0.056	0.124	0.050	0.109	↓ 11%	↓ 12%
	Mean	*0.060±0.003*	*0.156±0.03*	*0.041±0.01*	*0.10±0.01*	*↓ 32%*	*↓ 36%*
Mowed	3	0.172	0.202	0.116	0.127	↓ 33%	↓ 37%
	4	0.106	0.203	0.097	0.172	↓ 8.6%	↓ 15%
	5	0.023	0.041	0.070	0.065	↑ 205%	↑ 59%
	6	0.042	0.117	0.041	0.064	↓ 2.1%	↓ 46%
	7	0.041	0.101	0.0382	0.0716	↓ 6.1%	↓ 29%
	Mean	*0.077±0.056*	*0.133±0.06*	*0.072±0.03*	*0.100±0.04*	*↓ 5.6%*	*↓ 25%*

When comparing respiration as net raz turnover (Figure 3-7c), a decrease was observed as a result of mowing for all segments except segment 5 (Table 3-2). Respiration was 29% lower in mowed segments and 33% lower in unmowed segments, although this difference was not significant ($t(4) = 1.9292$, $p = 0.16$, $n = 5$).

Higher respiration (R_{coeff}) was generally observed at higher DO concentrations, although a significant relation could not be found using simple linear regression (not shown). The highest respiration activity was not found at the highest DO concentrations (segment 3), but just downstream of a fish ladder and decreased after mowing. Due to missing DO data from stations 4 and 7 this relation cannot be explored further.

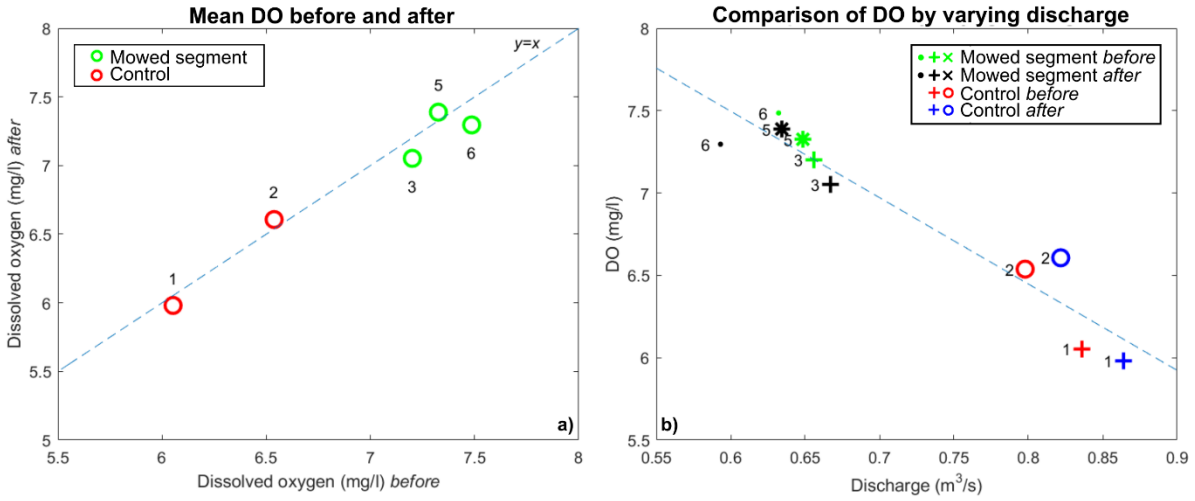

Figure 3-6. **a)** Difference in dissolved oxygen before and after macrophyte removal. **b)** Dissolved oxygen decreased with increasing discharge, described by a simple linear regression model. DO loggers of stations 4 and 7 did not record data and are therefore missing.

To explore possible effects of chosen reach length on estimates of R_{coeff}, several reach segments were combined and R_{coeff} calculated for those combinations. The initial chosen reach segment lengths (no combined segments) reflects the highest variation and captures widest range of microbial metabolic activity across several segments. Higher order

combinations increase the likelihood of masking potential hotspot activity that may take place. The mean R_{coeff} remains the same for all groups and properly reflect total stream respiration.

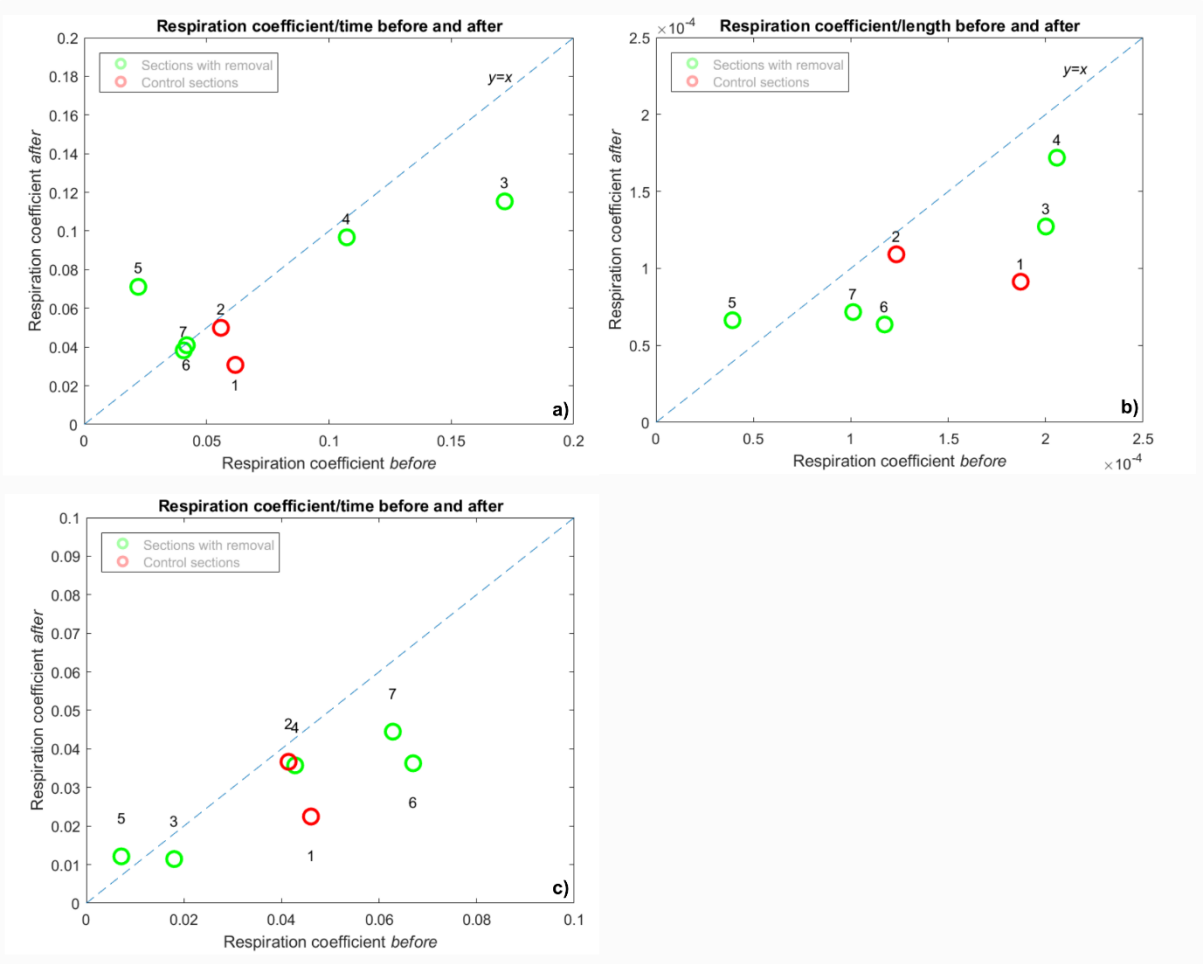

Figure 3-7. **a)** Respiration coefficients normalised for travel (residence) time. Text labels are segment numbers. R_{coeff} were calculated from resazurin turnover inside each segment and compared before and after mowing. **b)** Respiration coefficients normalised for reach length (meters). **c)** Respiration coefficients, as total raz turnover per reach segment.

3.4. Discussion

Removal of macrophytes led to a general decrease in advective time t_{ad} in the Erpe (Figure 3-4a), as was to be expected from the decrease in hydraulic resistance. The difference became larger more downstream. When comparing the times of t_w normalised by t_{ad} (Figure 3-4b), detection time increased after mowing for segments 5 and 6, while segment 7 was again

lower. The most likely explanation would be that for the most downstream station the peak concentrations were lower due to normal advective processes. As a result, a relatively smaller amount of the BTC was above the detection limit of the fluorometer and calculation of t_w may have been less robust.

The results indicate that noticeable changes in storage parameters could be observed resulting from mowing, yet none of them were significant. There was a marginal increase in transient storage for segments 5 and 6, but not for 7. While this increase was unexpected, as macrophyte stands provided storage zones which were removed, improved transient storage after macrophyte removal has previously been observed in a study in Flanders (Verschoren *et al.*, 2017). The authors of the Flanders study hypothesised that the increased transient storage was caused by increased in-channel storage, based on observations of increased longitudinal dispersion in vegetation-free reaches.

The resazurin method was able to pinpoint certain locations that were exhibiting hotspot activity in terms of microbial metabolic activity (Figure 3-7a). The highest respiration coefficients were measured in segments 3,4 and 5 (Figure 3-7a), which were all downstream of and close to fish ladders. Increased aeration due to turbulence or increased hyporheic exchange could have driven the higher respiration, similar to effects observed near large woody debris features (Blaen *et al.*, 2018). An explanation for the strong increase in respiration after mowing in segment 5 could not be identified.

After mowing, respiration in general was lower in all segments, both in mowed and unmowed. However, a 25% decrease in residence (travel) time through the mowed reach only resulted in a decreased respiration coefficient of 6%. R_{coeff} decreased as well in the unmowed segments 1 and 2 after mowing, suggesting that the observed decrease in respiration could

not be attributed directly to the mowing practice. The observed decrease in respiration in the unmowed segments was higher than in the mowed segments, suggesting that the reach metabolic activity was now relatively higher in the mowed segments as a result of the mowing activity. A possible explanation for the generally lower respiration after mowing could be a higher background concentration of pollutants from the WWTP, which was indicated by higher background conductivity (762±103 µS before and 819±62 µS after removal) or a slightly lower water temperature (19.44±0.61°C before and 18.91±0.34°C after removal), or a combination thereof. In other words, the studied section of the river Erpe as a whole was less active after macrophyte removal, but this could have been caused by factors beyond the scope of this experiment.

Surprisingly, R_{coeff}, which is normalised for travel time (Equation 3-6), did not decrease substantially nor significantly at all. Any observed effects were no worse than mild. A direct relation between TSI and R_{coeff} could not be found, although increased TSI may very well have played an important role by facilitating the increased respiration. By removing macrophytes, vertical water exchange may have improved (Heffernan *et al.*, 2008), e.g. by stronger hydrodynamically driven hyporheic exchange due to higher flow velocity over bedforms (Boano *et al.*, 2007), and thus forcing more water through the hyporheic zone. Improved hyporheic exchange also provides an explanation for the observed increase in skewness γ of the BTCs. Where previous work found similar results for increased transient storage after mowing and found the explanation in higher channel storage due to higher dispersion (Verschoren *et al.*, 2017), the results of this study support the hypothesis that increased TSI was due to increased exchange with the streambed. Although speculative, we find an explanation in the fact that respiration did not significantly decrease, especially considering the fact that the control section was much less active. If indeed more water was

exchanged with the streambed, this could explain this potentially buffering effect that was observed.

Macrophyte mowing may also have reduced clogging effects and improved potential for hyporheic exchange and microbial respiration (Nogaro *et al.*, 2010) by slightly ploughing the top of the streambed. Absence of macrophytes also improves water mixing, facilitated by lower water depth and higher flow velocities that can improve hyporheic exchange (Gomez-Velez *et al.*, 2014; Fox *et al.*, 2016), assuming a heterogeneous streambed structure.

Based on the presented results, the hypothesis is that macrophytes on the riverbed provide transient storage, but at shorter timescales than storage by hyporheic exchange. Macrophytes interfere with hyporheic exchange by reducing flow velocity, in particular close to the streambed. By mowing, the actual hyporheic exchange is improved and opens up a higher potential for nutrient attenuation inside the sediments colonised with microbial communities. Macrophyte stands are not always related to nutrient cycling (O'Brien *et al.*, 2014). By using mowing baskets, roots remain in the streambed and can serve as biofilm substrates. Nutrients such as ammonium and phosphates can be fixed by macrophytes (Castaldelli *et al.*, 2015; Levi *et al.*, 2015; García *et al.*, 2017) and then physically removed by mowing, which potentially leads to a net decrease of excess nutrients from stream water.

The dataset collected in this study was limited in size due to the cost of the tracer injections of raz in particular and the time available to perform the experiments as to not disturb other projects that were taking place in the river at the time. This may have led to a smaller dataset that would have been preferred with respect to the robustness of statistical analysis. Although other data analysis, such as PERMANOVA, was considered but dismissed as it is not always robust for unbalanced designs (Anderson *et al.*, 2013). Therefore, ANOVA was preferred

following the BA*CI procedure suggested by Schwarz (2018). Furthermore, in the case of a univariate analysis, a permutational test such as the PERMANOVA will give similar information as a univariate ANOVA (Anderson, 2001). Therefore, ANOVA was chosen as the test using type III sums of squares to correctly deal with the unbalanced data set from this study. Future studies could take into account a more balanced distribution of measurements between control and impact sites, which in this study was complicated due to the presence of other experiments in the reach that could not be disturbed. By combining mowing practices as a management practice with other measures to increase hyporheic exchange, such as improving sinuosity of a stream and adding large woody debris features or alternating mowing patterns (Vereecken *et al.*, 2006; Verschoren *et al.*, 2017), microbial respiration and pollutant attenuation could be further optimised. This could potentially be the best strategy to improve attenuation and maintain a sufficient storage capacity to safely deal with peak flows. While annual mowing of reaches may disturb the habitat in ways beyond the scope of this study, streambed environments appear to remain supportive for microbial metabolic activity in that is associated with the upper sediment layer (Hedin, 1990; O'Brien *et al.*, 2014; Alnoee *et al.*, 2016).

3.5. Conclusions

Macrophyte removal is a common management practise in urban streams to maintain good flow. This study measured impacts of such an application. Macrophytes were removed by mowing in an urban stream receiving a majority of its flow from wastewater treatment plant effluents. Contrary to what was expected, removal of macrophyte vegetation did not lead to significant reductions of transient storage. While increases in flow velocity were observed as expected, transient storage increased slightly. Although a generally lower respiration was observed, this relative decrease was much smaller than expected and mowed segments were

relatively less affected by mowing than unmowed segments. Contrasting previous research, we hypothesise that the increase in transient storage was attributed to improved hyporheic exchange due to a lack of vegetation. Consequently, stream water was exchanged with another storage compartment of higher quality where relatively larger or more active microbial communities are located. Although this conclusion is somewhat speculative, it provides a plausible explanation for both the increased transient storage and largely unchanged, and even slightly increased, respiration as a result of the macrophyte removal that were observed in this study. Macrophyte removal did not lead to significant losses of stream microbial activity and may therefore not significantly alter a streams' potential for nutrient and pollutant attenuation. Further research is suggested to confirm the potential impact of the increases in transient storage on nutrient cycling. The results of this study may be used to further improve management strategies, such as alternating mowing schedules.

Acknowledgements

We would like to thank Malte Posselt for providing the macrophyte species data, and Anna Jäger and Andrea Betterle for providing the discharge data and rating curves. This project has received funding from the European Union's Seventh Framework Programme for research, technological development and demonstration under grant agreement no 607150 as well as the European Union's H2020-MSCA-RISE-2016 project under grant agreement no 734317.

Author contributions

PR wrote the manuscript and was responsible for designing and conceptualising the study, performing the experiments, data collection and analysis. DMH provided support with manuscript revisions. SK instigated the study and advised on the experimental design and the

conceptualisation of the results, and supported the data analysis, interpretation, and manuscript revisions.

References

Alnoee AB, Riis T, Baattrup-Pedersen A (2016) Comparison of metabolic rates among macrophyte and nonmacrophyte habitats in streams. *Freshwater Science*, **35**, 834–844.

Anderson, M. J. (2001). A new method for non-parametric multivariate analysis of variance. Austral Ecology, **26**(1), 32–46. https://doi.org/10.1046/j.1442-9993.2001.01070.x

Anderson, M. J., & Walsh, D. C. I. (2013). PERMANOVA, ANOSIM, and the Mantel test in the face of heterogeneous dispersions: What null hypothesis are you testing? Ecological Monographs, **83**(4), 557–574. https://doi.org/10.1890/12-2010.1

Argerich A, Haggerty R, Martí E, Sabater F, Zarnetske JP (2011) Quantification of metabolically active transient storage (MATS) in two reaches with contrasting transient storage and ecosystem respiration. *Journal of Geophysical Research: Biogeosciences*, **116**.

Baattrup-Pedersen A, Göthe E, Riis T, O'Hare MT (2016) Functional trait composition of aquatic plants can serve to disentangle multiple interacting stressors in lowland streams. *Science of the Total Environment*, **543**, 230–238.

Baranov V, Lewandowski J, Romeijn P, Singer G, Krause S (2016a) Effects of bioirrigation of non-biting midges (Diptera: Chironomidae) on lake sediment respiration. *Scientific Reports*, **6**, 27329.

Baranov V, Lewandowski J, Krause S (2016b) Bioturbation enhances the aerobic respiration of lake sediments in warming lakes. *Biology letters*, **12**, 269–281.

Blaen PJ, Brekenfeld N, Comer-Warner S, Krause S (2017) Multitracer Field Fluorometry: Accounting for Temperature and Turbidity Variability During Stream Tracer Tests. *Water Resources Research*, **53**, 9118–9126.

Blaen PJ, Kurz MJ, Drummond JD et al. (2018) Woody debris is related to reach-scale hotspots of lowland stream ecosystem respiration under baseflow conditions. *Ecohydrology*, e1952.

Boano F, Revelli R, Ridolfi L (2007) Bedform-induced hyporheic exchange with unsteady

flows. *Advances in Water Resources*, **30**, 148–156.

Brown RR, Keath N, Wong THF (2009) Urban water management in cities: historical, current and future regimes. *Water Science and Technology*, **59**, 847–855.

Castaldelli G, Soana E, Racchetti E, Vincenzi F, Fano EA, Bartoli M (2015) Vegetated canals mitigate nitrogen surplus in agricultural watersheds. *Agriculture, Ecosystems & Environment*, **212**, 253–262.

Cotton JA, Wharton G, Bass JAB, Heppell CM, Wotton RS (2006) The effects of seasonal changes to in-stream vegetation cover on patterns of flow and accumulation of sediment. *Geomorphology*, **77**, 320–334.

Fox A, Laube G, Schmidt C, Fleckenstein JH, Arnon S (2016) The effect of losing and gaining flow conditions on hyporheic exchange in heterogeneous streambeds. *Water Resources Research*, **52**, 7460–7477.

García VJ, Gantes P, Giménez L, Hegoburu C, Ferreiro N, Sabater F, Feijoó C (2017) High nutrient retention in chronically nutrient-rich lowland streams. *Freshwater Science*, **36**, 26–40.

Gomez-Velez JD, Krause S, Wilson JL (2014) Effect of low-permeability layers on spatial patterns of hyporheic exchange and groundwater upwelling. *Water Resources Research*, **50**, 5196–5215.

González-Pinzón R, Haggerty R (2013) An efficient method to estimate processing rates in streams. *Water Resources Research*, **49**, 6096–6099.

González-Pinzón R, Haggerty R, Argerich A (2014) Quantifying spatial differences in metabolism in headwater streams. *Freshwater Science*, **33**, 798–811.

González-Pinzón R, Peipoch M, Haggerty R, Martí E, Fleckenstein JH (2016) Nighttime and daytime respiration in a headwater stream. *Ecohydrology*, **9**, 93–100.

Gooseff MN, Hall RO, Tank JL (2007) Relating transient storage to channel complexity in streams of varying land use in Jackson Hole, Wyoming. *Water Resources Research*, **43**.

Haggerty R, Argerich A, Martí E (2008) Development of a "smart" tracer for the assessment of microbiological activity and sediment-water interaction in natural waters: The resazurin-resorufin system. *Water Resources Research*, **44**, W00D01.

Haggerty R, Martí E, Argerich A, Von Schiller D, Grimm NB (2009) Resazurin as a "smart"

tracer for quantifying metabolically active transient storage in stream ecosystems. *Journal of Geophysical Research: Biogeosciences*, **114**.

Hedin LO (1990) Factors Controlling Sediment Community Respiration in Woodland Stream Ecosystems. *Oikos*, **57**, 94.

Heffernan JB, Sponseller RA, Fisher SG (2008) Consequences of a biogeomorphic regime shift for the hyporheic zone of a Sonoran Desert stream. *Freshwater Biology*, **53**, 1954–1968.

Hellström D, Jeppsson U, Kärrman E (2000) A framework for systems analysis of sustainable urban water management. *Environmental Impact Assessment Review*, **20**, 311–321.

Hensley RT, Cohen MJ (2012) Controls on solute transport in large spring-fed karst rivers. *Limnology and Oceanography*, **57**, 912–924.

Kaenel BR, Matthaei CD, Uehlinger U (1998) Disturbance by aquatic plant management in streams: Effects on benthic invertebrates. *Regulated Rivers: Research & Management*, **14**, 341–356.

Kaenel BR, Buehrer H, Uehlinger U (2000) Effects of aquatic plant management on stream metabolism and oxygen balance in streams. *Freshwater Biology*, **45**, 85–95.

Kantrud H (1990) *Sago pondweed (Potamogeton pectinatus L.): a literature review*.

Knapp JLA, Cirpka OA (2017) Determination of hyporheic travel time distributions and other parameters from concurrent conservative and reactive tracer tests by local-in-global optimization. *Water Resources Research*, **53**, 4984–5001.

Lemke D, Liao Z, Wöhling T, Osenbrück K, Cirpka O a. (2013b) Concurrent conservative and reactive tracer tests in a stream undergoing hyporheic exchange. *Water Resources Research*, **49**, 3024–3037.

Lemke D, Schnegg P-A, Schwientek M, Osenbrück K, Cirpka O a. (2013a) On-line fluorometry of multiple reactive and conservative tracers in streams. *Environmental Earth Sciences*, **69**, 349–358.

Levi PS, Riis T, Alnøe AB, Peipoch M, Maetzke K, Bruus C, Baattrup-Pedersen A (2015) Macrophyte complexity controls nutrient uptake in lowland streams. *Ecosystems*, **18**, 914–931.

Madsen JD, Chambers PA, James WF, Koch EW, Westlake DF (2001) The interaction

between water movement, sediment dynamics and submersed macrophytes. *Hydrobiologia*, **444**, 71–84.

Marlow DR, Moglia M, Cook S, Beale DJ (2013) Towards sustainable urban water management: A critical reassessment. *Water Research*, **47**, 7150–7161.

Nogaro G, Datry T, Mermillod-Blondin F, Descloux S, Montuelle B (2010) Influence of streambed sediment clogging on microbial processes in the hyporheic zone. *Freshwater Biology*, **55**, 1288–1302.

O'Brien JM, Lessard JL, Plew D, Graham SE, McIntosh AR (2014) Aquatic Macrophytes Alter Metabolism and Nutrient Cycling in Lowland Streams. *Ecosystems*, **17**, 405–417.

Ochs K, Rivaes RP, Ferreira T, Egger G (2018) Flow Management to Control Excessive Growth of Macrophytes – An Assessment Based on Habitat Suitability Modeling . *Frontiers in Plant Science* , **9**, 356.

Paul MJ, Meyer JL, Booth DB, Bledsoe BP, Gregory J, Chin K (2001) Streams in the Urban Landscape. *Annual Review of Ecology and Systematics*, **32**, 333–365.

Riis T, Dodds WK, Kristensen PB, Baisner AJ (2012) Nitrogen cycling and dynamics in a macrophyte-rich stream as determined by a release. *Freshwater Biology*, **57**, 1579–1591.

Sand-Jensen K (1998) Influence of submerged macrophytes on sediment composition and near-bed flow in lowland streams. *Freshwater Biology*, **39**, 663–679.

Schmadel NM, Ward AS, Kurz MJ et al. (2016) Stream solute tracer timescales changing with discharge and reach length confound process interpretation. *Water Resources Research*, **52**, 3227–3245.

Schwarz, C. J. (2018). Course Notes for Beginning and Intermediate Statistics. Department of Statistics and Actuarial Science, Simon Fraser University. Retrieved from http://www.stat.sfu.ca/~cschwarz/CourseNotes

Vereecken H, Baetens J, Viaene P, Mostaert F, Meire P (2006) Ecological management of aquatic plants: Effects in lowland streams. *Hydrobiologia*, **570**, 205–210.

Verschoren V, Schoelynck J, Cox T, Schoutens K, Temmerman S, Meire P (2017) Opposing effects of aquatic vegetation on hydraulic functioning and transport of dissolved and organic particulate matter in a lowland river: A field experiment. *Ecological Engineering*, **105**, 221–230.

Ward AS, Gooseff MN, Voltz TJ, Fitzgerald M, Singha K, Zarnetske JP (2013) How does rapidly changing discharge during storm events affect transient storage and channel water balance in a headwater mountain stream? *Water Resources Research*, **49**, 5473–5486.

Wilcock RJ, Champion PD, Nagels JW, Croker GF (1999) The influence of aquatic macrophytes on the hydraulic and physico-chemical properties of a New Zealand lowland stream. *Hydrobiologia*, **416**, 203–214.

Chapter 4. Groundwater flooding induced fertilisation and enhanced microbial metabolic activity of a dual-porosity aquifer system

Paul Romeijn, Anne Robertson, Julia Reiss, David M. Hannah, Stefan Krause

Abstract

Chalk aquifers in southern UK are important water resources used for drinking water production. Recharge with water from the surface to the aquifer mainly happens along fractures in the rock, causing sensitivity to rainfall events. In the case of prolonged rainfall, groundwater tables can rise high enough to cause flooding. The effects of groundwater flooding during the winter of 2013/2014 were investigated for possible effects of fertilisation on microbial communities that exist in groundwater. Microbial metabolic activity (MMA) was found to be higher at locations that were more directly affected by higher groundwater depth. Where water in boreholes was closer to the surface, MMA was found to be higher. Dissolved organic carbon was identified as the most important cause of increased MMA. Although nitrate concentrations were measured and higher during flooded situations, no relation between MMA and nitrate could be found. The results of this study can help understand how flooding events and increased water inputs can cause periods of reduced water quality inside aquifers.

4.1. Introduction

Groundwater aquifers are major water resources globally, used for drinking water and irrigation. Due to this use, the status of the quantity and quality of the water inside the

groundwater (GW) aquifers is important. In addition to the human consumption, the aquifers are also important for the GW habitat.

GW recharge is being investigated because of its importance for sustaining water supply. While aquifer recharge studies have focused on periods of drought (e.g. Darling *et al.*, 2012), less have focused on flooding events. However, with observed increase in winter precipitation and in the frequency of extreme events (Osborn *et al.*, 2000; Herrera-Pantoja & Hiscock, 2008), consequences of climate change on groundwater have not received as much attention (IPCC, 2014). Flooding events can be expected to include variations in groundwater level fluctuation, alteration of groundwater flow regimes (Scibek & Allen, 2006) and changes in the volume and quality of groundwater resources (Sherif & Singh, 1999; Brouyère *et al.*, 2004; Bloomfield *et al.*, 2006; Ranjan *et al.*, 2006a, 2006b).

The predicted climate change impact on GW recharge varies based on land use, vegetation types and soil thickness (Jackson *et al.*, 2011). Increased precipitation may increase the risk of groundwater flooding, where the groundwater table reaches above the soil surface and causes inundation (Robins & Finch, 2012). Effects of flood risks are mainly focused on water quantity (Macdonald *et al.*, 2012), despite observed biological responses to water quality in similar systems (Valett *et al.*, 2005; Hemme *et al.*, 2010). Although reports of extreme cases of groundwater flooding are rare, these occurrences had significant economic and social costs (Kreibich & Thieken, 2008; Macdonald *et al.*, 2008; Hughes *et al.*, 2011; Gotkowitz *et al.*, 2014; Fürst *et al.*, 2015). In recent years there has been progress in the field of GW flooding risk management (Cobby *et al.*, 2009; Naughton *et al.*, 2017). GW flood events can have implications for drinking water supply companies too. Flood events can create influxes of high-turbidity water into an aquifer, disrupting water supply to meet quality standards and costing the companies millions (Rivett *et al.*, 2007).

In general, the chemical signature of aquifer water is characterised by the land use above or near it (Banks *et al.*, 1995; Kim & Park, 2016). Consequently, microbial communities in aquifers have been observed to reflect land use (Kim *et al.*, 2015) or heavy metal pollution (Hemme *et al.*, 2010). While chemical response to flood pulses have been observed, the impacts of these fluxes on the microbial communities and their responses have rarely been studied, despite possible impacts on water turbidity and quality and the risk of contamination by microbes (Kistemann *et al.*, 2002).

During the aftermath of a period with a high number of GW floods in the UK, GW tables were substantially raised for up to several months (Muchan *et al.*, 2015). The aim of this study was to study the effects of a groundwater flood event on the fertilisation of the microbial communities in aquifers. It is hypothesised that pulses of nutrient inputs from the surface associated with groundwater flood events can cause increased microbial metabolic activity in groundwater aquifer, which may have implications for drinking water supply.

4.2. Methods

4.2.1. Groundwater boreholes and time series

For the analyses of groundwater flood dynamics and impacts, eight groundwater boreholes were analysed in Southwestern UK (Figure 4-1; Table 4-1). The boreholes were sampled from May 2014 to October 2014, as GW response to extreme water weather events are slow to respond, similar to drought events (Darling *et al.*, 2012). Groundwater microbial metabolic activity was measured by laboratory incubation. Borehole locations were located in Dorset and Berkshire, sampling water from Chalk aquifers. The groundwater aquifers are characterised as dual-porosity, where larger fracture systems in the rock have different hydraulic conductivity than the larger surrounding matrix, making them prone to flooding during high inputs of water from the surface (Pinault *et al.*, 2005). Land use in all borehole

surroundings is similar, predominantly agricultural land and pasture. Berkshire boreholes were on average deeper than Dorset boreholes (Table 4-1).

Sampling started three months after the highest water level of the January 2014 floods, thus the retreat towards baseline levels was observed. However, chemistry signatures were still present. Timeseries of GWD were obtained from the British Geological Survey for the past 10 years (Figure 4-1). One borehole in the catchment, Windmill Burrows (WM), collapsed early June 2014 and was substituted by the nearby Marley Bottom (MB). No time series are shown for WM.

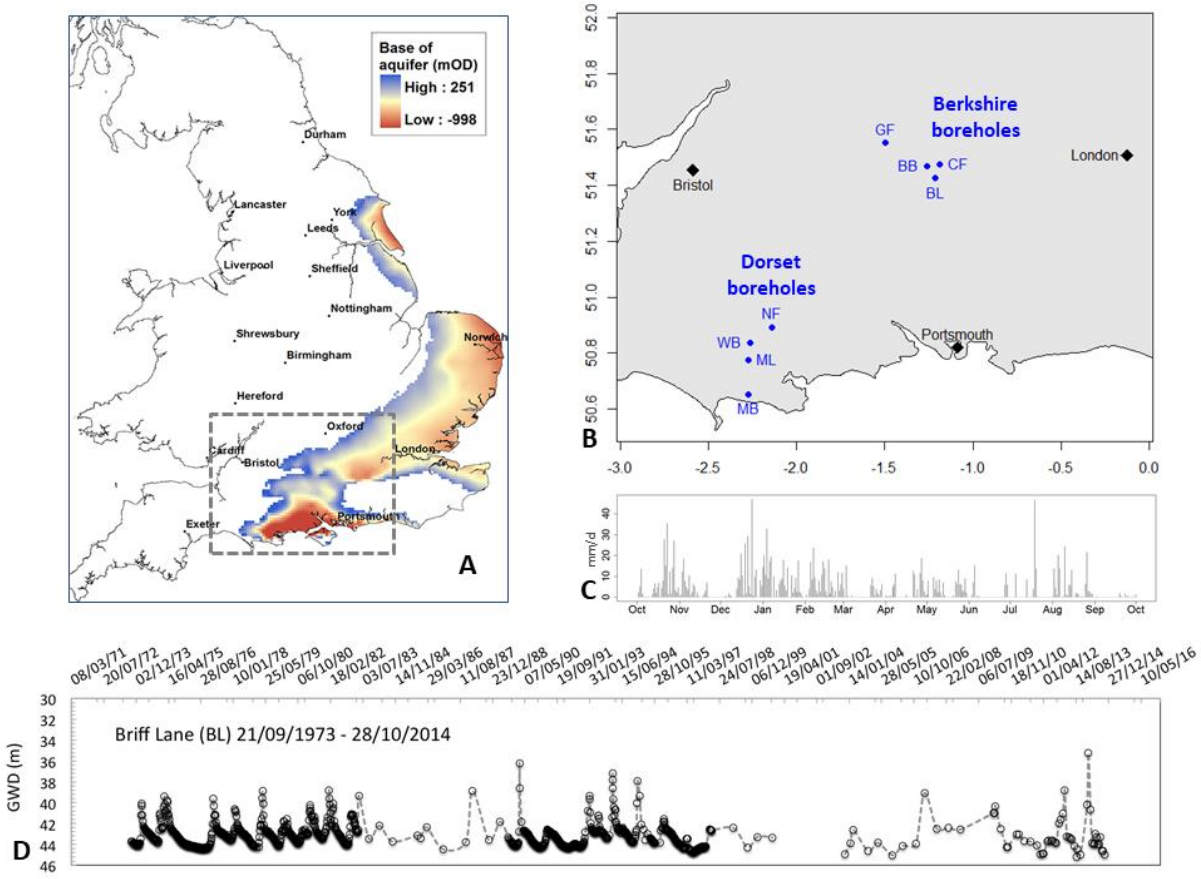

Figure 4-1. Spatial distribution of Chalk aquifers in the UK and base of aquifer, (data BGS – British Geological Survey) (**A**); Location of boreholes (**B**), daily precipitation between October 2013 and October 2014 (**C**), and long-term (1973-2015) groundwater depths at Brill Lane (BL) groundwater borehole (**D**).

4.2.2. Laboratory analyses

Boreholes were purged prior to the sampling using a sampling bailer lowered into the boreholes. Groundwater samples were filtered in the field through 0.45 μm Whatman polyamide filters and cooled for transport before being analysed at the University of Birmingham water quality laboratory. Analysis for nitrate concentrations was conducted on a Skalar San^{++} Continuous Injection Analyser (Skalar Analytical, Breda, NL) and dissolved organic carbon was analysed on a Shimadzu Catalyst Aided Combustion Analyser (Shimadzu, Kyoto, JP). All measured samples were within calibrated range.

Table 4-1. Details of groundwater boreholes.

Region	Name	Depth (m)	Notes
Berkshire	Bottom Barn (BB)	114.4	
	Calvesley Farm (CF)	119.8	
	Briff Lane (BL)	95	
	Greendown Farm (GF)	197	
Dorset	Newfields Farm (NF)	65.6	
	Winterbourne Heights (WB)	116.3	
	Millborne Lane (ML)	86.8	
	Marley Bottom (MB)	56.8	Sampling started June 2014
	Windmill Burrow		Sampling stopped due to borehole collapse June 2014. Close to MB.

4.2.3. Microbial metabolic activity

Microbial metabolic activity (MMA) in groundwater samples was quantified by the resazurin / resorufin smart tracer system (Haggerty *et al.*, 2009; González-Pinzón *et al.*, 2012; Kurz *et al.*, 2017). Resazurin (raz), a weakly-fluorescent substance transforms under mildly reducing conditions irreversibly to the highly-fluorescent resorufin (rru). It has been established as indicator of microbial metabolic activity with raz to rru conversion rates being correlated to aerobic respiration (McNicholl *et al.*, 2007; Haggerty *et al.*, 2008). Raz to rru transformation rates have been shown to be proportional to changes in oxygen, which is a common measurement of respiration rates (González-Pinzón *et al.*, 2012). Accordingly, the rate of raz to rru transformation represents an indicator of whole-stream metabolic functioning (González-Pinzón *et al.*, 2014) and as such has potential to improve our understanding of the relationships between stream solute transport and biogeochemical dynamics.

For the analysis of groundwater MMA, a set of samples was collected between 28 May 2014 and 30 May 2014. Samples were cooled and transferred to the University of Birmingham without filtering to preserve the microbial community that could be present. One of the samples for MMA analysis was Windmill Burrow (WB), which was still available in May 2014. Location Marley Bottom (MB) was not incubated as sampling had not started here. For incubations, 250 ml of sampled groundwater was incubated in 1000 ml microcosms with a concentration of 100 µg/l raz for 24 hrs. Each sample was incubated in duplicate. Two microcosms were prepared with only deionised water to act as control treatments. Incubations started on 9 June 2014.

The ratio of raz to rru conversion was quantified at t=0, 2, 4, 6, 8 and 24 hours of incubation. Therefore, fluorescence of raz and rru was measured for filtered samples using Albilla GGUN-FL 30 (Albillia, Neuchatel, CH) bench top fluorometers (Lemke *et al.*, 2013; Baranov

et al., 2016). Samples were discarded after measurement. Microcosms were incubated in a generic type incubation fridge, shielded from light, at 12.02±0.12°C. Temperature was monitored using a Tinytag Aquatic 2 temperature logger (Gemini Data Loggers Ltd, Chichester, United Kingdom). The raz-to-rru conversion rate was calculated as:

$$respiration_t = ln\left(\frac{rru_t}{raz_t} + C\right) \quad \text{Equation 4-1}$$

with $C = 1$, which is a constant value for amount of tracer recovered. Respiration at time t was calculated for each time step, through which a simple linear regression line was fitted. The slope of this line was then compared between all samples, where a higher value correlates with higher microbial metabolic activity.

4.2.4. Statistical analysis

Results are shown with standard deviation, unless specified otherwise. Bivariate analysis was performed using simple linear regression. Median values are sometimes shown together with mean values to illustrate skewness of a population.

4.3. Results

4.3.1. Hydro-meteorological conditions

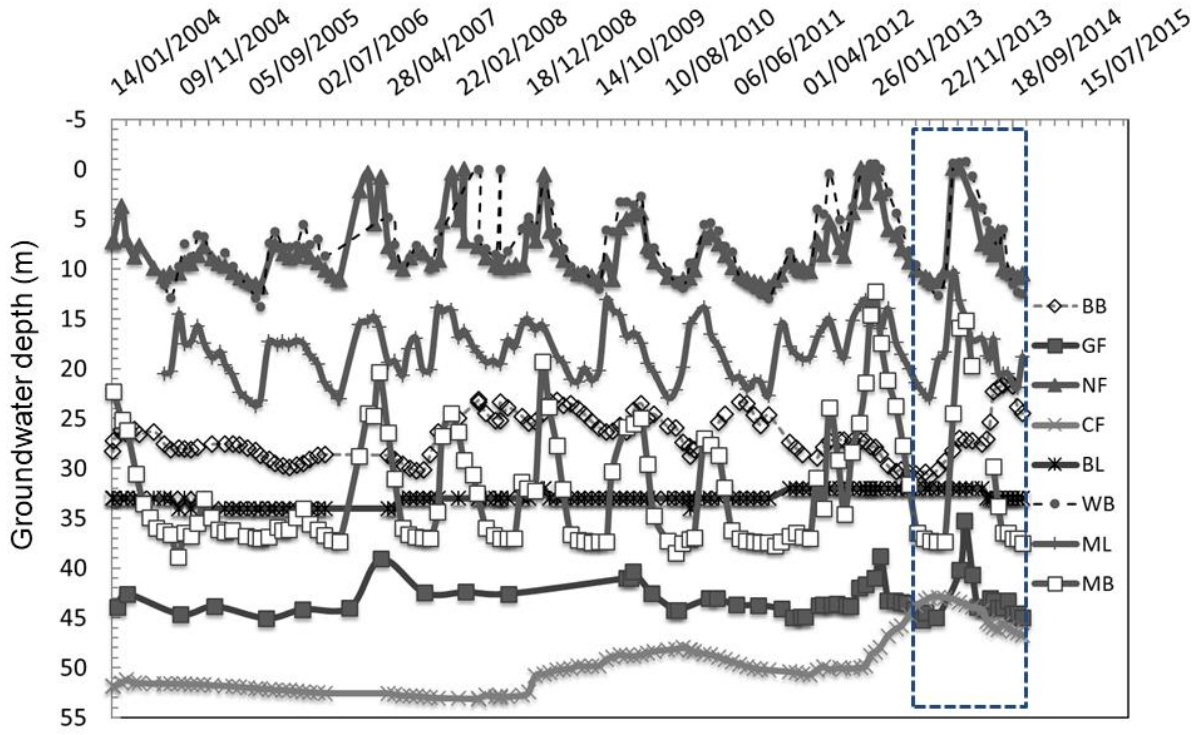

Figure 4-2. 10-year (2004-2014) groundwater depth time series of investigated Chalk boreholes. Marked box is the GW flood event of which the end was studied. Groundwater depth is water level below ground surface.

Long-term time series were constructed of groundwater depth (GWD) below surface (Figure 4-2) for a period of 10 years. These series display several GW flooding events that have taken place over the past 10 years. In general, boreholes closer to the surface show higher response to external water peaks. In the case of NF and WB, response from baseline to peak water level was around 1 month, whereas it took between 8 and 9 months for the GW to drop back to baseline depth.

4.3.2. Groundwater level time-series

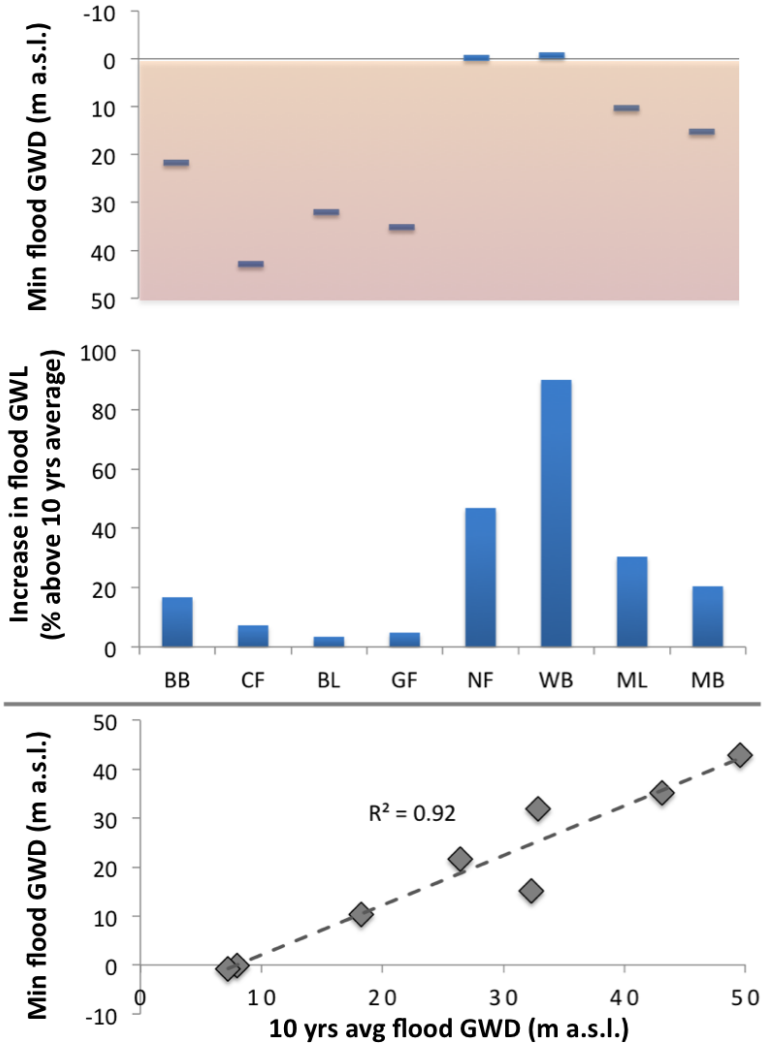

Figure 4-3. Minimum groundwater depth during 2014 flood (top), Relative (%) increase in flood groundwater levels (centre), and relationship between minimum and 10-year average groundwater depths for analysed boreholes (bottom). M.a.s.l. stands for meters above surface level.

Flood levels of GW were compared with the 10-year average flood level (Figure 4-3). Clearly the boreholes located in Dorset responded stronger to water inputs. For NF and WB, the flood level was reached and water rose to surface level (Figure 4-3a), where others remained below surface level. Water levels rose substantially more in Dorset boreholes: between 21% - 89% higher flood levels were measured, compared to 3% - 18% increases, for Dorset and Berkshire, respectively (Figure 4-3b). The measured flood levels were found to be

significantly correlated to the 10-year mean GW depth ($F(1, 6) = 71.09$, $p < 0.001$, $R^2 = 0.9222$, $n = 8$). In other words: areas with on average higher water levels see higher flood levels.

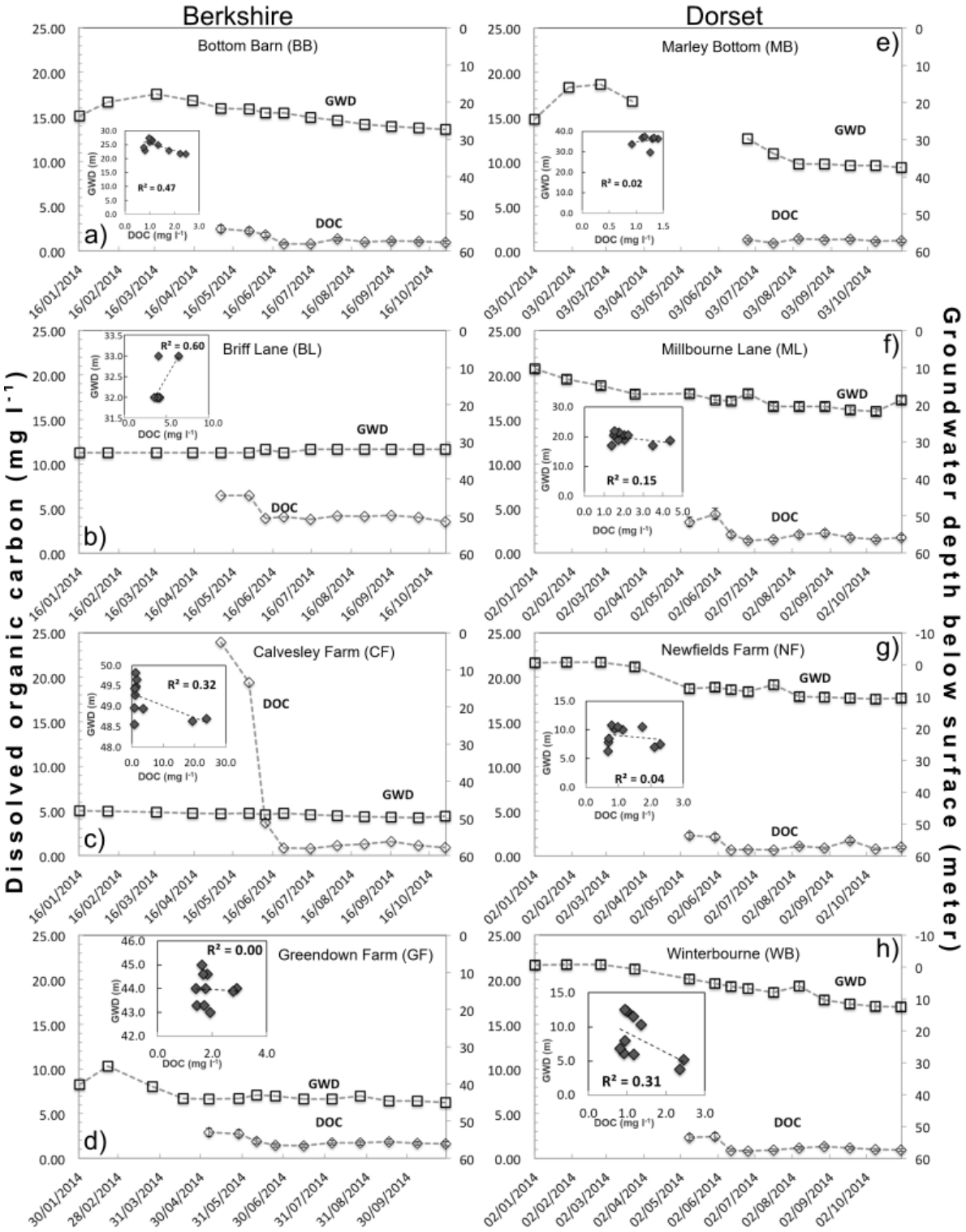

Figure 4-4. Groundwater depths and dissolved organic carbon (DOC) concentrations after the 2014 groundwater flooding for all analysed boreholes (Berkshire left; Dorset right), inlet figures indicating relationship between groundwater depth and DOC.

4.3.3. Groundwater quality time series

Water quality was monitored for all boreholes for DOC and nitrate (NO_3^-). In general, there was a falling trend in nutrient concentration with falling water table. DOC decreased for all locations after the flood and changes in concentration were similar for all but CF (Figure 4-4). A substantially higher DOC concentration was measured at CF, which dropped relatively rapidly back to its baseline value. There were no significant differences in concentration between sites with flooded situations (NF and WB) and those where the GWD was still under the surface. Highest DOC was measured in May 2014 in the Dorset borehole of CF with 21.67±3.22 mg/l, which dropped to below 4 mg/l in one month's time. The second highest DOC concentration was measured in BL, also Dorset, with 6.48±0.02 mg/l. Mean DOC concentration in Berkshire boreholes was 3.30±4.49 mg/l and median concentration was 1.77 mg/l. For Dorset boreholes, mean DOC concentration was 2.14±1.47 mg/l and a median of 1.49 mg/l.

For most boreholes there was a decrease in nitrate concentrations with falling GWD (Figure 4-5), suggesting concentrations were falling back to a baseline value after the floods. This observed pattern means that highest nitrate concentrations were measured at times when water was closest to or at the soil surface. Highest nitrate concentrations were measured in Berkshire borehole of GF with 94.23±10.09 mg/l, which remained high for several months. Highest nitrate concentration in Dorset was 43.06±2.18 mg/l. In general, mean nitrate concentrations in Berkshire boreholes were 32.95±33.17 mg/l and median concentration was 21.29 mg/l. For Dorset boreholes, mean nitrate concentration was 13.26±10.89 mg/l and a median of 13.05 mg/l.

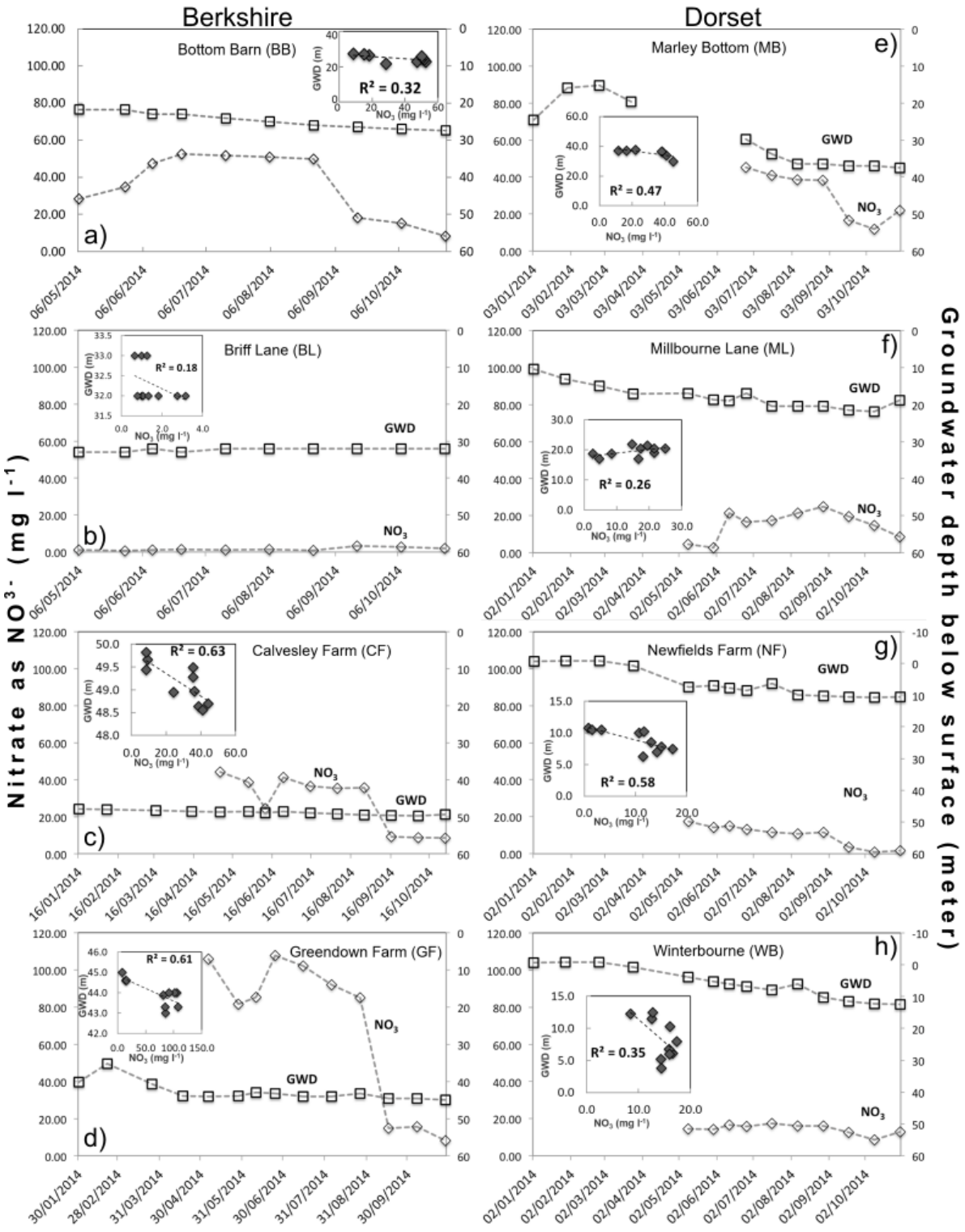

Figure 4-5. Groundwater depths and nitrate (NO_3) concentrations after the 2014 groundwater flooding for all analysed boreholes (Berkshire left, Dorset right), inset figures indicating relationship between groundwater depth and NO_3.

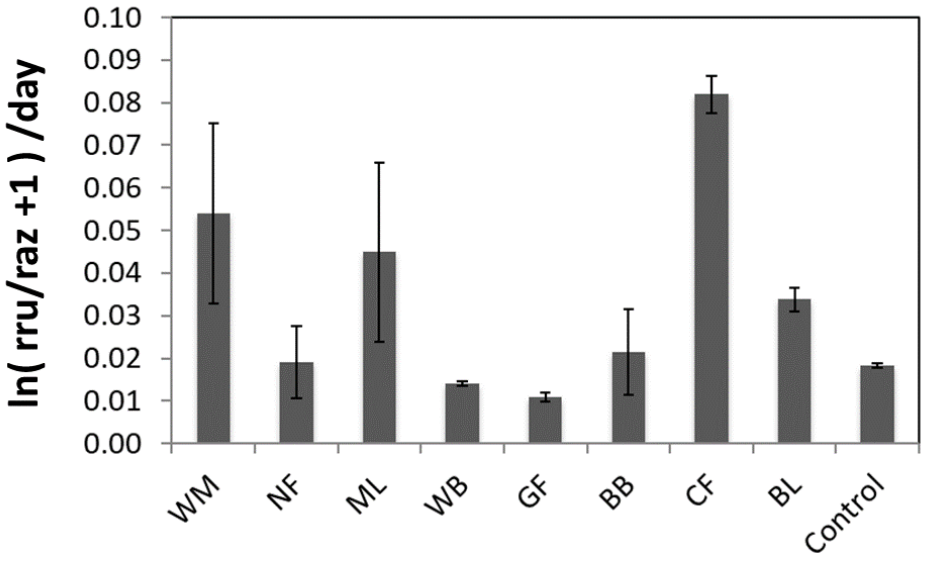

Figure 4-6. Microbial metabolic activity (as slope the of ln(Rru/Raz +1) per day, Equation 4-1) for all analysed boreholes (Table 4-1). Incubation was also possible for location WM. For location Marley Bottom (MB), incubation was not possible due to sampling schedule.

4.3.4. Groundwater microbial metabolic activity

Transformation of raz to rru was used to quantify microbial metabolic activity (MMA). A substantial amount of turnover was measured in several locations compared to control treatments (Figure 4-6). Highest MMA was measured in 0.082±0.004 day^{-1} in the water collected from Berkshire borehole CF. This was 52% higher than the second highest, with 0.054±0.021 day^{-1} in Dorset borehole WM. In half of the samples there was a substantial amount of microbial activity present. In samples WB and GF there was almost no observed difference compared to the control treatment. Sample sizes were n=2 and no reliable statistical testing was possible. In the control treatments there was limited transformation of raz to rru (0.0183±0.0004 day^{-1}).

Higher MMA was found in samples that contained a higher DOC concentration (Figure 4-7). The relation between DOC and MMA was found to be significant by simple linear regression

(F(1, 6) = 11.42, p = 0.0149, R^2 = 0.6556, n = 8). Although a wide variety in nitrate concentrations was present, there was no correlation found between the two (R^2 = 0.00).

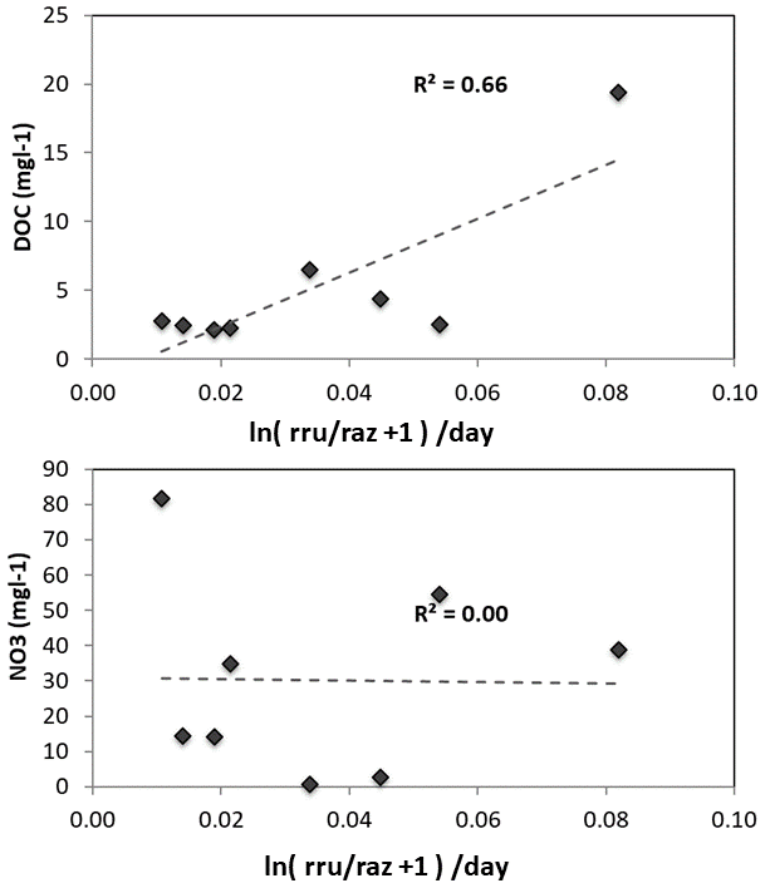

Figure 4-7. Relationship between DOC and microbial metabolic activity (top) and between nitrate and microbial metabolic activity (bottom) for all analysed boreholes.

4.4. Discussion

4.4.1. Spatio-temporal dynamics of groundwater levels

The groundwater flooding events in 2014 caused water levels in all boreholes to increase (Figure 4-2). The observed flood intensity was similar to previous flooding events. Sudden inputs of water from the surface during high-rainfall periods can move through fractures in dual-porosity aquifers. The stronger rise in GWD in Dorset boreholes could be related to local or regional differences in Chalk lithology (Macdonald & Allen, 2001) and complex

local exchange patterns between surface water and the Chalk aquifer (Allen *et al.*, 2010). Due to lower permeability superficial deposits in the Berkshire area, rainfall response times in the GW are known to be lower (Ascott *et al.*, 2017).

During the flood period there was a substantial increase in nutrients in the boreholes, suggesting that the influx reached the aquifer. Although there was no sampling during the rising part of the floods, the assumption can be made that the elevated observed concentrations were the result of flood water inputs (Figure 4-4, Figure 4-5). This rainwater quickly recharged the aquifer and therefore likely flowed along pathways that were connected by fractures (Macdonald & Allen, 2001). These pathways can be very responsive and cause nitrate and pesticides to be washed into the aquifer below (Haria *et al.*, 2003; Sorensen *et al.*, 2015). Along these pathways it is thought that most bacterial reduction of nitrate takes place (Bottrell *et al.*, 2000), although it may be difficult to reach conditions anaerobic enough to facilitate large-scale denitrification due to the relatively fast flow and oxygen transport (Rivett *et al.*, 2007).

In addition to contaminants, also DOC is known to be transported down with water in sandstone catchments (Lapworth *et al.*, 2008). However, rapid vertical transport does not fully explain the two observations of high DOC concentrations in borehole CF (Figure 4-4c). After the second observation near 20 mg/l DOC, the concentration dropped to around 5 mg/l and below, while nitrate remained more constant the whole time. Although evidence remains inconclusive, contamination of the borehole may have been possible.

4.4.2. Controls of groundwater microbial metabolic activity

While breakdown of excess nitrate is limited by organic carbon (Starr & Gillham, 1993), it may also act as a driver of MMA. DOC inputs are more short-lived and consumed quickly by

microbes compared to other pollutants that can accumulate in the Chalk aquifers over time (Manamsa *et al.*, 2016). Considering the dual-porosity nature of Chalk, DOC inputs by flood pulses can be expected to follow these same flow paths. Any MMA is expected along these flow paths, facilitating fertilisation of microbial communities, simply because microbes do not fit in the narrow (<1µm) matrix pores of the chalk (Bottrell *et al.*, 2000; Morris & Foster, 2000). Although data in this study did not cover the entire flood event, the results suggest that DOC inputs could be important for MMA (Figure 4-7a). DOC sensitivity of MMA was also observed in sandstone aquifers (Lapworth *et al.*, 2008) and more recently in alpine karst regions (Frank *et al.*, 2018).

MMA was generally highest in boreholes with water levels closer to the surface (Figure 4-2; Figure 4-6), suggesting that MMA was higher in locations that were experiencing an increased water level compared to their baseline level. MMA was lower in boreholes where the water level had increased less and lowest MMA was measured in water from boreholes where short-term water level changes were closest to zero (Figure 4-2). Higher MMA at higher water levels is explained by generally higher DOC at higher water levels. As the water levels are closer to the surface, flow paths of infiltrating water from the surface are shorter, possibly providing microorganisms with more and 'fresher' (more labile) DOC. This suggests that MMA was sensitive to flooding, similar to observations during flooding of riverbank infiltration points (Ascott *et al.*, 2016).

Although the results of this study suggest that DOC was an important driver of MMA (Figure 4-7), DOC quality measurements are needed to further explore this relation (Lapworth *et al.*, 2008), as not all DOC could have been bioavailable (Rivett *et al.*, 2007). Similarly, dissolved oxygen measurements can give insight whether zones were oxic or anoxic. In areas with river bank filtration for groundwater production it can take up to four weeks for dissolved oxygen

levels to drop from 4 to 2 mg/l after flood events (Ascott *et al.*, 2016), suggesting long lasting effects that may benefit MMA. Nitrate was not found to be an important variable for MMA. Dynamics of nitrate may only become clear when movement of the same body of water is studied over time while it moves down a certain flow path, for example from a confined to an unconfined zone (Moncaster *et al.*, 2000). The results show no significant differences between Berkshire and Dorset boreholes, although the response of MMA to DOC input does point towards the conclusion that higher pulses of nutrients due to flooding can fertilise MMA in a groundwater aquifer.

4.5. Conclusion

The effect of groundwater flooding events was studied in a Chalk aquifer in southern United Kingdom. These flooding events are known to negatively influence quality of the aquifer used for drinking water supply. The results of this study provide a lead to the source of the problem. Inputs of dissolved organic carbon (DOC) were found to influence microbial metabolic activity (MMA). Areas with groundwater depths more sensitive to flooding were found to have higher DOC, where also higher MMA was observed. Rapid transport of water down into the aquifer along fractures in the Chalk can cause a fertilisation effect from soil surface on MMA that could contribute to decreased quality of drinking water resources.

Further studies could focus on time series of MMA and DOC quality for spatio-temporal analysis, whereas this study focused more on spatial variation of MMA. Time series of MMA during a flood event may help to fully capture the sensitivity of a microbial community to flood inputs due to rainfall and DOC quality may be necessary to elucidate DOC sensitivity at lower DOC concentrations.

Acknowledgements

This project has received funding from the European Union's Seventh Framework Programme for research, technological development and demonstration under grant agreement no 607150 and we acknowledge funding from a NERC Urgency Grant NE/M005151/1.

Author contributions

PR wrote the manuscript and was responsible for the incubation experiment, laboratory analysis, data analysis and interpretation of the results. AR and JR designed and conceptualised the study, and collected field data. DMH provided support with manuscript revisions. AR and SK instigated the study. SK advised on the experimental design and the conceptualisation of the results, and supported the data analysis, interpretation, and manuscript revisions. AR and JR are affiliated with University of Roehampton, United Kingdom.

References

Allen DJ, Darling WG, Gooddy DC et al. (2010) Interaction between groundwater, the hyporheic zone and a Chalk stream: A case study from the River Lambourn, UK. *Hydrogeology Journal*, **18**, 1125–1141.

Ascott MJ, Lapworth DJ, Gooddy DC, Sage RC, Karapanos I (2016) Impacts of extreme flooding on riverbank filtration water quality. *Science of The Total Environment*, **554**–**555**, 89–101.

Ascott MJ, Marchant BP, Macdonald D, McKenzie AA, Bloomfield JP (2017) Improved understanding of spatio-temporal controls on regional scale groundwater flooding using hydrograph analysis and impulse response functions. *Hydrological Processes*, **31**, 4586–4599.

Banks D, Davies C, Davies W (1995) The Chalk as a karstic aquifer: evidence from a tracer test at Stanford Dingley, Berkshire, UK. *Quarterly Journal of Engineering Geology and Hydrogeology*, **28**, S31--S38.

Baranov V, Lewandowski J, Romeijn P, Singer G, Krause S (2016) Effects of bioirrigation of non-biting midges (Diptera: Chironomidae) on lake sediment respiration. *Scientific Reports*, **6**, 27329.

Bloomfield JP, Williams RJ, Gooddy DC, Cape JN, Guha P (2006) Impacts of climate change on the fate and behaviour of pesticides in surface and groundwater-a UK perspective. *Science of the Total Environment*, **369**, 163–177.

Bottrell SH, Moncaster SJ, Tellam JH, Lloyd JW, Fisher QJ, Newton RJ (2000) Controls on bacterial sulphate reduction in a dual porosity aquifer system: the Lincolnshire Limestone aquifer, England. *Chemical Geology*, **169**, 461–470.

Brouyère S, Carabin G, Dassargues A (2004) Climate change impacts on groundwater resources: modelled deficits in a chalky aquifer, Geer basin, Belgium. *Hydrogeology Journal*, **12**.

Cobby D, Morris S, Parkes A, Robinson V (2009) Groundwater flood risk management: advances towards meeting the requirements of the EU floods directive. *Journal of Flood Risk Management*, **2**, 111–119.

Darling WG, Gooddy DC, Morris BL, Peach DW (2012) The hydrochemistry of a Chalk aquifer during recovery from drought. *Quarterly Journal of Engineering Geology and Hydrogeology*, **45**, 473–486.

Frank S, Goeppert N, Goldscheider N (2018) Fluorescence-based multi-parameter approach to characterize dynamics of organic carbon, faecal bacteria and particles at alpine karst springs. *Science of the Total Environment*, **615**, 1446–1459.

Fürst J, Bichler A, Konecny F (2015) Regional frequency analysis of extreme groundwater levels. *Groundwater*, **53**, 414–423.

González-Pinzón R, Haggerty R, Myrold DD (2012) Measuring aerobic respiration in stream ecosystems using the resazurin-resorufin system. *Journal of Geophysical Research: Biogeosciences*, **117**, n/a-n/a.

González-Pinzón R, Haggerty R, Argerich A (2014) Quantifying spatial differences in metabolism in headwater streams. *Freshwater Science*, **33**, 798–811.

Gotkowitz MB, Attig JW, McDermott T (2014) Groundwater flood of a river terrace in southwest Wisconsin, USA. *Hydrogeology Journal*, **22**, 1421–1432.

Haggerty R, Argerich A, Martí E (2008) Development of a "smart" tracer for the assessment of microbiological activity and sediment-water interaction in natural waters: The resazurin-resorufin system. *Water Resources Research*, **44**, W00D01.

Haggerty R, Martí E, Argerich A, Von Schiller D, Grimm NB (2009) Resazurin as a "smart" tracer for quantifying metabolically active transient storage in stream ecosystems. *Journal of Geophysical Research: Biogeosciences*, **114**.

Haria AH, Hodnett MG, Johnson AC (2003) Mechanisms of groundwater recharge and pesticide penetration to a chalk aquifer in southern England. *Journal of Hydrology*, **275**, 122–137.

Hemme CL, Deng Y, Gentry TJ et al. (2010) Metagenomic insights into evolution of a heavy metal-contaminated groundwater microbial community. *ISME Journal*, **4**, 660–672.

Herrera-Pantoja M, Hiscock KM (2008) The effects of climate change on potential groundwater recharge in Great Britain. *Hydrological Processes*, **22**, 73–86.

Hughes AG, Vounaki T, Peach DW et al. (2011) Flood risk from groundwater: Examples from a Chalk catchment in southern England. *Journal of Flood Risk Management*, **4**, 143–155.

IPCC (2014) *Climate Change 2014: Impacts, Adaptation, and Vulnerability. Part A: Global and Sectoral Aspects. Contribution of Working Group II to the Fifth Assessment Report of the Intergovernmental Panel on Climate Change [Field, C.B., V.R. Barros, D.J. Dokken, K.J.* Cambridge University Press, Cambridge, United Kingdom and New York, NY, USA, 1132 pp.

Jackson CR, Meister R, Prudhomme C (2011) Modelling the effects of climate change and its uncertainty on UK Chalk groundwater resources from an ensemble of global climate model projections. *Journal of Hydrology*, **399**, 12–28.

Kim H, Park S (2016) Hydrogeochemical Characteristics of Groundwater Highly Polluted with Nitrate in an Agricultural Area of Hongseong, Korea. *Water*, **8**, 345.

Kim H, Kaown D, Mayer B, Lee J-Y, Hyun Y, Lee K-K (2015) Identifying the sources of nitrate contamination of groundwater in an agricultural area (Haean basin, Korea) using isotope and microbial community analyses. *Science of The Total Environment*, **533**, 566–575.

Kistemann T, Classen T, Koch C et al. (2002) Microbial Load of Drinking Water Reservoir Tributaries during Extreme Rainfall and Runoff. *Applied and Environmental Microbiology*, **68**, 2188–2197.

Kreibich H, Thieken AH (2008) Assessment of damage caused by high groundwater inundation. *Water Resources Research*, **44**, 1–14.

Kurz MJ, Drummond JD, Martí E et al. (2017) Impacts of water level on metabolism and transient storage in vegetated lowland rivers: Insights from a mesocosm study. *Journal of Geophysical Research: Biogeosciences*, **122**, 628–644.

Lapworth DJ, Gooddy DC, Butcher AS, Morris BL (2008) Tracing groundwater flow and sources of organic carbon in sandstone aquifers using fluorescence properties of dissolved organic matter (DOM). *Applied Geochemistry*, **23**, 3384–3390.

Lemke D, Schnegg P-A, Schwientek M, Osenbrück K, Cirpka O a. (2013) On-line fluorometry of multiple reactive and conservative tracers in streams. *Environmental Earth Sciences*, **69**, 349–358.

Macdonald AM, Allen DJ (2001) Aquifer properties of the Chalk of England. *Quarterly Journal of Engineering Geology and Hydrogeology*, **34**, 371–384.

Macdonald DDMJ, Bloomfield JPP, Hughes a. GG, MacDonald a. MM, Adams B, McKenzie a. a. (2008) Improving the understanding of the risk from groundwater flooding in the UK. In: *FLOODrisk 2008, European Conference on Flood Risk Management, Oxford, UK, 30 Sept - 2 Oct 2008. The Netherlands*, Vol. ~, p. 10.

Macdonald D, Dixon A, Newell A, Hallaways A (2012) Groundwater flooding within an urbanised flood plain. *Journal of Flood Risk Management*, **5**, 68–80.

Manamsa K, Lapworth DJ, Stuart ME (2016) Temporal variability of micro-organic contaminants in lowland chalk catchments: New insights into contaminant sources and hydrological processes. *Science of the Total Environment*, **568**, 566–577.

McNicholl BP, McGrath JW, Quinn JP (2007) Development and application of a resazurin-based biomass activity test for activated sludge plant management. *Water research*, **41**, 127–33.

Moncaster SJ, Bottrell SH, Tellam JH, Lloyd JW, Konhauser KO (2000) Migration and attenuation of agrochemical pollutants: Insights from isotopic analysis of groundwater

sulphate. *Journal of Contaminant Hydrology*, **43**, 147–163.

Morris BL, Foster SD (2000) Cryptosporidium contamination hazard assessment and risk management for British groundwater sources. *Water Science and Technology*, **41**, 67–77.

Muchan K, Lewis M, Hannaford J, Parry S (2015) The winter storms of 2013/2014 in the UK: hydrological responses and impacts. *Weather*, **70**, 55–61.

Naughton O, Johnston PM, McCormack T, Gill LW (2017) Groundwater flood risk mapping and management: examples from a lowland karst catchment in Ireland. *Journal of Flood Risk Management*, **10**, 53–64.

Osborn TJ, Hulme M, Jones PD, Basnett TA (2000) Observed trends in the daily intensity of United Kingdom precipitation. *International Journal of Climatology*, **20**, 347–364.

Pinault J-L, Amraoui N, Golaz C (2005) Groundwater-induced flooding in macropore-dominated hydrological system in the context of climate changes. *Water Resources Research*, **41**, 1–16.

Ranjan P, Kazama S, Sawamoto M (2006a) Effects of climate and land use changes on groundwater resources in coastal aquifers. *Journal of Environmental Management*, **80**, 25–35.

Ranjan P, Kazama S, Sawamoto M (2006b) Effects of climate change on coastal fresh groundwater resources. *Global Environmental Change*, **16**, 388–399.

Rivett MO, Smith JWN, Buss SR, Morgan P (2007) Nitrate occurrence and attenuation in the major aquifers of England and Wales. *Quarterly Journal of Engineering Geology and Hydrogeology*, **40**, 335–352.

Robins NS, Finch JW (2012) Groundwater flood or groundwater-induced flood? *Quarterly Journal of Engineering Geology and Hydrogeology*, **45**, 119–122.

Scibek J, Allen DM (2006) Comparing modelled responses of two high-permeability, unconfined aquifers to predicted climate change. *Global and Planetary Change*, **50**, 50–62.

Sherif MM, Singh VP (1999) Effect of climate change on sea water intrusion in coastal aquifers. *Hydrological Processes*, **13**, 1277–1287.

Sorensen JPR, Butcher AS, Stuart ME, Townsend BR (2015) Nitrate fluctuations at the water table: implications for recharge processes and solute transport in the Chalk aquifer. *Hydrological Processes*, **29**, 3355–3367.

Starr RC, Gillham RW (1993) Denitrification and Organic Carbon Availability in 2 Aquifers. *Ground Water*, **31**, 934–947.

Valett HM, Baker MA, Morrice JA et al. (2005) Biogeochemical and metabolic responses to the flood pulse in a semiarid floodplain. *Ecology*, **86**, 220–234.

Conclusions

The work performed in this thesis aimed at contributing to closing specific knowledge gaps on microbial metabolic activity (MMA) at groundwater-surface water (GW-SW) interfaces. Novel tracer methods were successfully applied to study MMA across several contrasting but connected GW-SW interfaces.

In the first chapter the importance of the GW-SW interface at the streambed surface level was demonstrated. By means of an incubation experiment, it was shown that streambed sediments in agricultural streams produce substantial amounts of the greenhouse gases carbon dioxide and methane and that production varied between sediments of a Chalk background and a Sandstone background. Production of these greenhouse gases (GHG) was driven by organic matter (OM) contents. Like GHG production, MMA was also observed to respond to OM contents. However, not only quantity, but also quality of OM played an important role. OM properties in streambed environments typically reflect the geological background of a certain reach. Quality of OM was measured by aromaticity and also found to drive MMA and associated GHG production. The quantities of CO_2 production were compared with previous studies and the amount of CO_2 produced by MMA inside the streambed sediments of the top layer can explain up to 35% of previously measured excess CO_2 fluxes. Methane production varied even stronger with OM quality. The results of this chapter suggest that microbial communities exhibit strong spatial patterns that vary with the geologic background of the substrate. It is not only the amount of OM that controls microbial metabolic OM mineralisation, OM quality needs to be considered too. This is especially important in areas with strong anthropogenic disturbances.

After the first chapter demonstrated the potential of GHG production and MMA at the streambed surface, Chapter 2 continues to explore spatial variability of MMA and nutrient cycling. This study used a novel *in situ* push-pull injection experiment to measure MMA by vertical spatial variability in a heterogeneous streambed environment. The lowland River Tern experienced net groundwater upwelling from the Sandstone substrate and a strong nutrient loading from the surrounding agriculture in the present and the past. Detailed imaging of the streambed sediment structure allowed precise planning of measurement of residence times, MMA and nutrient concentrations around structures of low hydraulic conductivity (K_h). Residence time was controlled by K_h. While dissolved organic carbon (DOC) was not found to be limiting as opposed to the observed OM controls in Chapter 1, residence time was identified as an important control on dissolved oxygen, MMA and nutrient concentrations. Streambed structures with high OM contents were found to be a source of ammonium to the top of the streambed and possibly into the stream. Streambed heterogeneity, and thus residence time, can be very local. Sampling locations should be selected with care to properly cover the entire range of spatial variety, including possible hotspots that may be present.

In Chapter 3 the scale was increased from plot to the reach. The focus shifted from local streambed heterogeneities and hydraulic features towards larger scale impacts. Concurrent slug injections of reactive and conservative tracer injections were performed in an urban stream receiving wastewater treatment effluents, before and after removal of macrophytes by mowing. The hypothesis before commencing the experiment was that mowing would lead to shorter residence times and thus reduced MMA. Although flow velocity increased, transient storage was not found to be shorter and had even slightly increased after mowing. It was concluded that one transient storage zone replaces another: storage between macrophytes was removed, but this facilitated improved hyporheic exchange. The results suggest that storage

in the hyporheic zone was of a higher quality for MMA, since the decrease in MMA due to mowing was much lower than expected, and even remained unchanged. This supports findings from Chapter 2, where residence time controls were found to be important for nutrient cycling and pollutant attenuation in the hyporheic zone as well. The results have implications for application of management principles and help understand the consequences of potentially disturbing mowing practices.

In Chapter 1 it was shown how OM acts as a driver of MMA inside the streambed sediments and Chapter 2 demonstrated the importance of residence time as a driver of MMA, which was supported by findings in Chapter 3. Chapter 4 enters the last area of GW-SW interactions that was not fully explored yet in this thesis, namely groundwater itself. In the last chapter it was demonstrated that MMA in groundwater was sensitive to fertilisation by carbon that can be introduced during groundwater flood events. In dual-porosity Chalk aquifers in the south of the UK, groundwater flows preferentially along fractures. In these fractures a matrix is present that hosts microbial communities, an ecotone that shares similarities with the heterogeneous streambed environment from Chapter 2: preferential flow around and between areas low hydraulic conductivity. MMA in these fractures was positively correlated to DOC concentrations, suggesting sensitivity to fertilisation. Improved knowledge may help to predict decreases in groundwater quality and to help drinking water supply companies to anticipate when to take measures.

The work in this thesis sheds new light on MMA in different parts of the groundwater-surface water interfaces across several scales. The main drivers of MMA were identified in this thesis as carbon (as organic matter and depending on the quality or DOC) and residence time. Effects of carbon were observed not only at the GW-SW interface in the top of the streambed (Chapter 1), but also in the groundwater compartment (Chapter 4). Residence time was found

to be important in heterogeneous streambed subsurface and, on the reach scale, in stream water (Chapter 3). Recent technological advances in 'smart' tracers (resazurin) combined with high-resolution fluorometric detection have enabled analysis of MMA in novel ways at the groundwater-surface water interface. The resazurin method results suggest MMA was important for carbon turnover. Since the method is a measure for aerobic respiration, turnover of nitrate and ammonium may not be directly related to resazurin turnover. However, the results do suggest residence time controls are important for most biogeochemical processes from the plot scale to the reach scale.

Future directions

The findings presented here illustrate the importance of the availability of carbon (as organic matter or DOC), as well as its quality, is an important control on potential greenhouse gas emissions. Considering the location of the studied areas, it is essential to learn about the potential impacts of human-induced land use change in lowland streams. High-frequency fluorescence resazurin measurements are promising technologies that can provide a rapid and effective method to compare MMA between several reaches. This is a useful tool when there are questions about the impact of certain treatments (such as described in Chapter 3) on the reach level on microbial activity, but also to compare seasonal changes or land use changes.

Measurements of MMA inside the streambed using injections of resazurin have proven useful, albeit difficult. Although the design of mini-piezometers used in Chapter 2 was similar to some previous experiments, some challenging technical difficulties remain. Measurements are subject to dilution by flow, while the flow direction cannot be determined. A multi-point approach could be applied to determine (1) flow direction in the subsurface, (2) flow velocity and (3) MMA and (4) advanced insights into nutrient cycling. Dissolved GHG

analysis would be less feasible in combination with this type of experiment due to small porewater sample sizes of approximately 15 ml required for fluorometric analysis.

On the reach scale there is great potential to combine several methods used in this thesis. After reviewing the results from Chapter 3, an open question remains about potential increases of MMA and GHG production inside the streambed. An interesting approach would be to use mini-piezometers at certain locations and perform high-frequency resazurin concentrations combined with *in situ* carbon dioxide and methane concentrations. This could verify assumptions about increased streambed MMA and provide a strong basis for new urban stream management strategies, including improvements on pollutant attenuation.

The connection between groundwater and surface water, such as was demonstrated in Chapter 4, should be explored in further detail. Various, if not most, climate change scenarios generally agree on increases in extreme rainfall and a shift towards stronger separation between dry and wet periods in the United Kingdom in the near future. Combined with higher amounts of rainfall, dual-porosity aquifers in Chalk areas of the UK and elsewhere could be at risk of uncontained contaminations by sharp turbidity increases. Reliable predictions of the scale of such contaminations may help anticipate these events and secure reliable water supply.

Appendices

Appendix A. Supporting information Chapter 1

Full results statistical analysis

Table A-1. Results from comparing hourly microbial metabolic activity between the different sediment groups. Values are P-values from the corresponding tests. Whole groups are also compared, indicated with 'all'. For groups CH, CM, CL, SH, SM, SL and Control, n=12 and, depending on group normality, T-test or Mann-Whitney U test was used. For Chalk (all) and Sandst. (all), n=36 and, depending on group normality, T-test or Kruskall-Wallis test was used. T or U values are in brackets.

	CM	*CL*	*SH*	*SM*	*SL*	*Control*	*Sandst. (all)*
CH	*0.002 (U=123)*	*7.63E-05 (U=141)*	*0.078 (U=103)*	*0.0002 (U=136)*	*3.60E-05 (U=144)*	*1.03E-05 (U=144)*	
CM		*0.099 (T=1.761)*	*0.22 (U=50)*	*0.11 (T=1.688)*	*0.013 (T=2.851)*	*1.03E-05 (U=144)*	
CL			*0.01 (U=27)*	*0.73 (T=0.358)*	*0.06 (T=1.963)*	*0.000125 (U=132)*	
SH				*0.012 (U=116)*	*0.0009 (U=130)*	*1.03E-05 (U=126)*	
SM					*0.46 (T=0.756)*	*0.005874 (U=144)*	
SL						*0.0004 (U=114)*	
Chalk (all)						*8.73E-07 (χ^2=24.189)*	*0.012 (χ^2=6.316)*
Sandst. (all)						*3.96E-05 (χ^2=16.888)*	

Table A-2. Results from comparing hourly CO_2 between the different sediment groups. Values are P-values from the corresponding tests. Whole groups are also compared, indicated with 'all'. For groups CH, CM, CL, SH, SM, SL and Control, n=12 and, depending on group normality, T-test or Mann-Whitney U test was used. For Chalk (all) and Sandst. (all), n=36 and, depending on group normality, T-test or Kruskall-Wallis test was used. T or U values are in brackets.

	CM	CL	SH	SM	SL	Control	Sandst. (all)
CH	6.7E-06 *(T=6.391)*	2.3E-07 *(T=10.749)*	0.009 *(T=2.881)*	2.1E-06 *(T=8.274)*	1.4E-06 *(T=9.031)*	7.4E-07 *(U=0.000)*	
CM		2.7E-05 *(T=6.352)*	0.0006 *(T=4.063)*	0.053 *(T=2.091)*	0.006 *(T=3.295)*	0.0002 *(U=0.000)*	
CL			4.5E-07 *(T=9.762)*	2.5E-07 *(T=7.877)*	1.6E-07 *(T=7.524)*	0.017 *(U=0.000)*	
SH				1.9E-05 *(T=6.410)*	7.4E-06 *(T=7.440)*	7.4E-07 *(U=0.000)*	
SM					0.054 *(T=2.055)*	7.4E-07 *(U=0.000)*	
SL						7.4E-07 *(U=0.000)*	
Chalk (all)						3.8E-05 *(χ^2=16.967)*	0.86 *(χ^2=0.032)*
Sandst. (all)						2.7E-07 *(χ^2=26.449)*	

Table A-3. Results from comparing hourly methane production between the different sediment groups. Values are P-values from the corresponding tests. Whole groups are also compared, indicated with 'all'. For groups CH, CM, CL, SH, SM, SL and Control, n=12 and, depending on group normality, T-test or Mann-Whitney U test was used. For Chalk (all) and Sandst. (all), n=36 and, depending on group normality, T-test or Kruskall-Wallis test was used. T or U values are in brackets.

	CM	CL	SH	SM	SL	Control	Sandst. (all)
CH	7.4E-07 *(U=144)*	5.9E-06 *(T=8.091)*	1.8E-05 *(T=6.921)*	3.6E-05 *(U=144)*	5.8E-06 *(T=8.099)*	5.8E-06 *(T=8.102)*	
CM		0.0001 *(U=133)*	0.003 *(U=22)*	0.0005 *(U=133)*	0.0006 *(U=132)*	0.0001 *(U=134)*	
CL			0.0001 *(T=5.859)*	0.285 *(U=91)*	0.207 *(T=1.310)*	0.113 *(T=1.656)*	
SH				3.6E-05 *(U=144)*	0.0001 *(T=5.904)*	9.9E-05 *(T=5.919)*	
SM					0.773 *(U=77.5)*	0.885 *(U=75)*	
SL						0.573 *(T=0.573)*	
Chalk (all)						9.4E-05 *(χ^2=15.247)*	0.004 *(χ^2=8.119)*
Sandst. (all)						0.051 *(χ^2=3.812)*	

Appendix B. Supporting information Chapter 2

Table B-1. Multilevel piezometer properties.

Name	Description	Sampling depths (cm)
MP-1 peat/clay	50 cm from bank, crossing a peat layer between 50 and 70 cm. (GPR location 80) 6 depths.	10, 20, 40, 60, 80, 115
MP-2 peat/clay		10, 20, 40, 60, 80, 115
MP-3 peat/clay		10, 20, 40, 60, 80, 115
MP-4 sand	Near GPR 88 5 depths.	10, 20, 40, 70, 115
MP-5 sand		10, 20, 40, 70, 115
MP-6 sand		10, 20, 40, 70, 115
MP-7 sand	Streambed, GPR location 110, sandy throughout with some gravel. 5 depths.	10, 20, 40, 70, 115
MP-8 sand		10, 20, 40, 70, 115
MP-9 sand		10, 20, 40, 70, 115
MP-10 sand	Streambed, GPR location 120, sandy throughout with some gravel. 5 depths.	10, 20, 40, 70, 115
MP-11 sand		10, 20, 40, 70, 115
MP-12 sand		10, 20, 40, 70, 115
MP-13 peat/clay	after the bend, approx 155 GPR. 4 depths.	10, 20, 50, 115
MP-14 peat/clay		10, 20, 50, 115
MP-15 peat/clay		10, 20, 50, 115
MP-16 peat/clay	after the bend, approx 160 GPR to 170 5 depths.	10, 20, 30, 70, 115
MP-17 peat/clay		10, 20, 30, 70, 115
MP-18 peat/clay		10, 20, 30, 70, 115

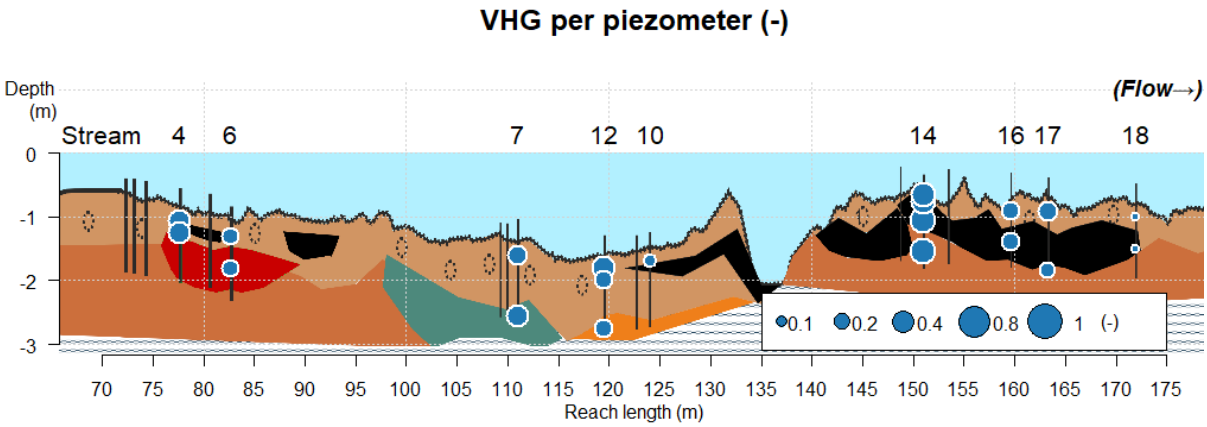

Figure B-1. Vertical hydraulic gradients during each experiment. During all experiments the VHG was positive, indicating net upwelling in the entire reach.